

**Nitrogen Cycling in the Past and in the Present Mediterranean Sea and
Arabian Sea – Implications from Stable Isotope Studies**

Dissertation

Zur Erlangung des Doktorgrades der Naturwissenschaften im Department
Geowissenschaften der Universität Hamburg

vorgelegt von

Jürgen Henning Möbius

aus

Hamburg

Hamburg

2010

Als Dissertation angenommen vom Department Geowissenschaften der
Universität Hamburg

auf Grund der Gutachten von

Prof. Dr. Kay-Christian Emeis

und

Dr. Birgit Gaye

Hamburg, den 7. Mai 2010

Prof. Dr. Jürgen Oßenbrügge

Leiter des Department Geowissenschaften

Zusammenfassung

Das Atomverhältnis der stabilen Stickstoffisotope ($R = {}^{15}\text{N}/{}^{14}\text{N}$, ausgedrückt als $\delta^{15}\text{N}$) in festen und gelösten Stickstoffverbindungen wird oft genutzt, um N-Quellen und -Umsatzprozesse in aquatischen Systemen zu verfolgen. In dieser Arbeit verwende ich isotopische Methoden mit dem Schwerpunkt auf $\delta^{15}\text{N}$, um einzelne Bereiche des rezenten N-Kreislaufs im östlichen Mittelmeer genauer zu untersuchen (Kapitel 3). Des Weiteren überprüfe ich anhand von kombinierten $\delta^{15}\text{N}$ -Daten und der Aminosäurezusammensetzung (ein Indikator für den Abbaugrad des organischen Materials) aus Sinkstoffen, Oberflächensedimenten und Sedimentkernen die Anwendbarkeit des $\delta^{15}\text{N}$ als paläozeanografisches Werkzeug im östlichen Mittelmeer und im Arabischen Meer (Kapitel 4 und 5).

Das äußerst nährstoffarme östliche Mittelmeer weist in fast allen reaktiven Stickstoffkompartimenten (also allen anorganischen und organischen Formen von N außer N_2) ungewöhnlich niedrige $\delta^{15}\text{N}$ Werte auf. Als Grund dafür wurde diazotrophe N-Fixierung vermutet, die bisher allerdings kaum beobachtet wurde und die zudem wegen des Nitratüberschusses im Tiefen- und Zwischenwasser (Nitrat zu Phosphat- Verhältnisse bis zu 28) biogeochemisch wenig sinnvoll erscheint. Um diese Umstände weiter zu klären, wurden isotopische Daten der wichtigsten reaktiven N-Spezies (NO_3^- , gelöster reduzierter N, suspendierter partikulärer N und sinkender partikulärer N) während einer Probenahmekampagne im Winter/beginnenden Frühjahr 2007 im östlichen Mittelmeer bestimmt und nun in Kapitel 3 diskutiert und modelliert. Dabei zeigen die Mess- und Modellergebnisse, dass die wichtigste NO_3^- -Quelle für den Nitratpool während der Probenahme höchstwahrscheinlich remineralisiertes NO_3^- ist, welches durch die Nitrifizierung von absinkendem, im durchmischten Oberflächenwasser produzierten partikulärem N entstanden ist. Außerdem wird ein signifikanter Beitrag von atmosphärisch eingetragenen, industriell in Europa emittierten Stickoxiden auf das $\delta^{15}\text{N}$ -Signal im Oberflächenwasser deutlich.

Die paläozeanografische Anwendung von $\delta^{15}\text{N}$ als Proxy wird generell dadurch erschwert, dass das ursprüngliche Signal aus den biologisch produktiven oberen Wasserschichten während des Absinkens der Partikel und nach der Sedimentation eine frühdiagenetische Überprägung erfährt. Diesen frühdiagenetischen Effekt versuche ich in den Kapiteln 4 und 5 zu erfassen, um das ursprüngliche isotopische Signal des in der euphotischen Zone assimilierten reaktiven N im östlichen Mittelmeer (Kapitel 4) und im Arabischen Meer (Kapitel 5) während des Holozäns und des späten Pleistozäns anhand von Sedimentkernen zu rekonstruieren. Dies ist durch eine Kombination von $\delta^{15}\text{N}$ -Werten mit der Aminosäurezusammensetzung möglich, wobei letztere genutzt wird, um den Abbaugrad des organischen Materials zu bestimmen. Die derart

normalisierten Sedimentkerndaten aus dem östlichen Mittelmeer zeigen, dass die großskaligen (Jahrzehntausende umfassende) Veränderungen im $\delta^{15}\text{N}$ -Signal und die horizontalen Gradienten im $\delta^{15}\text{N}$ von Sapropelen (isochrone, organisch-reiche Lagen) im wesentlichen durch unterschiedliche Erhaltung aufgrund wechselnder Sauerstoffsättigung im Tiefen- bzw. Bodenwasser bestimmt sind. Die erhöhten Akkumulationsraten von organischem Kohlenstoff, die zur Bildung des jüngsten Sapropels (S1) führten, sind möglicherweise ebenfalls größtenteils auf verhinderten Abbau unter sauerstoffdefizitären Bedingungen an der Sedimentoberfläche zurückzuführen und damit weniger ein Ausdruck von erhöhter Primärproduktion.

Die großskaligen Schwankungen im $\delta^{15}\text{N}$ -Signal der Kerne aus dem Arabischen Meer (Kapitel 5) werden primär von Veränderungen im $\delta^{15}\text{N}$ des assimilierten Nitrats hervorgerufen. Hier wird die Variabilität hauptsächlich von externen klimatischen Veränderungen in der Monsunstärke und damit einhergehenden unterschiedlichen Zirkulationsmustern im Zwischenwasser gesteuert; diese bestimmen wiederum die Sauerstoffgehalte des Zwischenwassers im Arabischen Meer und damit letztendlich die Isotopie des Nitrats. Die Verteilungsmuster von $\delta^{15}\text{N}$ in Oberflächensedimenten und in isochronen Zeitscheiben aus Sedimentkernen sind hingegen als unterschiedliche Erhaltung des originalen Signals aus der Primärproduktion und Nitratassimilation zu deuten.

Die Evaluierung von zwei Abbauidizes auf Aminosäurebasis (Reactivity Index, RI und Degradation Index, DI) in rezenten Sedimenten und Sedimentkernen aus dem Arabischen Meer legt nahe, dass der RI eher geeignet ist, den Erhaltungsgrad von organischem Material in Sedimentkernen anzuzeigen als der DI. Durch die eindeutige Beziehung zwischen $\delta^{15}\text{N}$ und dem RI ist eine Rekonstruktion des originalen $\delta^{15}\text{N}$ vor der diagenetischen Überprägung möglich.

Abstract

The $^{15}\text{N}/^{14}\text{N}$ isotope ratio ($\delta^{15}\text{N}$) of particulate and dissolved N-species is widely used to trace N sources and turnover processes in aquatic environments. In this thesis, I apply isotopic methods with a focus on $^{15}\text{N}/^{14}\text{N}$ ratios to elucidate the recent N-cycle in the Eastern Mediterranean Sea (EMS) (Chapter 3). I further use data on the isotopic composition of N in conjunction with amino acid composition (reflecting the state of degradation of organic matter) of sinking particulate nitrogen (sediment traps), surface sediments and sediment cores to gauge the use of $\delta^{15}\text{N}$ as a paleoceanographic tool in recent sediments and sediment cores of the EMS and the Arabian Sea (Chapters 4 and 5).

Unusually low $\delta^{15}\text{N}$ values in many compartments of reactive N in the extremely nutrient poor EMS have been attributed to diazotrophic N_2 fixation - although observational evidence is scarce and the surplus of nitrate over phosphate (N to P ratios up to 28) in deep and intermediate waters argue against the biogeochemical need of N_2 fixation. Isotope data raised on major N species involved in the cycling of reactive N (NO_3^- , total dissolved reduced N, suspended particulate N and sinking particulate N) in the EMS during winter/early spring of 2007 are discussed and modeled in Chapter 3. Analytical and model results suggest that recycled NO_3^- from nitrification of sinking particulate N produced in the surface mixed layer is the most likely source of NO_3^- during the winter sampling. Additionally, a strong imprint of atmospherically deposited nitrous oxides of industrial origin in Europe on the $\delta^{15}\text{N}$ of the mixed layer NO_3^- is indicated.

The paleoceanographic application of $\delta^{15}\text{N}$ as a proxy is generally hampered by an early diagenetic overprint of the signal formed in the ocean surface mixed layer that occurs during particle sinking and after sedimentation. In Chapter 4 and 5, I quantify the effect of early diagenetic alterations on sedimentary N-isotope composition in order to reconstruct the pristine signal of N assimilated in the euphotic zone of the EMS (Chapter 4) and the Arabian Sea (Chapter 5) during the Holocene and late Pleistocene. This is possible by using paired data of $\delta^{15}\text{N}$ and amino acid composition, which can be applied to estimate the degree of organic matter degradation. The normalized records for the EMS reveal that millennial scale oscillations in $\delta^{15}\text{N}$, and its spatial gradients in organic rich layers (sapropels) are driven mainly by differences in preservation under oxygen-poor and oxygen-replete bottom water conditions. The EMS study gives further evidence that enhanced organic carbon accumulation in the youngest sapropel S1 may be due to better preservation under suboxic to anoxic conditions at the sediment-water interface, and to a lesser extent to elevated productivity.

In the Arabian Sea $\delta^{15}\text{N}$ records, millennial scale oscillations are mainly controlled by changes of the $\delta^{15}\text{N}$ of assimilated source nitrate; these changes are to a large extent caused by

external climatic variability in the monsoon dynamics and associated circulation of the intermediate water masses in the Arabian Sea, which in turn determine oxygen levels in mid-water and nitrate isotopic composition. Most of the $\delta^{15}\text{N}$ amplitude in spatial patterns of surface sediments and isochronous time slices in sediment cores can be attributed to differences in preservation of the original $\delta^{15}\text{N}$ signal exported from the sea surface. An evaluation of two preservation indexes based on amino acid composition (Reactivity Index, RI, and Degradation Index, DI) in both recent sediments and core samples from the Arabian Sea suggest that the RI is more suitable than the DI in estimating the state of organic matter degradation in core sediments that have undergone progressive degradation. The relationship between $\delta^{15}\text{N}$ and the RI allowed a reconstruction of the original $\delta^{15}\text{N}$ prior to diagenetic overprinting.

Contents:

Zusammenfassung	i
Abstract	iii
Contents	v
1. Introduction	1
2. Working areas, projects and thesis outline	7
3. N-isotope ratios of nitrate, dissolved organic nitrogen and particulate nitrogen in the Eastern Mediterranean Sea	11
4. Diagenetic control of nitrogen isotope ratios in Holocene sapropels and recent sediments from the Eastern Mediterranean Sea	39
5. Influence of diagenesis on sedimentary $\delta^{15}\text{N}$ in the Arabian Sea over the last 130 kyr	59
6. Conclusions and outlook	83
Acknowledgements	86
Figure captions	87
Table captions	91
List of abbreviations	93
References	94
Curriculum Vitae	110

1. Introduction

1.1. The marine nitrogen cycle

Reactive inorganic nitrogen, together with carbon and phosphorus, is the most important nutrient for plant growth. In marine phytoplankton and in seawater these nutrients occur in the so called Redfield-Ratio of 106 C : 16 N : 1 P, implying an equilibrium and that nutrient availability in this proportion promotes optimal growth (Redfield, 1934). Whereas carbon is assimilated from the abundant atmospheric pool and from CO₂ dissolved in seawater, atmospheric dinitrogen (N₂) is bioavailable only for specialized prokaryotes containing the enzyme nitrogenase (diazotrophic N₂ fixation; e.g., Sprent and Sprent, 1990); for other primary producers it has to be present as nitrate (NO₃⁻), nitrite (NO₂⁻), ammonium (NH₄⁺), or dissolved organic nitrogen (DON) to be assimilated. Hence, either phosphate or reactive N limit primary production in large parts of the ocean (e.g., Tyrell, 1999), and only in specific areas production is limited by micronutrients such as iron (e.g., Martin et al., 1990).

Whereas supply of phosphate to the ocean is governed by external inputs and internal recycling (Benitez-Nelson, 2000), nitrate supply and turnover in the ocean is considerably more complex. A schematic overview of the marine N-cycle is given in Figure 1.1 and briefly explained in the following paragraph.

The major source of reactive N in marine systems is atmospheric N₂ that is fixed as NH₄⁺ and further assimilated to organic N. Detrital organic N will either (i) settle through the water column to the sediment, be buried and taken out of the marine N cycle, or (ii) be remineralized to NH₄⁺ (ammonification) during organic matter breakdown in the water column or in the sediment. NH₄⁺ is either oxidized (by nitrification) in several intermediate steps to NO₃⁻ (which is the most important bioavailable N species and the largest oceanic pool of reactive N), or assimilated and again transformed to organic N. Residual NO₃⁻ remains in the oxic water column/sediment, or is reduced to NO₂⁻ (denitrification) under oxygen-deficient conditions in the water column or in the sediment. NO₂⁻ is either (i) assimilated to organic N, or (ii) a reactant of the anammox reaction and is transformed to N₂, or (iii) is reduced to N₂ via NO and N₂O (denitrification). Gaseous species such as N₂O and N₂ will be either fixed and assimilated, or released to the atmosphere and leave the marine N-pool. Note that all transformations in the marine N-cycle are biologically mediated processes. For an in-depth description of the intricacies of the natural N cycle, the reader is referred to Canfield et al. (2005).

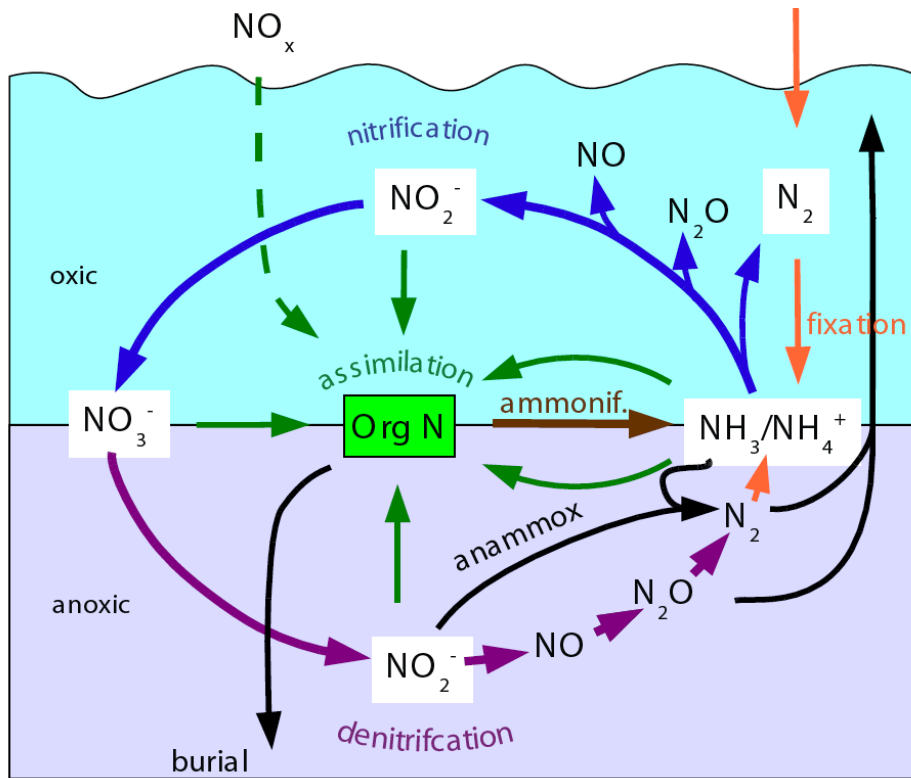


Figure 1.1: The marine nitrogen cycle

On a global scale and over time scales of centuries to decades, natural sources and sinks of marine bioavailable N species should be in equilibrium (e.g., Codispoti et al., 2001). Diazotrophic N_2 fixation and terrestrial/riverine inputs (the major sources) are balanced with N-loss during denitrification and nitrification, and burial of particulate N in the sediment (e.g., Brandes and Devol, 2002), although this balance has recently been questioned (e.g., Codispoti et al., 2001; Codispoti, 2007). Over the last decades, anthropogenic input of fertilizers via rivers and atmospheric total nitrogen inputs (NO_x) became important contributors (Galloway et al., 2003; Duce et al., 2008); they derive from industrial fixation of atmospheric N_2 in the Haber-Bosch process and fossil fuel burning that annually introduce $125 \cdot 10^6$ Tg of reactive N in addition to natural sources (Gruber and Galloway, 2008).

Because the marine N-cycle determines the magnitude of the organic carbon pump in the ocean, it is an important variable in validating and budgeting global variations of atmospheric CO_2 concentrations (Gruber and Galloway, 2008). Another link to global climate is given by the powerful greenhouse gas properties of N_2O (e.g., Badr and Probert, 1993).

1.2. Stable N-isotopes ($\delta^{15}\text{N}$) - use as a proxy

The two stable isotopes of nitrogen, ^{14}N and ^{15}N occur in natural abundances of 99.6337 atomic% ^{14}N and 0.3663 atomic% ^{15}N in atmospheric N_2 . The ratio (R) of both isotopes is expressed in relation to a standard as $\delta^{15}\text{N}$:

$$\delta^{15}\text{N} (\text{‰}) = \frac{(R_{\text{sample}} - R_{\text{standard}})}{R_{\text{standard}}} * 1000 \quad R = \frac{^{15}\text{N}}{^{14}\text{N}} \quad (1.1)$$

The standard is atmospheric N_2 , defined as $\delta^{15}\text{N} = 0 \text{‰}$ (Mariotti et al., 1981).

As the ^{15}N atom is heavier than the ^{14}N atom and its vibrational frequencies are lower, its molecular bonds are stronger and molecules containing ^{15}N are usually less reactive than those containing ^{14}N . This leads to a slight discrimination against ^{15}N , in every non-equilibrium transformation in the N-cycle (N_2 -fixation, $\text{NH}_4^+/\text{NO}_2^-/\text{NO}_3^-$ assimilation, ammonification, nitrification, denitrification, anammox). An exception of the ^{14}N preference is an inverse fractionation occurring during the nitrite oxidation step (NO_2^- to NO_3^-) of nitrification (Casciotti, 2009). According to the “normal” ^{14}N preference, residual substrate of any reaction (e.g., NO_3^- that is not assimilated) becomes enriched in ^{15}N , whereas the product (assimilated N) is depleted in ^{15}N compared to the substrate. In a closed system the accumulated product and substrate will have the same isotopic composition after complete turnover. This “Rayleigh”-type called fractionation process is schematically illustrated in Figure 1.2, using the example of NO_3^- assimilation in a closed system.

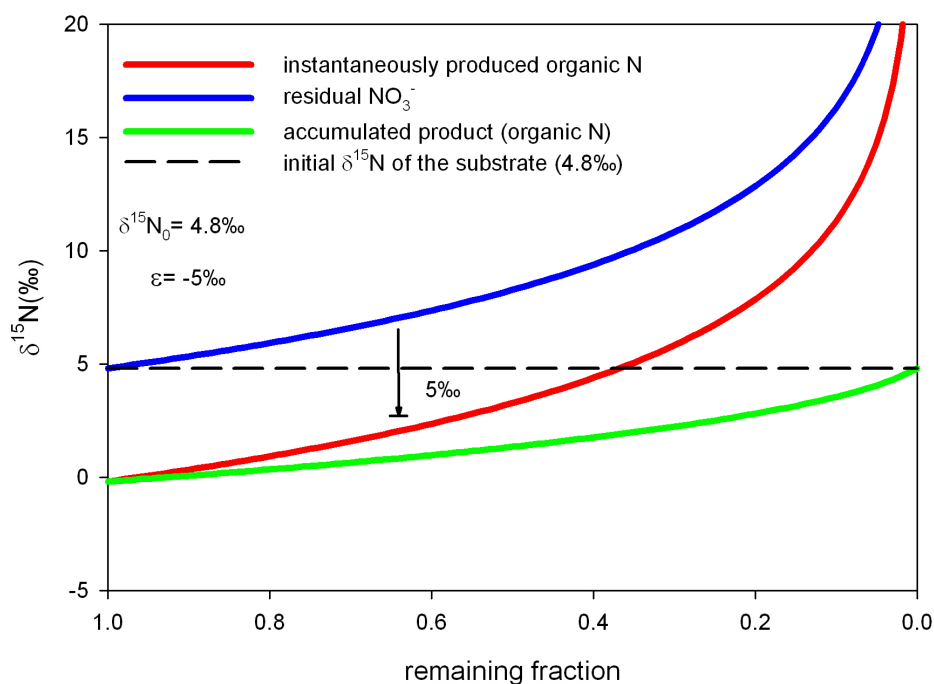


Figure 1.2: Rayleigh fractionation during NO_3^- assimilation in a closed system

Chapter 1

The degree of fractionation is process-specific and fractionation factors ϵ for several processes in the N-cycle are listed in Table 1.1. ϵ is defined as $(R_{\text{product}}/R_{\text{substrate}} - 1) \cdot 1000$ and is approximated by the difference in $\delta^{15}\text{N}$ between the substrate and the initial instantaneous product. The preference for ^{14}N or ^{15}N is expressed by negative values, if the lighter isotope is preferred. Variability in ϵ is driven by physical parameters such as diffusivity and exchange rates of pore waters, availability of the substrate, and biological factors related to enzymatic and “vital” effects of organisms and assemblages of microorganisms involved.

Table 1.1: Fractionation factors ϵ for major transformation processes in the marine N-cycle. ^{14}N preference is expressed by negative values. ϵ -values for the anammox process have not been published yet; the published ϵ of 0‰ for ammonification (Kendall, 1998) appears unrealistic considering this study.

Process	Reaction	Fractionation factor ϵ (‰)	Reference
N_2 fixation	$\text{N}_2 \rightarrow \text{NH}_4^+$	0 to -3.6	Carpenter et al., 1997 Brandes and Devol 2002
Ammonification	$\text{N}_{\text{org}} \rightarrow \text{NH}_4^+$	0	Kendall, 1998
NO_3^- assimilation	$\text{NO}_3^- \rightarrow \text{N}_{\text{org}}$	-6 to -20	Granger et al., 2004
NH_4^+ assimilation	$\text{NH}_4^+ \rightarrow \text{N}_{\text{org}}$	-11 to -14	Hoch et al., 1992 Voss et al., 1997
Nitrification (Ammonium oxidation)	$\text{NH}_4^+ \rightarrow \text{NO}_2^-$	-14 to -38	Casciotti et al., 2003
Nitrification (Nitrite oxidation)	$\text{NO}_2^- \rightarrow \text{NO}_3^-$	+12.8	Casciotti, 2009
Denitrification	$\text{NO}_3^- \rightarrow \text{N}_2$	-22 to -30	Brandes et al., 1998
Anammox	$\text{NO}_2^- + \text{NH}_4^+ \rightarrow \text{N}_2$?	

As a consequence, each N-pool has a specific isotopic signature (Table 1.2.) resulting from the balance of source and sink terms and their isotopic fractionation.

Table 1.2: Isotopic signatures of selected N-pools

Source	$\delta^{15}\text{N}$ (‰)	Reference
Atmospheric N_2 - fixed N	0	Mariotti et al., 1981
Atmospheric NO_x	-15 to 15	Kendall et al., 2007
Global ocean deep water NO_3^-	5 ± 0.5	Sigman et al., 2000
Pristine rivers NO_3^-	-0.1 to 5	Mayer et al., 2002 Voss et al., 2006
Polluted rivers NO_3^-	5 to 22	Mayer et al., 2002 Voss et al., 2006 Johannsen et al., 2008

Fractionation during N transformation processes often modifies original source values. If known, the $\delta^{15}\text{N}$ values can be used as a proxy to trace N sources and turnover processes in core records archiving past geological conditions, or to budget recent N-cycles. Systematic relationships to other proxies can help to evaluate and quantify the impact of transformation processes on $\delta^{15}\text{N}$.

Degradation of organic matter (OM) is a pathway of ammonification in a broader sense that is usually accompanied by an enrichment in $\delta^{15}\text{N}$ resulting from preferential loss of ^{15}N depleted compounds (Altabet, 1996; Freudenthal et al., 2001; Gaye-Haake et al., 2005) during protein hydrolysis (Bada et al., 1989; Silfer et al., 1992) and deamination (Macko and Estep, 1984). In this study I investigate and define the relationship between OM degradation and ^{15}N enrichment in particulate N using paired data of $\delta^{15}\text{N}$ and different indexes based on the amino acid composition of the samples that are sensitive for OM degradation.

1.3. The use of amino acid composition as a proxy for organic matter preservation

Amino acids (AAs) are the building blocks of proteins and are ubiquitous in the OM preserved in marine sediments. As they are differentially degraded during OM decay, changes in the concentration of individual AAs and changes in the overall AA composition can be used as indicators for the degree of OM degradation in younger sediments (Cowie and Hedges, 1992; Dauwe and Middelburg, 1998). To gauge the OM degradation status from AA, molar contributions of individual AA to total AA are expressed by two indexes that have been established over the last ten years: (i) the Reactivity Index (RI; Jennerjahn and Ittekkot, 1997), which is calculated as the ratio of aromatic to non-proteinogenic AAs (the latter do not exist in living organic tissue but enrich during OM decay), and (ii) the Degradation Index (DI; Dauwe et al., 1999) derived from a statistical treatment (principal component analysis) of data sets of 14 individual AAs. The DI will be introduced in Chapter 4 and both indexes will be introduced and discussed in detail in Chapter 5.

As shown by the linear relationship between the DI and $\delta^{15}\text{N}$ in surface sediments and sinking particles from the Arabian Sea and from the South China Sea (Gaye-Haake et al., 2005; Gaye et al., 2009), decomposition of AA goes in concert with an enrichment of $\delta^{15}\text{N}$ in the residual OM fraction. This systematic relationship will be used in the following to correct the $\delta^{15}\text{N}$ record of sediment cores for early diagenetic enrichment.

2. Working Areas, Projects and Thesis Outline

2.1. The Mediterranean Sea – a natural laboratory

The Mediterranean Sea is the smallest ocean - or the biggest enclosed marine basin in the world. Relatively low exchange rates with the Atlantic Ocean, low concentration levels of nitrate and phosphate, and the relatively fast turn over rates of limiting nutrients (as characteristic for oligotrophic environments) make it an ideal place to study the impact of man-made and natural environmental changes on external and internal nitrogen cycling on short time scales. Atmospheric deposition of anthropogenic NO_x increased by factor five to six since the 1920s (Preunkert et al., 2003) and presently is considered to be the largest individual source of reactive N that has changed the N inventory and N cycling of the Eastern Mediterranean Sea (EMS) dramatically (Mara et al., 2009). The relative contribution of this new source to the reactive nitrate pool in the mixed layer and the recycling rates of fixed N are calculated in Chapter 3 by budgeting the $\delta^{15}\text{N}$ of major involved N species.

For the past, repetitive deposition of organic rich sediment layers (sapropels) gives evidence of dramatic changes in circulation patterns and nutrient cycling of the EMS (e.g., Emeis and Weissert, 2009). It is widely accepted that Mediterranean sapropel formation is a result of water column stratification and anoxic deep water conditions that developed as a consequence of enormous fresh water inputs (e.g., Kullenberg, 1952; Cita et al., 1977). In most cases, these were caused by northward shifts of the African monsoon belt (into the catchment area of the Mediterranean Sea) that are driven by variations in solar radiation in the 23 kyr precession mode of the Milankovitch cycles (Rossignol-Strick et al., 1982; 1983; Rossignol-Strick, 1985). To what proportion enhanced productivity (as a consequence of enhanced nutrient supply; e.g., Calvert et al., 1992) or preservation (due to the absence of oxygen in deep water; e.g., Cheddadi and Rossignol-Strick, 1995) were responsible for OM accumulation is unclear. In the framework of the European Science Foundation (ESF) project MERF (Marine Ecosystem Response to Fertilization), my project attempted to develop and calibrate $\delta^{15}\text{N}$ as a proxy for nitrogen cycling and nitrate utilization in order to trace the impact of recent anthropogenic fertilization and to explore temporal and spatial gradients in the possibly natural fertilized S1 sapropel (the most recent) time slice (Chapter 4).

2.2. The Arabian Sea – a key area of the global N-cycle

In contrast to the EMS, the Arabian Sea is one of the most productive areas in the world ocean. Monsoon induced upwelling of nutrient-rich intermediate water to the euphotic zone seasonally arises primary productivity up to more than $1.5 \text{ g C} \cdot \text{m}^{-2} \cdot \text{d}^{-1}$ (Barber et al., 2001). Due to the remineralization of high export production flux in mid-water and oceanographic processes, oxygen levels in subsurface waters and intermediate waters almost drop to zero resulting in a permanent oxygen minimum zone (OMZ) roughly between 200 m and 1200 m water depth in the central Arabian Sea (Wyrski, 1971). As a consequence, large amounts of NO_3^- are reduced to N_2O and N_2 by denitrifying and anammox bacteria and are no longer bioavailable in the marine N-cycle (Naqvi, 1994; Jaeschke et al., 2007). Accordingly, the Arabian Sea is both an important source of the greenhouse gas N_2O and an important sink of fixed marine N. Orbitally driven and millennial-scale oscillations in monsoon intensity alter the OMZ in extent and intensity; this is reflected for instance in sedimentary TOC and $\delta^{15}\text{N}$ records (Altabet et al., 1995; Schulz et al., 1998). My investigation aimed to appraise the diagenetic and environmental influences on $\delta^{15}\text{N}$ in basin-wide surface sediments and in core records of the last 130 kyr from various locations in the Arabian Sea (Chapter 5).

The following individual chapters of this thesis constitute the basis of 3 articles that are under review in, or submitted to peer-reviewed scientific journals:

Chapter 3

Emeis, K.-C., Mara, P., Schlarbaum, T., Möbius, J., Dähnke, K., Struck, U., Mihalopoulos, N. and Krom, M.,: **N-isotope ratios of nitrate, dissolved organic nitrogen and particulate nitrogen in the Eastern Mediterranean Sea.** Under review in *Journal of Geophysical Research – Biogeochemistry*

My contribution to Chapter 3 (Emeis et al., under review):

- recovery, analysis and interpretation of suspended matter samples and sediment trap samples (MID 03)
- determination of stable isotope pairs $^{15}\text{N}/^{14}\text{N}$ and $^{18}\text{O}/^{16}\text{O}$ in NO_3^- (part of the data set).
- Co-work in discussion and manuscript preparation

Chapter 4

Möbius, J., Lahajnar, N. and Emeis, K.-C., 2010: **Diagenetic control of nitrogen isotope ratios in Holocene sapropels and recent sediments from the Eastern Mediterranean Sea.** *Biogeosciences Discussions* 7, 1131-1165.

Chapter 5

Möbius, J., Gaye, B., Lahajnar, N., Bahlmann, E. and Emeis, K.-C.,: **Influence of diagenesis on sedimentary $\delta^{15}\text{N}$ in the Arabian Sea over the last 130 kyr.** Submitted to *Marine Geology*

3. Isotope Ratios of Nitrate, Dissolved Reduced and Particulate Nitrogen in the Eastern Mediterranean Sea Trace External N-inputs and Internal N-cycling

Abstract

The eastern Mediterranean Sea (EMS) is an unusually nutrient-poor ocean basin where the $^{15}\text{N}/^{14}\text{N}$ isotope ratios in many compartments of reactive N are lower than in comparable oceanic settings. To elucidate possible reasons, we determined stable isotope ratios in nitrate, suspended particulate, total dissolved reduced nitrogen, and sinking particulate N for stations across the Eastern Mediterranean Sea (EMS) occupied in January and February 2007. The absolute level of $\delta^{15}\text{N}$ integrated over all reactive N compartments in waters of the EMS is very low (grand average 2.6‰) compared to other oceanic environments. The $\delta^{15}\text{N}$ of deep-water nitrate was lower than nitrate generally found in the global ocean, whereas the $\delta^{15}\text{N}$ of particulate N and reduced dissolved N was significantly higher than that of nitrate and particulate N intercepted in sediment traps. We infer that extensive mineralisation is the immediate cause of the isotopic makeup of reactive N in deep water. Partial nitrate assimilation in the mixed layer had reduced concentrations and raised $\delta^{15}\text{N}$ and $\delta^{18}\text{O}$ in nitrate, but an additional external source of nitrate with a low $\delta^{15}\text{N}$, probably anthropogenic NO_x rather than fixed nitrogen, was required to describe the isotope distribution adequately. To explain the observed nitrate isotope anomaly $\Delta(15,18)$ in the mixed layer, either the ammonium formed by OM breakdown must be predominantly nitrified, or atmospheric NO_x with characteristically high $\delta^{18}\text{O}$ was present.

3.1. Introduction

The modern Eastern Mediterranean Sea (EMS) is a highly oligotrophic oceanic environment (Béthoux, 1989; Antoine et al., 1995) where primary production is approximately half the values observed in the mid-ocean gyres such as the Sargasso Sea or the Northeast Pacific (Krom et al., 2003). This low productivity is caused by the anti-estuarine circulation in the EMS: Modified Atlantic Water (MAW) flows in through the Strait of Sicily at the surface, sinks in the eastern part of the EMS and feeds the Levantine Intermediate Water (LIW), a high temperature, high salinity water mass at depths between 200 and 500 m that leaves the EMS as a westward current through the Strait of Sicily. This intermediate water mass collects and exports the bulk of mineralisation products sinking out of the mixed layer. Below (>500 m) this surface circulation cell is the Eastern Mediterranean Deep Water (EMDW) (Wüst, 1961; Malanotte-Rizzoli and Bergamasco, 1989) which forms when LIW entrained into surface waters of the two northern sub-basins (Aegean or Adriatic Seas) gains sufficient density after winter cooling (Lascaratos et al., 1999).

The export of nutrients with LIW causes the deep waters of the EMS to be nutrient depleted relative to the deep water in all other parts of the global ocean: Nitrate concentrations in EMDW are 4-6 μM compared to 8 μM in deep water of the adjacent Western Mediterranean Sea, and 20 μM at similar depths in the Atlantic Ocean. The EMS is also unusual in that it has a high nitrate:phosphate ratio (28:1) in the deep water (Krom et al., 1991) and is phosphate-starved (Krom et al., 2005a). As a result, primary production during the winter phytoplankton bloom is limited by phosphate rather than by nitrate (Krom et al., 1991). In winter, the phosphate in the surface water is entirely depleted while excess nitrate remains (Kress and Herut, 2001). However, soon after the seasonal thermocline develops in spring, both nitrate and phosphate become depleted in the photic zone (Kress and Herut, 2001; Krom et al., 2005b) and phytoplankton productivity becomes N- and P- co-limited (Thingstad et al., 2005; Zohary et al., 2005).

Another unusual feature of the EMS is the low $\delta^{15}\text{N}$ levels of deep-water nitrate, suspended matter, and surface sediments in the EMS (Struck et al., 2001; Pantoja et al., 2002; Coban-Yildiz et al., 2006) relative to values in other open-ocean environments. $\delta^{15}\text{N}$ expresses the ratio in the abundance of ^{15}N and ^{14}N in relation to that ratio (R) in a standard: $\delta^{15}\text{N}_{\text{sample}} = (\text{R}_{\text{sample}}/\text{R}_{\text{standard}} - 1) * 1000$ in ‰; the international standard being $\delta^{15}\text{N}_{\text{air N}_2} = 0$ ‰. The low levels of $\delta^{15}\text{N}$ in the EMS are unusual, and three possible reasons have been suggested. The first is incomplete nitrate utilisation (Altabet and Francois, 1994; Struck et al., 2001): Because most biological processes discriminate against ^{15}N , incomplete nitrate uptake during phosphate-limited assimilation by phytoplankton would result in products (such as particulate nitrogen, PN, or dissolved organic

nitrogen, DON) depleted in ^{15}N , while unprocessed residual nitrate would be enriched in ^{15}N over the original nitrate. Together, residue and products have the original nitrate signature, and establishing isotope fingerprints of all compartments is a tool to quantify individual processes in the N-cycle (Altabet, 1988). Establishing the relationships between mixed layer nitrate levels and its $\delta^{15}\text{NO}_3^-$ helps to decide if supply by deep winter mixing and subsequent nitrate utilisation governs isotopic compositions entirely, or alternatively to identify situations where other sources besides thermocline nitrate contribute to nitrate in the mixed layer.

One of the possible external sources that has been invoked to explain low $\delta^{15}\text{N}$ levels (and high N:P ratios) in the EMS is significant levels of diazotrophic N_2 fixation (Sachs and Repeta, 1999; Pantoja et al., 2002), because newly fixed nitrogen is isotopically depleted ($\delta^{15}\text{N} = -2$ to 0‰) (Minagawa and Wada, 1986; Montoya et al., 2002). This interpretation is in line with other authors' inference from N:P ratios that N_2 fixation is the most important source of new nitrogen to the EMS (Béthoux and Copin-Montegut, 1986; Gruber and Sarmiento, 1997; Mahaffey et al., 2005). At present, however, observational evidence for N_2 -fixation in the EMS is ambiguous (Rees et al., 2006; Berman-Frank et al., 2007; Ibello et al., in press), and annual input estimates range from nil (Krom et al., 2004) to $120 \cdot 10^9$ mol/a (Béthoux and Copin-Montegut, 1986), the latter estimate being $\sim 2/3$ of the total nitrate exported through the Straits of Sicily.

A third possible reason for low $\delta^{15}\text{N}$ levels is significant atmospheric NO_x input to the EMS that is bordered by heavily industrialised regions to the North and is a busy shipping route. This basin is distinct from other oligotrophic settings of the world ocean (Duce et al., 2008) in that atmospheric deposition of NO_x presently dominates the external nitrogen inputs (Krom et al., 2004; Mara et al., 2009). Furthermore, regional atmospheric loads have increased dramatically over the last decades (Kouvarakis et al., 2001; Preunkert et al., 2003; Fagerli et al., 2007), and the input of new nitrate from the atmosphere to the surface water mass of the EMS presently accounts for almost 60% of reactive N inputs (Krom et al., 2004; Mara et al., 2009). The atmospheric source (NO_3^- in dry and wet deposition) in the EMS has a low annually averaged (flux-weighted) $\delta^{15}\text{NO}_3^-$ of -3.1‰ (Mara et al., 2009) and thus is a strong candidate for depressing the $\delta^{15}\text{NO}_3^-$ levels in the EMS. Both N_2 fixation and atmospheric inputs have similarly low $\delta^{15}\text{N}$ signatures and cannot be separated based on $\delta^{15}\text{N}$. But whereas fixed N has to be oxidised to nitrate in the mixed layer, atmospheric NO_x is a preformed input of nitrate, and is known to have a high $\delta\text{N}^{18}\text{O}_3^-$ (Kendall, 1998; Sigman et al., 2009; Wankel et al., 2009).

The denitrifier method (Sigman et al., 2001; Casciotti et al., 2002) to simultaneously determine the $\delta\text{N}^{18}\text{O}_3^-$ and $\delta^{15}\text{NO}_3^-$, has provided the analytical tool to investigate global (Sigman et al., 2009) and regional (Lehmann et al., 2005; Sigman et al., 2005; Wankel et al., 2006; Casciotti et al., 2008; Knapp et al., 2008) N-cycles that involve internal oceanic sources and sinks. The largest source of nitrate to the oceanic mixed layer is thermocline nitrate. But in oligotrophic oceanic settings, nitrate regenerated from particulate nitrogen (PN) and possibly from dissolved organic nitrogen (DON) via ammonia and nitrite oxidation contributes significantly to primary production (Yool et al., 2007) and is thought to be particularly important in the oligotrophic Mediterranean Sea (Diaz and Raimbault, 2000). Nitrification imparts a characteristic isotopic signature on the $\delta\text{N}^{18}\text{O}_3^-$ and $\delta^{15}\text{NO}_3^-$ of regenerated nitrate (Casciotti et al., 2003; Wankel et al., 2006) that can be used to quantify the contribution of regenerated nitrate (Sigman et al., 2009). Regenerated nitrate can either derive from PN or DON (Bronk, 2002; Knapp et al., 2008). Should dissolved total reduced nitrogen (TRN, dissolved organic nitrogen and ammonia) indeed be a key component in the recycling of reactive N in the EMS (Thingstad et al., 2005), its isotopic composition must reflect active participation in the N-cycle (Knapp et al., 2005).

In this study, we determined the stable isotope ratios in nitrate ($\delta^{15}\text{NO}_3^-$, $\delta\text{N}^{18}\text{O}_3^-$), in dissolved total reduced nitrogen ($\delta^{15}\text{TRN}$, composed of $\text{DON}+\text{NH}_4^+$) and in particulate N ($\delta^{15}\text{PN}$) of both suspended particles obtained from filtration from the mixed-layer and deep-water pools for a set of 17 stations occupied in the EMS in 2007 (Figure 3.1). Furthermore, mass flux and $\delta^{15}\text{N}$ data of sinking particles intercepted by sediment trap moorings in several periods from 1999 to 2007 at one of the stations in the Ierapetra Gyre south of Crete are reported and discussed. Aims of this study are 1) to provide a comprehensive data set of $\delta^{15}\text{N}$ in several relevant N-pools of the water column, covering pelagic and more nearshore provinces of the EMS and different water masses; 2) to explain the processes which cause the unusual isotopic ratios in the deep water, and 3) to test if the unusually low levels of $\delta^{15}\text{N}$ are a consequence of incomplete nitrate utilisation in the euphotic zone of the EMS due to P-limited phytoplankton blooms, or if internal N-recycling or external inputs (N_2 fixation or NO_x inputs) are a significant source of mixed-layer nitrate.

3.2. Materials and methods

Samples were obtained during an expedition with r/v METEOR in 2007, which visited 17 stations in the EMS in January/February 2007 (Figure 3.1).

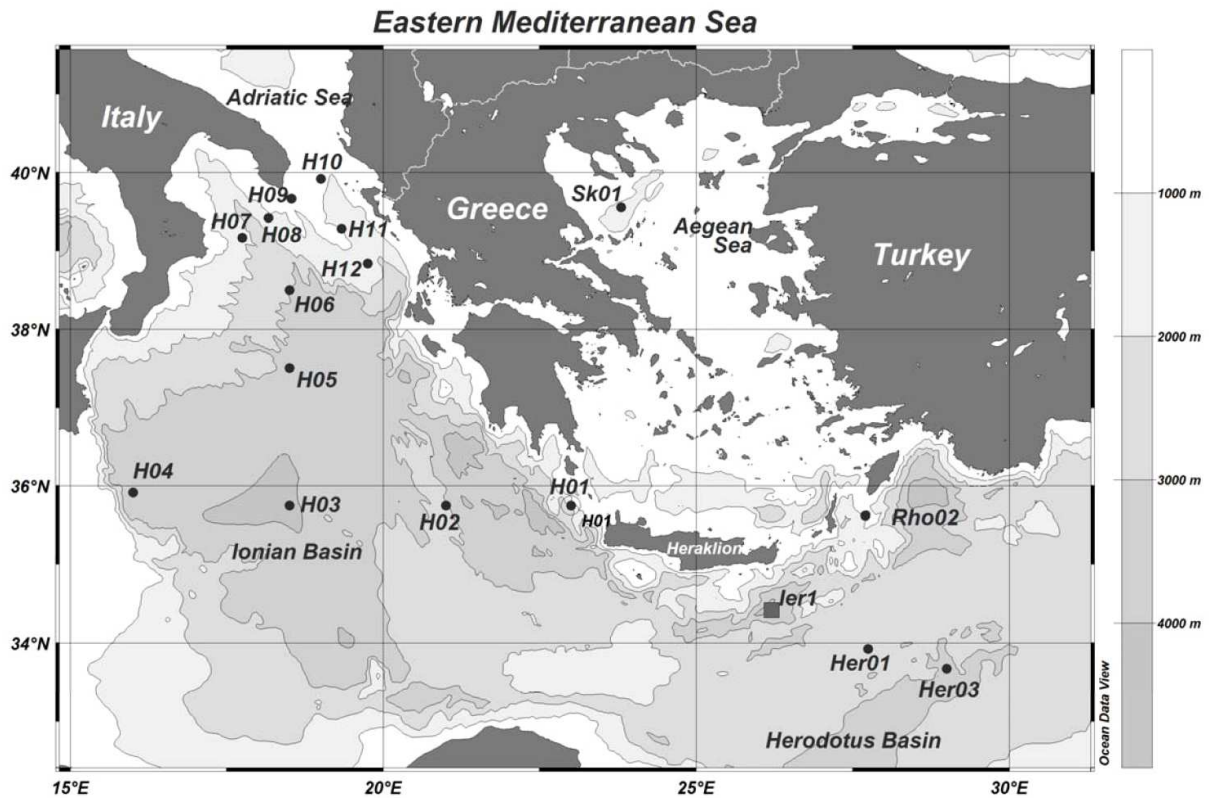


Figure 3.1: Map of stations occupied in the Eastern Mediterranean Sea during r/v Meteor cruise 71-3 (January-February, 2007). NIS stations referred to in the text are stations H07 to H12. The black square SE of Crete (water column sampling station Jer1) marks the location of the sediment trap deployment station (MID).

Water samples were taken with a rosette sampler equipped with a Seabird 911 CTD; an aliquot of the bottom water at the sediment-water interface was also taken from multicorer deployments. Water samples were immediately filtered through pre-combusted, rinsed GF/C filters and transferred into PE bottles for shore based analyses of nutrient concentrations, total dissolved nitrogen (TDN) content and N-isotopic signature ($\delta^{15}\text{TDN}$), and $\delta^{15}\text{N}/\delta^{18}\text{O}$ of nitrate ($\delta^{15}\text{NO}_3^-$ and $\delta\text{N}^{18}\text{O}_3^-$). Samples for nitrate isotope analysis were frozen on board ship for further analysis onshore, samples for TDN analysis were oxidised immediately after filtration on the ship with persulfate and then stored frozen in brown glass bottles until further analysis in the shore-based laboratory (Schlarbaum et al., in revision). Samples for nutrient analyses were poisoned with 3.5% mercury chloride solution and stored at room temperature. Nutrient and TDN concentrations were analysed immediately after the expedition using a Bran+Luebbe Autoanalyzer 2 in the home laboratory and standard colorimetric techniques (Grasshoff et al., 1999).

Large water samples (10-50 L) were filtered through pre-combusted and tared GF/F filters for analyses of total nitrogen concentrations in suspended solids (particulate nitrogen, PN), as well as for $\delta^{15}\text{N}$ of PN ($\delta^{15}\text{PN}$). Filters were frozen on board, lyophilised in the home laboratory and weighed before further analysis.

On January 29, 2007, a mooring system MID-03 (Mediterranean Ierapetra Deep) was deployed in the Ierapetra Deep off Crete ($34^{\circ}26.63'$ N, $026^{\circ}11.58'$ E, bottom depth 3620 m) (Figure 3.1). The system consisted of one sediment trap McLane PARFLUX MARK 7G-21 at 1508 m water depth (MID-03 Shallow) and one Kiel Sediment Trap K/MT 234 at 2689 m water depth (MID-03 Deep). The cups were filled with filtered (GF/F, combusted) sea water from the respective depths. In addition, 35 g l^{-1} NaCl and 3.3 g l^{-1} HgCl_2 were added in order to avoid diffusion and bacterial decomposition during the deployment. Sampling period started on 30 January 2007 and ended on September 03, 2007. The particle flux was sampled at intervals of 12 days and the mooring was recovered in September 2007. Subsequent to trap recovery, trapped materials were sieved into >1 and <1 mm fractions, the wet sample material was filtered onto pre-weighed nucleopore filters and dried at 40°C . The dry weights of the <1 mm fraction are used for calculating the total fluxes, and the filter cake was homogenised with an agate mortar prior to analysis. The same site has seen intermittent sediment trap deployments at 2700 m water depth in 1999 (30 January to 13 April, 1999) and in 2001/2002 (5 November 2001 to 1 April, 2002) (Warnken, 2003), and we use data from these earlier deployments to complement data obtained from the last trapping period.

The samples for determinations of $\delta^{15}\text{NO}_3^-$ and $\delta\text{N}^{18}\text{O}_3^-$ and $\delta^{15}\text{TDN}$ were thawed in the shore-based laboratory, and nitrate isotopic composition was determined with the denitrifier method (Sigman et al., 2001; Casciotti et al., 2002; Dähnke et al., 2008). The untreated filtered water samples or persulfate-digested TDN samples were injected into a suspension of *Pseudomonas aureofaciens* for combined analysis of $\delta^{15}\text{N}$ and $\delta^{18}\text{O}$, or *Ps. chlororaphis* for $\delta^{15}\text{N}$ analysis of TDN only. The resulting N_2O gas was flushed by purging the sample vials with helium, concentrated and purified on a GasBench II (ThermoFinnigan), and analyzed on a Delta Plus XP mass spectrometer (ThermoFinnigan). To avoid concentration-dependent fractionation effects, sample size in deep and thermocline water samples was adjusted to achieve a final gas amount of 10 nmol. Many mixed-layer samples, where nitrate concentrations were low, yielded smaller N_2O amounts. For each sample, replicate measurements were performed, and an international standard (IAEA-N3) was measured with each batch of samples; we used a $\delta^{15}\text{N}$ value of 4.7‰ and a $\delta^{18}\text{O}$ value of 25.6‰ for IAEA-N3 referenced to Standard Mean Ocean Water ($\delta^{18}\text{O}$ SMOW=0‰) (Böhlke et al., 2003; Lehmann et al., 2003; Sigman et al., 2005). The contribution of nitrite was always below one per cent and will

therefore not be considered further in our calculations, because the effect on $\delta^{18}\text{O}$ values is negligible (Casciotti and McIlvin, 2007). The standard deviation for IAEA-N3 was better than 0.2‰ ($n = 5$) for $\delta^{15}\text{NO}_3^-$ and better than 0.4‰ for $\delta\text{N}^{18}\text{O}_3^-$. For further quality assurance of the results, we used an internal potassium nitrate standard that was measured with each batch of samples. The standard deviation for the internal standard was within the same specification for both $\delta^{15}\text{N}$ and $\delta^{18}\text{O}$ as IAEA-N3. The duplicate analyses suggest an overall average standard deviation for $\delta^{15}\text{NO}_3^-$ of 0.2‰ and for $\delta\text{N}^{18}\text{O}_3^-$ of 0.3‰. The standard deviations of duplicate analyses of $\delta\text{N}^{18}\text{O}_3^-$ increased to of 0.5‰ in samples with low nitrate concentrations in the mixed layer and upper thermocline. The majority of 85 samples analysed from the mixed layer gave unacceptable standard deviations and are not reported.

For calculations of the $\delta^{15}\text{N}$ of total reduced nitrogen (TRN, the sum of DON and ammonia) mass balance calculations were made using the measured concentrations (c) of nitrate and TRN, and $\delta^{15}\text{TDN}$ values of the oxidised sample, the reagent blank and the $\delta^{15}\text{NO}_3^-$ of the original (not oxidised) sample (Knapp et al., 2005):

$$\delta^{15}\text{TRN} = \delta^{15}\text{TDN} * c(\text{TDN})/c(\text{TRN}) - [\delta^{15}\text{NO}_3^- * c(\text{NO}_3^-) + \delta^{15}\text{N}_{\text{Blank}} * c(\text{Blank})]/c(\text{TRN})$$

Because of low concentrations and error propagation, the calculated standard deviation of $\delta^{15}\text{TRN}$ analyses ranged from 0.2 to 2.0‰ with a mean value of 0.9‰, and the calculated mean standard deviation for TRN concentration was 1.7 μM . Note that $\delta^{15}\text{TRN}$ was not corrected for any contribution by ammonium. However, the only published data on ammonium from the EMS found values in the range of 40-80 nM with no major trend with depth (Krom et al., 2005a). In the same profiles the DON concentration was ~2-4 μM in deeper water, similar to the values measured in this study. It is thus likely that most of the isotopic signal is due to DON.

Total particulate nitrogen concentrations (PN) in suspended solids and in sinking material captured by the sediment trap (SPN) were analysed after high-temperature flash combustion in a Carlo Erba NA-2500 elemental analyzer at 1100°C (Rixen et al., 2000). $\delta^{15}\text{N}$ values were determined using a Finnigan MAT 252 gas isotope mass spectrometer coupled to an elemental analyzer. Pure tank N_2 calibrated against the reference standards International Atomic Energy Agency (IAEA)-N-1 and IAEA-N-2 was used as a working standard. The within-lab standard-deviation was found to be <0.2‰ based on a set of replicate measurements of 6 sediment samples (Bahlmann et al., 2009).

3.3. Results

3.3.1. Concentrations of N-bearing compounds

The study took place in winter when the water column at most stations was well mixed with a thermocline situated at depths of around 100m (stations H07 to H12 in the northern Ionian Basin, in the following abbreviated NIS, maximum water depth 1688 m, and station Sk01 in the northern Aegean Sea; see Figure 3.1) to 250 m (stations in the deep Ionian Basin, Ierapetra and Herodotus Basin, termed pelagic stations in the following) water depth.

Fluorescence profiles (Figure 3.2a) show elevated fluorescence (uncalibrated chlorophyll concentrations) in the surface mixed layer typical of the winter phytoplankton bloom observed in the EMS (Krom et al., 2003); these mixed layers were <100 m in the NIS station set and at station Sk01, and >200 m deep in pelagic stations (Figure 3.2b). Concentration versus depth plots of nitrate, phosphate, TRN and PN for all stations shown in Figure 3.3 in each of the individual station profiles showed that the thermocline (coincident with the base of the fluorescence increase) in all cases coincided with the nitracline. Based on the criterion of nitrate concentrations, we distinguished samples above the nitracline, in the nitracline, and deep-water samples below the nitracline for each station set (Table 3.1).

Nitrate concentrations were low but measurable in the mixed layers of both the NIS and the pelagic stations, while phosphate concentrations (Figures 3.3a,b and Table 3.1) were below the effective detection limit of the nutrient procedures being used (estimated to $0.05 \mu\text{mol}\cdot\text{L}^{-1}$) (Li et al., 2008). TRN concentrations varied around averages of $1.6 \mu\text{mol}\cdot\text{L}^{-1}$ in the mixed layer of NIS and pelagic stations, and $3.3 \mu\text{mol}\cdot\text{L}^{-1}$ in the northern Aegean (Figure 3.3c and Table 3.1). PN concentrations in the mixed layer of the NIS were on average $0.5 \mu\text{mol N}\cdot\text{L}^{-1}$ ($0.4 \mu\text{mol N}\cdot\text{L}^{-1}$ in the mixed layer of the pelagic stations, and $0.5 \mu\text{mol N}\cdot\text{L}^{-1}$ in the northern Aegean) (Figure 3.3d, Table 3.1).

Isotope ratios of nitrate, dissolved reduced and particulate N in the EMS

Table 3.1: Comparison of averages in water above, in and below the nitracline for samples taken in stations of the Northern Ionian Sea (6 stations, Table 3.1a), at pelagic stations (10 stations, Table 3.1b) and at one station in the northern Aegean Sea (Table 3.1c) in the EMS in January/February 2007 during Meteor expedition 71-3.

Table 3.1a: Average concentrations and isotopic composition/northern Ionian Sea stations

	Nitrate ($\mu\text{mol L}^{-1}$)	Phosphate ($\mu\text{mol L}^{-1}$)	TRN ($\mu\text{mol L}^{-1}$)	PN ($\mu\text{mol L}^{-1}$)	$\delta^{15}\text{N}$ nitrate (‰)	$\delta^{18}\text{O}$ nitrate (‰)	$\delta^{15}\text{TRN}$ (‰)	$\delta^{15}\text{PN}$ (‰)
<i>mixed layer above nitracline</i>								
average	0.48	0.02	1.6	0.5	5.6	10.7	-0.2	2.2
sd	0.32	0.01	0.8	0.1	2.7	7.1	1.8	1.1
n	24	24	24	3	11	7	2	3
range	0.06-0.97	0.01-0.04	0.6-3.5	0.4-0.6	1.0-9.9	3.1-21.5	-1.1-1.5	1.0-3.1
<i>in nitracline</i>								
average	3.55	0.1	1.5	n.d.	2.1	5.1	2.9	n.d.
sd	0.95	0.04	0.7		0.8	2.5	3.3	
n	14	14	14		13	10	7	
range	1.75-4.45	0.03-0.14	0.6-3.2		1.3-3.8	2.8-9.5	-2.4-6.6	
<i>below nitracline to total depth</i>								
average	4.49	0.16	1.4	0.2	2.0	3.2	2.4	7.9
sd	0.47	0.02	0.7	0.0	0.3	0.7	3.5	0.6
n	25	25	25	3	24	11	8	3
range	3.53-5.09	0.11-0.19	0.6-3.2	0.1-0.2	1.1-2.5	2.3-4.4	-1.4-7.7	7.3-8.4

Table 3.1b: Average concentrations and isotopic composition/pelagic stations

<i>mixed layer above nitracline</i>								
average	0.24	0.02	1.6	0.4	2.3	5.2	1.1	1.1
sd	0.26	0.01	1.1	0.1	3.4	0.0	1.1	0.5
n	57	57	56	24	3	2	2	23
range	0.03-0.93	0.01-0.04	0.8-5.4	0.2-0.5	0.1-6.3	5.2	0.8-2.4	0.1-2.4
<i>in nitracline</i>								
average	3.45	0.12	1.6	0.2	1.6	5.0	3.4	7
sd	1.44	0.06	1.6	0.1	0.5	1.4	3.5	0.7
n	21	20	20	10	20	13	9	10
range	0.93-5.53	0.02-0.21	0.6-7.0	0.1-0.3	0.6-3.3	2.8-7.2	0.6-12.2	6.0-8.1
<i>below nitracline to total depth</i>								
average	4.77	0.18	1.3	0.1	2.2	3.8	6.7	7.2
sd	0.45	0.02	0.7	0.1	0.3	0.8	3.5	0.8
n	52	52	52	21	47	14	33	20
range	3.76-5.98	0.13-0.22	0.5-3.6	0.0-0.4	1.3-2.9	2.4-5.5	1.1-14.4	5.2-8.5

Table 3.1c: Average concentrations and isotopic composition/North Aegean station

<i>mixed layer above nitracline</i>								
average	0.33	0.02	3.3	0.5	4.1	n.d.	-0.6	1.9
sd	0.31	0.01	0.3	0.0	2.6		n.d.	0.3
n	4	4	4	2	2		1	2
range	0.07-0.67	0.02-0.03	3.1-3.6	0.5-0.6	2.2-5.9			1.7-2.1
<i>in nitracline</i>								
average	2.27	0.1	3.6	0.2	2.0	4.4	2.8	7.7
sd	0.9	0.05	1.8	n.d.	0.4	2.3	0.8	n.d.
n	5	5	5	1	5	4	5	1
range	1.28-3.53	0.05-0.17	2.2-6.6	n.d.	1.6-2.5	2.7-7.7	2.2-4.0	n.d.
<i>below nitracline to total depth</i>								
average	4.7	0.23	3.6	0.1	2.3	n.d.	3.6	8.1
sd	0.11	0.01	0.8	0.0	0.1		1.3	0.3
n	3	3	3	2	3		3	2
range	4.61-4.82	0.22-0.24	2.7-4.2	0.1	2.2-2.4		2.1-4.5	7.8-8.3

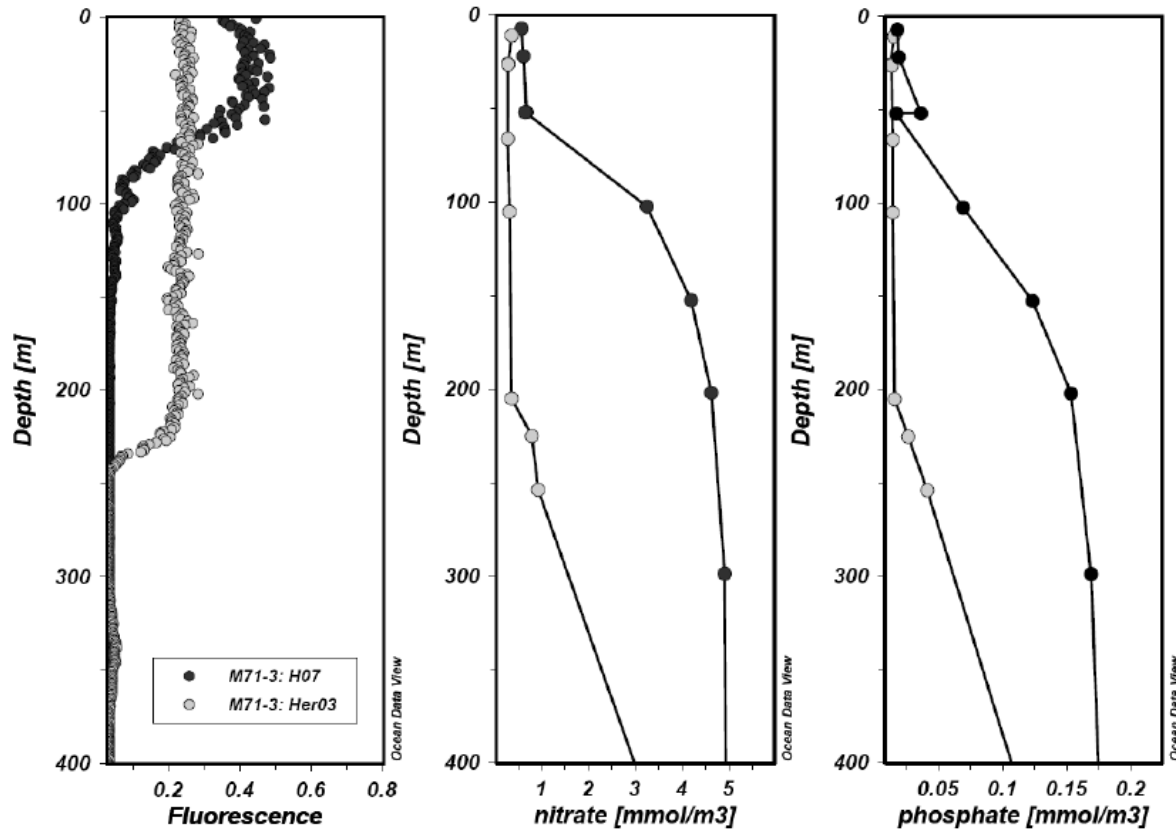


Figure 3.2: Profiles of fluorescence (a; arbitrary units), nitrate (b) and phosphate (c) concentrations in the upper 400 m at 2 stations representative of NIS (H07) and pelagic stations (Her03) show stratification between 80 and 230 m water depth and indicate the biologically active mixed layer. An ongoing phytoplankton bloom in the northern Ionian Sea (at station H07) is sustained by nitrate and phosphate provided from ongoing regional thermocline deepening, whereas station Her03 illustrates the mature and thick mixed layer with very low nutrient concentrations at pelagic sites.

The intermediate water mass had average nitrate concentrations around $3.5 \mu\text{mol}\cdot\text{L}^{-1}$ and average phosphate concentrations between 0.10 and $0.12 \mu\text{mol}\cdot\text{L}^{-1}$; the mean N:P in the intermediate water was around 30. TRN concentrations were around $1.5 \mu\text{mol N}\cdot\text{L}^{-1}$ in intermediate waters at NIS and pelagic stations, and $3.6 \mu\text{mol N}\cdot\text{L}^{-1}$ in Aegean station. The TRN concentrations in the intermediate water mass depth interval scatter widely due to measurement uncertainties at the low concentration levels measured. PN (not determined in the intermediate water mass of NIS stations) averaged $0.2 \mu\text{mol N}\cdot\text{L}^{-1}$ at both pelagic stations and the single northern Aegean station.

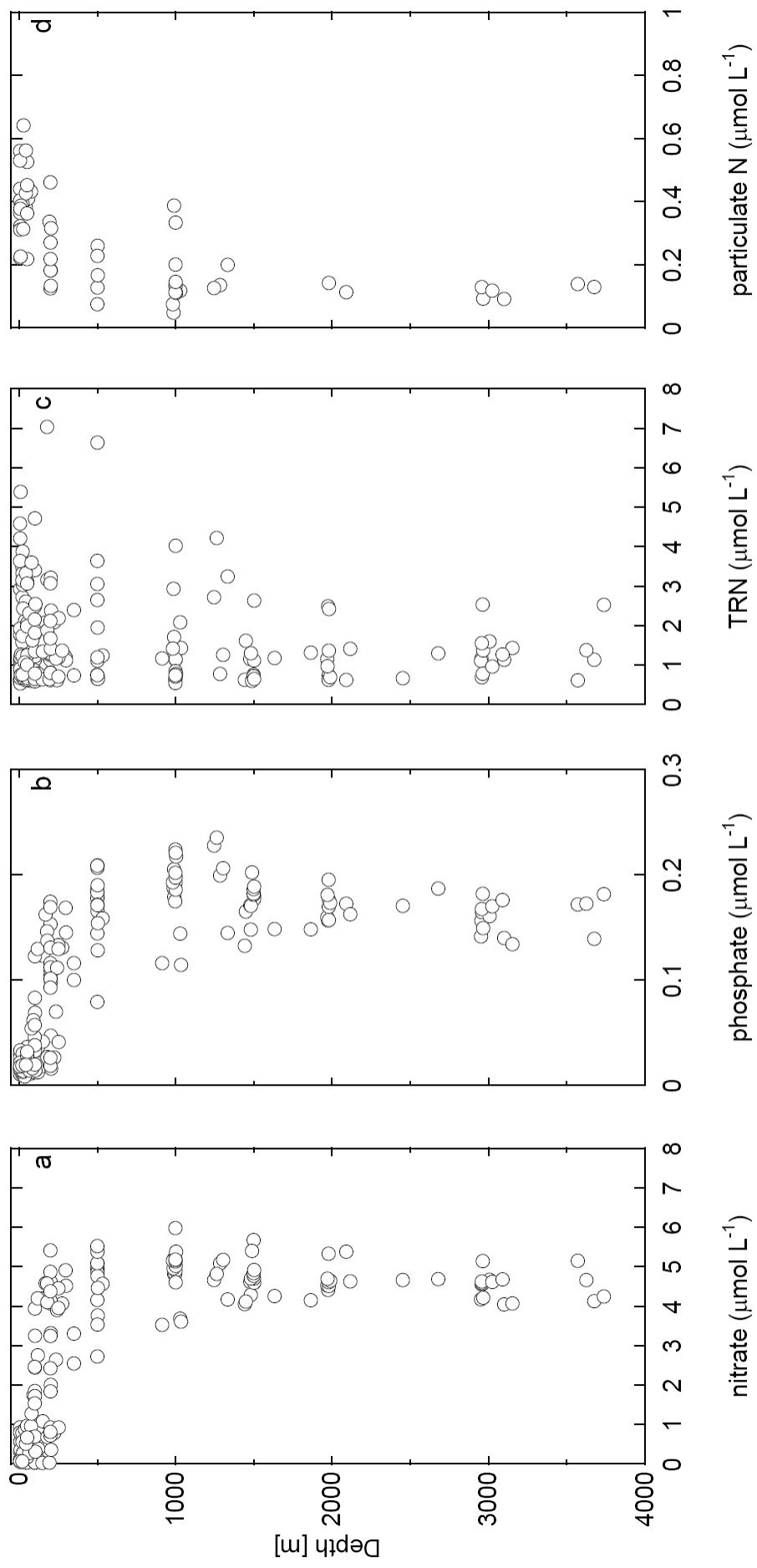


Figure 3.3: Concentrations of nitrate (a), phosphate (b), TRN (c) and particulate N in total suspended solids (d) plotted against water depth for all stations.

Concentrations of most dissolved and particulate constituents in samples below the nitracline to total depth were more uniform than in the biologically active surface (Figure 3.3; Table 3.1): Average nitrate (4.5 to $4.8 \mu\text{mol}\cdot\text{L}^{-1}$) and phosphate (0.16 to $0.23 \mu\text{mol}\cdot\text{L}^{-1}$) concentrations over all station sets resulted in an average N:P ratio of >27 , similar to previous measurements across the EMS (Kress and Herut, 2001). Average TRN concentrations varied around $1.3 \mu\text{mol N}\cdot\text{L}^{-1}$ in deep water at NIS and pelagic stations, but were elevated (average $3.6 \mu\text{mol N}\cdot\text{L}^{-1}$) in the northern Aegean. Average PN concentration was below $0.2 \mu\text{mol N}\cdot\text{L}^{-1}$ in all waters below the nitracline to total depth.

The two sediment traps deployed over 216 days from February to September 2007 at station Ierapetra (SE of Crete, Fig. 1) monitored a total SPN flux in the shallow trap (at 1500 m) of $5.7 \text{ mmol N m}^{-2}$ (or $26.3 \mu\text{mol N}\cdot\text{m}^{-2}\cdot\text{d}^{-1}$) over that period, while the deep trap (at 2700 m) collected $1.4 \text{ mmol N m}^{-2}$ ($6.5 \mu\text{mol N}\cdot\text{m}^{-2}\cdot\text{d}^{-1}$) of SPN over the same period. Earlier sediment trap deployments at the MID location (Warnken, 2003) reported similar N fluxes in the deep traps (MID-01, February to April 1999, $4.5 \mu\text{mol N}\cdot\text{m}^{-2}\cdot\text{d}^{-1}$; and MID-02, November 2001 to March 2002, $6.0 \mu\text{mol N}\cdot\text{m}^{-2}\cdot\text{d}^{-1}$); unfortunately, sampling in the shallower trap failed during those deployments.

3.3.2. Isotopic composition of N-bearing compounds

At all stations, the isotopic composition of N-bearing species differed not only between the mixed layer and the intermediate and deep water masses (Figure 3.4, Table 3.1), but also among station sets. Mixed-layer nitrate had average $\delta^{15}\text{NO}_3^-$ of 5.6‰ , 2.3‰ , and 4.1‰ at NIS, pelagic, and northern Aegean stations, respectively; $\delta\text{N}^{18}\text{O}_3^-$ was 10.7‰ at NIS stations, and 5.2‰ at pelagic stations; no sample yielded a reliable value in the northern Aegean (Table 3.1). Particulate N in the mixed layer was low ($\delta^{15}\text{PN}$ average of all stations = $1.3\pm 0.7\text{‰}$), and TRN in the surface layer (average $\delta^{15}\text{TRN}$ of all stations = $0.0\pm 1.1\text{‰}$) was roughly similar to PN in isotopic composition.

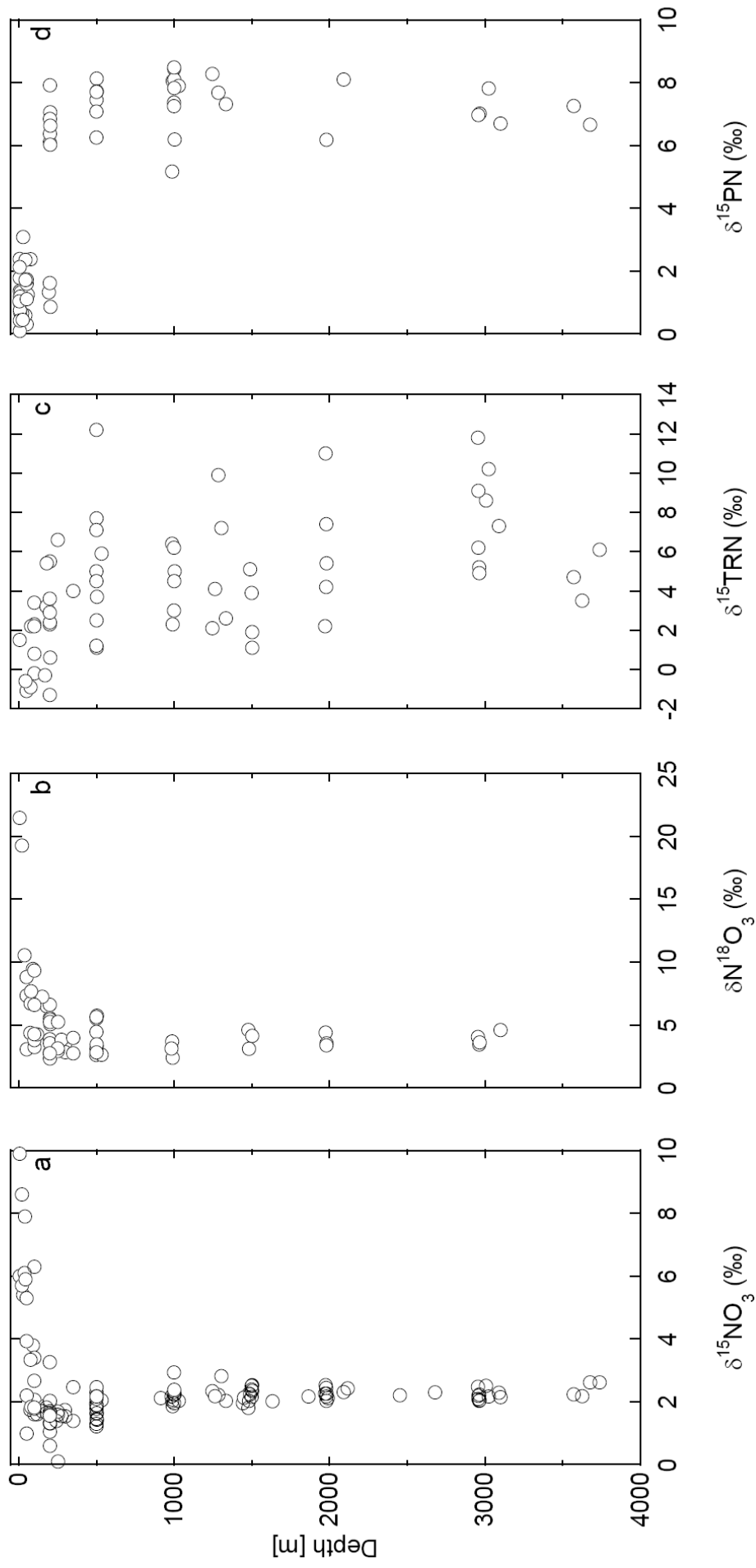


Figure 3.4: Isotopic composition $\delta^{15}\text{NO}_3^-$ (a), $\delta\text{N}^{18}\text{O}_3^-$ (b), $\delta^{15}\text{TRN}$ (c), and $\delta^{15}\text{PN}$ (d) plotted against water depth for all stations.

The average isotopic composition of nitrate in samples from the nitracline was similar in all station sets: $\delta^{15}\text{NO}_3^-$ averaged 1.6 and 2.1‰ in samples below the mixed layers of the pelagic and NIS stations, respectively, and 2.0‰ in the thick nitracline in the northern Aegean. $\delta\text{N}^{18}\text{O}_3^-$ of samples from the nitracline had averages of 5.1‰ (NIS stations), 5.0‰ (pelagic stations), and 4.4‰ in the northern Aegean nitracline. Values of $\delta^{15}\text{TRN}$ and $\delta^{15}\text{PN}$ were higher in the thermocline samples than in the mixed layer (Table 3.1).

In deep waters, $\delta^{15}\text{NO}_3^-$ averaged between 2.0‰ and 2.3‰ in the three stations sets, and $\delta\text{N}^{18}\text{O}_3^-$ was on average between 3.2‰ (NIS stations) and 3.8‰ for pelagic sites, respectively, and these deep water values were not statistically different. Suspended matter in deep waters at all sites had high $\delta^{15}\text{PN}$ averages of 7.2‰ to 8.1‰, while $\delta^{15}\text{TRN}$ measurements averaged between 2.4‰ and 6.7‰ over all sites. We attribute part of the high variability to measurement artefacts at the low concentrations encountered. Samples of deep waters below the nitracline at pelagic sites, where a relatively large sample pool was measured, had an average $\delta^{15}\text{TRN}$ of $6.7\pm 3.5\%$ (Table 3.1).

The $\delta^{15}\text{SPN}$ of material captured by the two sediment traps during the deployment in 2007 (MID-03) differed significantly from $\delta^{15}\text{PN}$ of suspended matter collected by filtration in deep water, and was essentially the same as PN found in the mixed layer during the expedition: The upper trap had an average $\delta^{15}\text{SPN}$ of $0.9\pm 0.8\%$ within the 216 days sampling period (1.0‰ flux weighted), whereas the lower trap average $\delta^{15}\text{SPN}$ was $0.8\pm 1.0\%$. This is somewhat lower than $\delta^{15}\text{SPN}$ for the 1999 deployment (MID-01; $\delta^{15}\text{SPN} = 2.2\pm 0.4\%$), but is in agreement with data from trap MID-02 (deployment 2001/2002) that collected sinking particles with a mean $\delta^{15}\text{SPN}$ of $1.2\pm 0.6\%$ (Warnken, 2003). Together the three deployments cover a period from November to October, and thus the biologically active season for which we can expect the bulk of particle transport out of the mixed layer to occur. In a composite annual cycle constructed from all three deployments at 2700 m water depth (Figure 3.5, Table 3.2), SPN- flux peaks in March, whereas highest $\delta^{15}\text{SPN}$ (1.8‰) are indicated for the months of November and December. In general, seasonality in $\delta^{15}\text{SPN}$ is subdued and varies around an annual average of 1.1‰ with low values from April to May (0.3-0.5‰) and higher values (1.2–1.8‰) later in the year from June to December.

Isotope ratios of nitrate, dissolved reduced and particulate N in the EMS

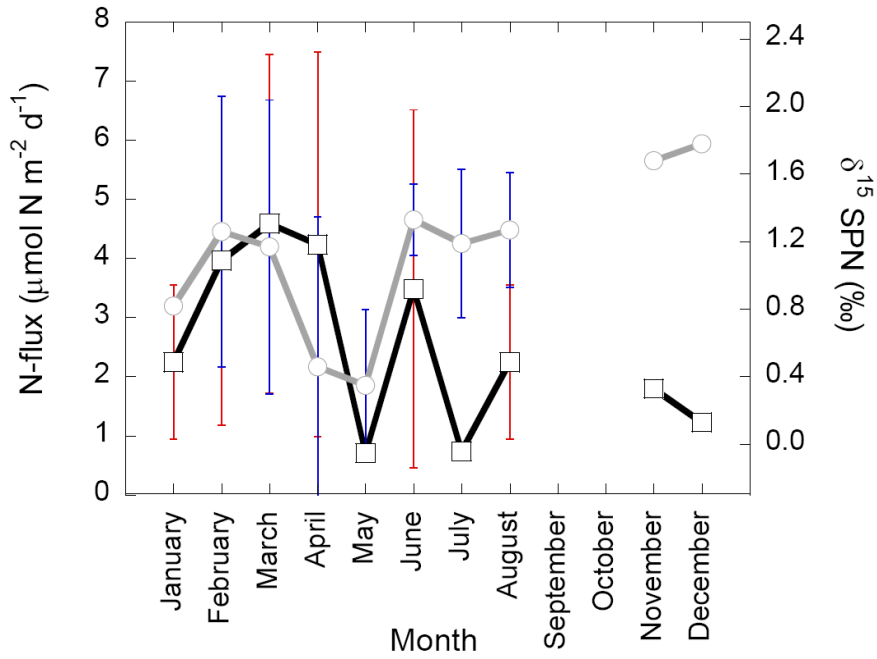


Figure 3.5: Composite seasonal diagram of SPN fluxes (squares) and $\delta^{15}\text{SPN}$ (circles) and their standard deviations at 2600 m water depth at station Ierapetra ($34^{\circ}26'\text{N}$, $26^{\circ}11'\text{E}$, water depth 3750 m). Fluxes (squares, black line and s.d. in red) and $\delta^{15}\text{SPN}$ (circles, grey line, s.d. in blue) for three deployment periods (MID-1: 01/30/1999 to 04/13/1999), MID-2: 11/05/2001 to 04/01/2002 and MID-3: 01/30/2007 to 09/05/2007) at 2700 m water depth have been assembled in a surrogate annual cycle.

Table 3.2: Composite seasonal course of N-flux and $\delta^{15}\text{N}$ of sinking particulate matter at station MID (Ierapetra), water depth 2700 m. Data are from three separate and discontinuous deployment periods starting in 1999 and ending in 2007, as explained in the text.

Month	Flux ($\mu\text{mol N m}^{-2} \text{d}^{-1}$)	$\pm 1s$	n	$\delta^{15}\text{SPN}$ (‰)	$\pm 1s$	n
January	2.25	1.30	2	0.82	0.03	2
February	3.97	2.78	6	1.26	0.80	7
March	4.58	2.86	6	1.17	0.87	6
April	4.24	3.25	4	0.46	0.89	4
May	0.71		1	0.35	0.45	2
June	3.49	3.03	2	1.33	0.21	3
July	0.74	0.14	2	1.19	0.44	3
August	2.25	1.30	2	1.27	0.34	3
September	n.d.					
October	n.d.					
November	1.80		1	1.68		1
December	1.23		1	1.78		1

3.4. Discussion

Table 3.3 is a compilation of inventories and $\delta^{15}\text{N}$ of different water masses in the EMS and in different compartments of reactive N based on our data, according to which the mass-weighted and depth-integrated $\delta^{15}\text{N}$ of the EMS is 2.8‰. Judging from that value, the inventory of reactive N in the EMS is fundamentally different from the inventories of other oceans or regional marine systems studied so far, because the overall level of $\delta^{15}\text{N}$ is clearly lower than elsewhere. In the following, we will first compare our new measurements on the individual compartments of N in the EMS with previous data and those of other areas, discuss possible reasons for the unusual ^{15}N depletion, and finally test these possible reasons against the isotopic evidence.

Table 3.3: Estimate of reactive N-inventories of the EMS in different depth intervals and mass-weighted $\delta^{15}\text{N}$ of the different components (nitrate, particulate nitrogen PN, and total reduced nitrogen, TRN). We calculated inventories (given in gigamol N) based on interval water volumes for the EMS without Adriatic and Aegean sub-basins (R. Grimm, pers. comm., 2009) and weight $\delta^{15}\text{N}$ values by average concentrations found during our cruise. The last column is the integrated and mass-weighted $\delta^{15}\text{N}$ over all components of reactive N for each interval, the last line are the integrated inventories and $\delta^{15}\text{N}$ of the entire water column.

Interval (m)	volume (km ³)	mass nitrate (Gmol)	interval weighted $\delta^{15}\text{N}$ (‰)	mass PN (Gmol)	interval weighted $\delta^{15}\text{N}$ (‰)	mass TRN (Gmol)	interval weighted $\delta^{15}\text{N}$ (‰)	mass reactive N (Gmol)	weighted $\delta^{15}\text{N}$ all (‰)
0-200	306200	357	2.4	112	1.6	876	1.1	1345	1.5
200-500	365300	1411	1.8	59	6.4	700	6.2	2171	3.3
>500	1719000	7949	2.2	249	7.2	3510	5.2	11709	3.2
all	2390500	9717	2.1	421	5.6	5086	4.6	15224	3.0

3.4.1. Isotopic composition of reactive nitrogen in sub-nitracline and deep water masses

The starting point for our discussion is the isotopic composition of the large reactive nitrogen in the deep-water pool and the depth interval below the nitracline and in the deep-water pool, which integrates the isotopic signal over all internal and external nitrate sources over the deep-water residence time of 50-80 years (Roether et al., 1996). Differing from the pool in surface waters (see below), this deep nitrate pool is isotopically homogeneous in the EMS. There are three previous data sets of widely differing $\delta^{15}\text{NO}_3^-$ in deep and intermediate water masses: One group (Sachs and Repeta, 1999) determined $\delta^{15}\text{NO}_3^-$ to $-0.7 \pm 0.1\text{‰}$ in two samples of deep water (depths not given) from the EMS, analysed by the ammonia diffusion method (Sigman et al., 1997). Another group (Struck et al., 2001), also by the ammonia diffusion method, gave a mean of

$7.3 \pm 2.8\%$ in 6 samples of waters from between 200 m and 400 m water depth. A third group (Pantoja et al., 2002), who used the denitrifier method, show 6 data points below 500 m in the EMS but give a $\delta^{15}\text{NO}_3^-$ of $2.5 \pm 0.1\%$ of only 4 samples (in the text of that publication, the mean is given as 2.4%).

Our data confirm that $\delta^{15}\text{NO}_3^-$ of nitrate in the deep water of the EMS (average of samples below 500 m) is indeed lower ($2.2 \pm 0.3\%$; $n=68$) compared to the narrow range of 4.7 to 5.4‰ for global ocean deep-water nitrate (Sigman et al., 2009), and our data set further shows that nitrate in the LIW water mass from the base of nitracline to 500 m is even more ^{15}N -depleted ($1.8 \pm 0.4\%$; $n=29$) (Table 3.3). Deep water nitrate in the western Mediterranean Sea has a $\delta^{15}\text{NO}_3^-$ of $3.0 \pm 0.1\%$ below 1500 m water depth (Pantoja et al., 2002), while in the adjacent NE subtropical Atlantic Ocean, $\delta^{15}\text{NO}_3^-$ is around 5‰ in waters >800 m depth (Bourbonnais et al., 2009). The residence time of deep-water nitrate in the EMS has been estimated to be 125 years (Mara et al., 2009). The pool is not directly linked to deep waters outside the EMS. It is fed mainly by mineralisation/nitrification of particles sinking from the mixed layer and by preformed nitrate downwelled during deep-water formation without subsequent modification by denitrification. The main nitrate sink is the LIW water mass that exports nitrate to the western Mediterranean Sea at depths between 150 and 500m. Plausible external sources are N_2 -fixation, atmospheric NO_x deposition, and river runoff.

The comparatively small size of the deep-water nitrate pool in the EMS ($5\text{-}6 \mu\text{mol L}^{-1}$), its relatively short residence time compared to that of other oceans, and the low $\delta^{15}\text{N}$ of external nitrate sources (runoff and atmospheric deposition without N_2 fixation have an annual load-weighted $\delta^{15}\text{NO}_3^-$ estimated at 0.5 to 1.5‰) (Mara et al., 2009) mean that over one residence time (~ 125 yrs) the deep-water $\delta^{15}\text{NO}_3^-$ should be depressed to approach the $\delta^{15}\text{NO}_3^-$ of inputs (Mara et al., 2009). The only data of $\delta^{15}\text{NO}_3^-$ available (also determined by the denitrifier method and with the same internal standard deviation of the method) to gauge possible systematic time-dependent changes are those for 4 samples taken in 1999 in the EMS (Pantoja et al., 2002). These data had an average of $2.5 \pm 0.1\%$ below 500 m depth. Average $\delta^{15}\text{NO}_3^-$ in our samples taken from below 500 m water depth 8 years later is $2.2 \pm 0.3\%$ ($n=68$). While the difference in isotopic ratio is in the predicted direction, the magnitude of the change is not large enough to confirm the hypothesis. We point out, however, that the interval-integrated and mass-weighted $\delta^{15}\text{N}$ of reactive N in the EMS (Table 3.3) has a gradient from lighter to heavier values with depth, and that the surface layer, which has a much lower residence time than deep water (on the order of years), is within

the $\delta^{15}\text{N}$ range of estimated external N inputs. Furthermore the intermediate water which is being exported from the EMS has a value ($1.8\pm 0.4\text{‰}$) close to the external supply.

The EMS deep-water (>500 m) nitrate pool is further unusual in that it has higher $\delta\text{N}^{18}\text{O}_3^-$ ($3.7\pm 0.9\text{‰}$, $n=25$) than other deep-water pools in the world ocean (Sigman et al., 2009). In table 2 of that publication, available data for the $\delta\text{N}^{18}\text{O}_3^-$ of deep nitrate from a variety of other deep oceanic environments are reported, and all are lower (1.8 to 2.8‰, except in the water depth interval from 300 to 1500 m eastern tropical Pacific with a $\delta\text{N}^{18}\text{O}_3^-$ of 7.0‰) than the EMS deep nitrate pool. One previous reported value for the $\delta\text{N}^{18}\text{O}_3^-$ of deep water in the westernmost Mediterranean Sea (Sigman et al., 2009) was 2.6‰ for the depth range of 1500 m to the seafloor, and $3.1\pm 0.1\text{‰}$ for a composite value of in parallel measurements of 4 samples in deep water.

A probable reason for higher $\delta\text{N}^{18}\text{O}_3^-$ in EMS deep water than in other deep ocean pools may be that the EMS is a concentration basin where evaporation exceeds precipitation and river runoff (E/P+R ratio of 1.2 in winter and 1.83 in summer) (Gat et al., 1996). The average $\delta^{18}\text{O}$ in water samples deeper than 500 m is $1.43\pm 0.18\text{‰}$ and $1.44\pm 0.16\text{‰}$ in the 0-500 m depth range (Pierre, 1999), and thus is around 1.4‰ heavier than in other ocean basins (LeGrande and Schmidt, 2006). Based on experiments (Granger et al., 2004), it has been suggested that nitrification does not involve dissolved O_2 for the required electron transfer to oxidise NH_4^+ to NO_2^- and subsequently to NO_3^- (Sigman et al., 2009). These authors argue that it is very likely that the $\delta\text{N}^{18}\text{O}_3^-$ is inherited from the $\delta^{18}\text{O}$ of ambient water with a positive offset of approximately 2‰, and the higher $\delta\text{N}^{18}\text{O}_3^-$ in the EMS is in agreement with that concept.

Concentrations of TRN (predominantly DON) in EMS deep and sub-nitracline intermediate waters are also very low compared with other environments (Berman and Bronk, 2003) and match low PN concentrations (Table 1). To our knowledge, no data exist on $\delta^{15}\text{TRN}$ from deep waters of the global ocean, but $\delta^{15}\text{TRN}$ in the deep (>500m) EMS is clearly higher ($6.0\pm 3.7\text{‰}$, $n=39$) than in EMS surface waters. It is also higher than in the subtropical ($3.9\pm 0.4\text{‰}$) and equatorial NW Atlantic ($4.1\pm 0.6\text{‰}$), and the subtropical NE Atlantic ($2.6\pm 0.4\text{‰}$), but in the range of values reported from shallower depths of the subtropical North Pacific ($5.4\pm 0.8\text{‰}$) (Knapp et al., 2005; Meador et al., 2007; Bourbonnais et al., 2009).

This ^{15}N -enriched TRN in EMS deep water coexists with low concentrations of even more ^{15}N enriched suspended PN, whereas our sediment trap data suggest that the $\delta^{15}\text{N}$ of material sinking rapidly from the mixed layer is low over the entire year and – differing from other observations

(Altabet, 1988; Gaye-Haake et al., 2005) – is apparently not enriched in ^{15}N during its passage through the water column. There was a significant decrease in the flux measured at different water depths, with the flux of particulate sinking N in the upper sediment trap being $5.7 \text{ mmol N m}^{-2}$ over the period of 216 days, decreasing to $1.4 \text{ mmol N m}^{-2}$ at 2700 m water depth (second trap), or to roughly 25%. This implies a loss 75% of particulate N flux to disintegration and remineralisation over a 1100 m water column. Because both the concentrations of PN and TRN in ambient water are low, and also decrease with depth (or are at best invariant), most of the loss must be to ammonification and rapid nitrification to nitrate. In consequence, both TRN and PN in deep water are very likely enriched residues of mineralisation, from which some lighter product originated. Because at the same time all meso-zooplankton size classes in EMS deep waters (Koppelman et al., 2009) and surface sediments (Struck et al., 2001) are also enriched, the product with low $\delta^{15}\text{N}$ is likely to be nitrate. The data illustrate the efficient cycling of labile PN in this ultra-oligotrophic system resulting in depleted nitrate and enriched TRN and suspended PN.

3.4.2. Nitrate in the surface layer: Testing the model of incomplete nitrate utilisation

The intermediate water nitrate pool provides the bulk of nitrate available for assimilation in the euphotic zone of the EMS. The EMS is unusual in that the phytoplankton bloom takes place over the winter period (October-March), as indicated in 2006/2007 by Chl-a concentrations from satellites (<http://reason.gsfc.nasa.gov/OPS/Giovanni/ocean.aqua.shtml>). Soon after the seasonal thermocline breaks down in autumn (October), nutrients are mixed into the surface layer. Since the winter period in the Mediterranean typically consists of short periods (few days) of cold and often wet weather interspersed with several days of warm sunny weather, this results in an immediate growth of phytoplankton which can be observed by remote sensing imagery and by fluorescence and nitrate profiles of NIS stations (exemplified in Figure 3.2). After each mixing event, nutrients are removed from the mixed layer, until all of the phosphate has been taken up and excess nitrate remains, together with biomass and TRN produced; sinking particles exit the mixed layer across the pycnocline. This incomplete assimilation of nitrate has been previously seen as a mechanism to explain low $\delta^{15}\text{N}$ values in sediments and suspended matter of the EMS (Struck et al., 2001).

At all stations sampled during M71-3, there was excess nitrate remaining in the surface mixed layer. The average nitrate remaining in the euphotic zone was between 0.24 and $0.48 \mu\text{M}$, and the actual amount of residual nitrate varied with location and stage of thermocline evolution. These concentrations are similar to those found previously for the average winter residual nitrate across

the Southern Levantine basin ($0.6 \pm 0.5 \mu\text{M}$) (Kress and Herut, 2001). In contrast, phosphate was entirely depleted in most surface water samples, with all values being below the detection limit for dissolved phosphate in samples from the EMS that have been preserved by freezing prior to analysis ($<20 \text{ nM}$) (Krom et al., 2005a). This depletion of phosphate in the surface mixed layer - while excess nitrate remained - during the winter phytoplankton bloom has been used as direct evidence that the waters of the EMS are P limited (Krom et al., 1991).

If the concept of incomplete nitrate utilisation is correct, it requires that residual nitrate and products of assimilation together have the original isotopic mixture of nitrate provided by mixing (Mariotti et al., 1981). Products of assimilation in the mixed layer are those parts of PN and TRN that are present in excess of their concentrations below the thermocline (which were mixed up during homogenisation), and SPN exported by sinking particles. If an initial mixed-layer nitrate pool in a closed system is progressively assimilated, it will be enriched in ^{15}N (and ^{18}O) in the course of assimilation, in analogy to the Rayleigh distillation process. The enrichment can be approximated by (Mariotti et al., 1981):

$$\delta^{15}\text{NO}_3^-_{\text{residual}} = \delta^{15}\text{NO}_3^-_{\text{initial}} + 15\epsilon \times \ln(f)$$

with $f = [\text{NO}_3^-]_{\text{residual}}/[\text{NO}_3^-]_{\text{initial}}$, and $^{15}\epsilon$ expressing the fractionation factor (in ‰) between product and substrate. Similarly, the isotopic composition of instantaneous and accumulated products at any fraction of substrate remaining in the course of assimilation can be calculated (Mariotti et al., 1981).

The range of $^{15}\epsilon$ reported in the literature is large and differs for different primary producers. A recent compilation (York et al., 2007) reports $^{15}\epsilon$ from -16 to 6‰ (negative values meaning that ^{14}N is preferentially assimilated), but is commonly assumed to be -5‰. Available field and experimental data suggest equal separation factors $^{15}\epsilon$ and $^{18}\epsilon$ for nitrate assimilation (Casciotti et al., 2002; Granger et al., 2004; Lehmann et al., 2005).

Simplifying the EMS mixed layer to closed systems and using the Rayleigh closed-system approach, we can test if progressive assimilation of thermocline nitrate matches observed isotopic enrichment in residual nitrate and the $\delta^{15}\text{N}$ of instantaneous and accumulated products (calculated according to Mariotti et al., 1981) for pelagic and NIS stations (Figure 3.6 and Table 3.4a, b). We assume an initial nitrate concentration in the mixed layer of half the concentration below the thermocline due to mixing of essentially nitrate-free surface waters with sub-thermocline waters, and at the nitrate isotope signature of water below the thermocline (Table 3.1) before the onset of phytoplankton assimilation. This assumed starting stock of nitrate is similar in value to previous estimates for the amount of nitrate mixed into surface waters in the EMS (Krom et al., 2003).

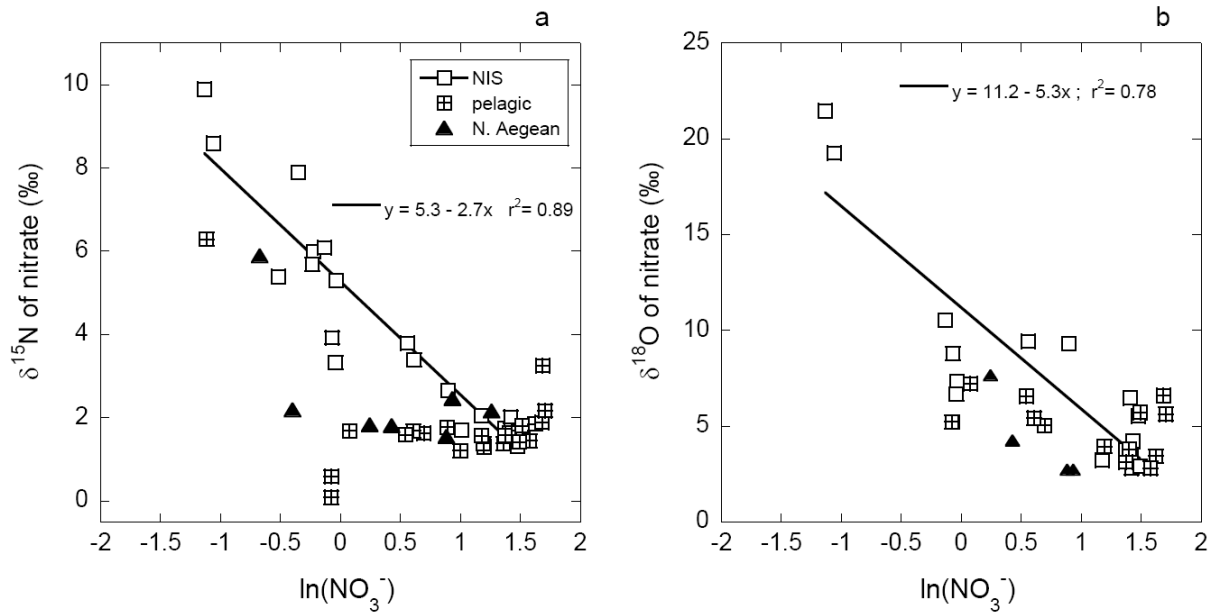


Figure 3.6: Plots of log-normal nitrate concentrations (X-axis) versus $\delta^{15}\text{NO}_3^-$ (a) and $\delta^{18}\text{O}_3^-$ (b) found in samples in and above the nitraclines for individual station. The solid regression line in Figure 6a is for samples in the northern Ionian Sea (NIS) where nitrate is replenished from thermocline deepening ($r^2=0.89$). In these samples, ^{15}N in nitrate is enriched in the course of ongoing nitrate assimilation with an apparent separation factor $^{15}\epsilon$ close to -3‰ . In samples from the open Ionian Sea and Herodotus Basin (pelagic stations), where the mixed layer was thick and nitrate poor at the time of sampling, $\ln(\text{nitrate})$ and $\delta^{15}\text{NO}_3^-$ are uncorrelated. In Figure 6b, the correlation between $\ln(\text{nitrate})$ and $\delta^{18}\text{O}_3^-$ for NIS samples is also significant ($r^2=0.78$), with an apparent separation factor $^{18}\epsilon$ close to -5‰ . There is no significant correlation in samples from pelagic stations and from the northern Aegean station.

Table 3.4: Calculation of the isotopic composition of residual nitrate ($\delta^{15}\text{N}$ and $\delta^{18}\text{O}$) and instantaneous and accumulated products of nitrate assimilation expected from Rayleigh-fractionation in closed systems (a = NIS and b = pelagic mixed layers) with starting concentrations and isotopic compositions corresponding to thermocline nitrate from Table 1. Note that the permil fractionation factors $^{15}\epsilon$ and $^{18}\epsilon$ have been set to -5‰. Results of measurements are also shown.

a)

Northern Ionian Sea stations ($\delta^{15}\text{NO}_3$ _{3initial}=2.1‰; $\delta\text{N}^{18}\text{O}_3$ _{3initial}=5.1‰)

Initial NO_3 ($\mu\text{mol L}^{-1}$)	remaining NO_3 ($\mu\text{mol L}^{-1}$)	fraction remaining	expected $\delta^{15}\text{NO}_3$ residual nitrate (‰)	expected $\delta\text{N}^{18}\text{O}_3$ residual nitrate (‰)	$\delta^{15}\text{N}$ instanta- neous product (‰)	$\delta^{15}\text{N}$ accumulat ed prod. expected (‰)
1.8	0.48	0.27	8.6	11.6	3.6	-0.3
	$\delta^{15}\text{NO}_3$ found (‰)	found $\delta\text{N}^{18}\text{O}_3$ residual nitrate (‰)	estimated $\delta^{15}\text{N}$ PN+ DON+SPN found (‰), mass- weighted*	$\delta^{15}\text{TRN}$ found (‰)	$\delta^{15}\text{PN}$ found (‰)	$\delta^{15}\text{SPN}$ found (‰), assumed to the same as in pelagic trap
	5.6	10.7	0.7	-0.2	2.2	0.9 (*)

* calculated with 4 mmol N in 4 months [Boldrin et al., 2002]

b)

Pelagic stations ($\delta^{15}\text{NO}_3$ _{3initial}=1.6‰; $\delta\text{N}^{18}\text{O}_3$ _{3initial}=5.0‰)

Initial c NO_3 (μM)	remaining c NO_3 (μM)	fraction remaining	expected $\delta^{15}\text{NO}_3$ residual nitrate (‰)	expected $\delta\text{N}^{18}\text{O}_3$ residual nitrate (‰)	$\delta^{15}\text{N}$ instanta- neous product (‰)	$\delta^{15}\text{N}$ accumulat ed prod. expected (‰)
1.7	0.24	0.14	11.5	14.9	6.5	0.0
	$\delta^{15}\text{NO}_3$ found (‰)	found $\delta\text{N}^{18}\text{O}_3$ residual nitrate (‰)	mass- weighted $\delta^{15}\text{N}$ PN+ DON+SPN found (‰)	$\delta^{15}\text{TRN}$ found (‰)	$\delta^{15}\text{PN}$ found (‰)	$\delta^{15}\text{SPN}$ found (‰), flux weighted
	2.3	5.2	1.0	1.1	1.1	0.9

Isotopic composition of substrate and products at NIS stations, where the thermocline was as yet thin (<100 m) and deepening, was roughly balanced with respect to the $\delta^{15}\text{N}$ of nitrate supplied by thermocline mixing and products of assimilation found. However, the apparent separation factor $^{15}\epsilon$ suggested by the relationship between the natural logarithm of nitrate concentration and $\delta^{15}\text{NO}_3^-$ is only -3‰ (Figure 3.6a), whereas the apparent $^{18}\epsilon$ is close to -5‰. The Rayleigh model predicts that by the time that 73% of the initial nitrate in the NIS mixed layer

is assimilated into PN, SPN and TRN (such as is the case in the average profile over all stations there), the residual nitrate should have a $\delta^{15}\text{NO}_3^-$ of 8.6‰, which is higher than the 5.6‰ found (Table 3.4a), and a $\delta\text{N}^{18}\text{O}_3^-$ of 11.6‰ (found 10.7‰). The theoretical accumulated products of nitrate assimilation (PN, TRN, SPN) should have a $\delta^{15}\text{N}$ of -0.3‰. The mass-weighted $\delta^{15}\text{N}$ found in all products (including an estimate of the amount and $\delta^{15}\text{N}$ of SPN exported from the mixed layer based on the sediment trap data) was around 0.7‰. The found values are similar to those predicted by a closed system approach for the NIS stations, although (as will be shown below), the different values for the apparent separation factors $^{15}\epsilon$ and $^{18}\epsilon$ suggest that nitrate isotopic composition can be better described by also including externally supplied N.

By contrast, the isotopic compositions in the pelagic stations that had a mature thermocline and a thick nitrate-depleted mixed layer deviate significantly from a simple closed system: Only 14% of the initially mixed nitrate remained (Table 3.4b) and should have a $\delta^{15}\text{NO}_3^-$ of 11.5‰, and $\delta\text{N}^{18}\text{O}_3^-$ of 14.9‰, whereas we found 2.3‰, and 5.2‰, respectively. Expected accumulated and instantaneous products should have a $\delta^{15}\text{N}$ of 0.0‰ and 6.5‰, respectively. While the value found for the mass-weighted $\delta^{15}\text{N}$ of products (PN, TON, SPN: 1.0‰) could be a mixture of accumulated and instantaneous products, the deviations in $\delta^{15}\text{NO}_3^-$ of the nitrate-poor pelagic mixed layer clearly require an additional source of nitrate with a low $\delta^{15}\text{NO}_3^-$.

3.4.3. Constraints from differences in $\delta^{15}\text{NO}_3^-$ and $\delta^{18}\text{NO}_3^-$

At all stations (NIS and pelagic), a second and related indicator for a deviation from simple enrichment due to assimilation of thermocline nitrate is the differential behaviour of $\delta^{15}\text{NO}_3^-$ and $\delta\text{N}^{18}\text{O}_3^-$ of residual nitrate in the mixed layer. This could be an effect of unequal separation factors suggested by data for NIS stations (see Figure 3.6), but this assumption would run counter to available evidence (Casciotti et al., 2002; Granger et al., 2004; Lehmann et al., 2005). The deviation from the expected 1:1 enrichment line originating from the composition of nitrate at the base of the thermocline in samples from the mixed layers may be expressed as a nitrate isotope deviation $\Delta(15,18)$ (Sigman et al., 2005) from the dual isotope composition of the nitrate source:

$$\Delta(15,18) = (\delta^{15}\text{N}_{\text{measured}} - \delta^{15}\text{N}_{\text{source}}) - \epsilon^{15}/\epsilon^{18} \times (\delta^{18}\text{O}_{\text{measured}} - \delta^{18}\text{O}_{\text{source}})$$

Figure 3.7 is a depth plot of $\Delta(15,18)$ for different station sets in the EMS over the top 500 m and is calculated by using the average $\delta^{15}\text{NO}_3^-$ and $\delta\text{N}^{18}\text{O}_3^-$ of EMS deep water as $\delta^{15}\text{N}_{\text{source}}$ and $\delta^{18}\text{O}_{\text{source}}$, respectively. Our data points are scarce in the nitrate-depleted mixed layers, but suggest

an average $\Delta(15,18)$ of EMS mixed layer nitrate of around -3‰, and both station sets suggest a decrease towards the sea surface. The negative values imply an additional source with lower $\delta^{15}\text{NO}_3^-$ than the residual thermocline nitrate, and suggest either nitrate generation via nitrification while nitrate in the mixed layer is being assimilated, or external input of nitrate with a different isotopic makeup than the nitrate being assimilated (Sigman et al., 2005).

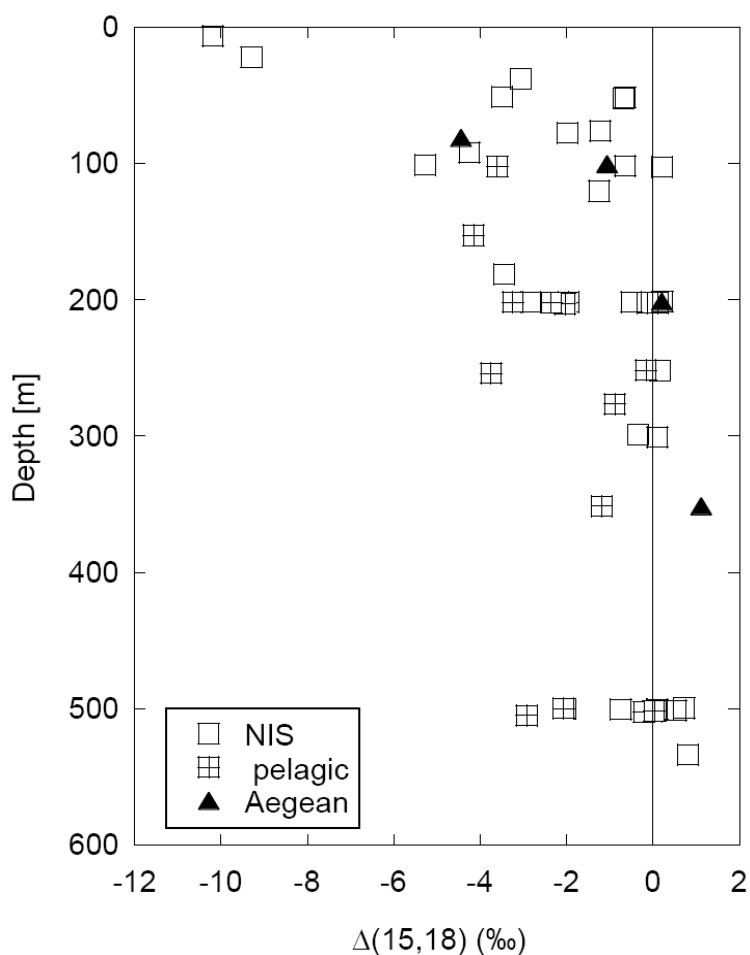


Figure 3.7: Depth plot of $\Delta(15,18)$ of nitrate for different station sets in the upper 500 m of the water column.

3.4.4. Nitrification of fixed N or recycled N

Nitrification in the presence of nitrate assimilation, via ammonification of particulate N and/or DON, is the standard mechanism to cause a negative $\Delta(15,18)$. In the few oligotrophic environments studied so far, observed negative $\Delta(15,18)$ have been attributed to nitrification of comparatively light PN produced from fixation and possibly DON (Casciotti et al., 2008; Knapp et al., 2008; Bourbonnais et al., 2009). In these cases, the isotopic composition of (in this case “new”) nitrate is set by the $\delta^{15}\text{N}$ of fixed N ($\sim -1\text{‰}$) on the one hand, and by the $\delta^{18}\text{O}$ of ambient

seawater with a positive offset of 2‰, so that nitrate deriving from N₂ fixation is added to the mixed-layer nitrate pool with a $\delta^{15}\text{NO}_3^-$ of $\sim -1\text{‰}$ and $\delta\text{N}^{18}\text{O}_3^-$ of $\sim 2\text{‰}$ (Bourbonnais et al., 2009). In the EMS with its higher $\delta^{18}\text{O}$ of seawater, we would expect the recycled nitrate to have a $\delta^{15}\text{NO}_3^-$ equivalent to $\delta^{15}\text{SPN}$ and a $\delta\text{N}^{18}\text{O}_3^-$ of $\sim 3.4\text{‰}$.

Partitioning of ammonium released from PN to either nitrification or ammonium uptake has also been shown to cause a range of $\Delta(15,18)$, because both processes have different $^{15}\epsilon$ (Sigman et al., 2005; Wankel et al., 2006). Negative $\Delta(15,18)$ in residual nitrate may ensue, because nitrate returned from PN mineralisation via ammonium oxidation is relatively more depleted in ^{15}N than the residual nitrate pool, whereas its $\delta^{18}\text{O}$ is pegged to ambient water. Because on the other hand ammonium uptake has a lower preference for ^{15}N than nitrification, significant ratios of ammonium assimilation versus nitrification will cause biomass and thus PN to be relatively enriched over the recycled nitrate. Because we find no indication for enriched SPN or PN in the mixed layers, and the sediment trap data suggest that SPN is on annual average even more depleted in ^{15}N than thermocline nitrate in the EMS, we believe that assimilation of mineralised ammonium is unlikely to play a major role as a substrate for phytoplankton growth in the EMS mixed layer, and as a cause for negative $\Delta(15,18)$.

3.4.5. Input of NO_x

Aside from an internal source of nitrate, there must be a second source that potentially causes negative $\Delta(15,18)$ in the mixed layer of the EMS, namely atmospheric inputs of NO_x. Two previous studies (Knapp et al., 2008; Bourbonnais et al., 2009) acknowledge (but dismiss) the possibility that the negative $\Delta(15,18)$ observed in mixed layer nitrate of the oligotrophic Sargasso Sea and subtropical NE Atlantic Ocean indicate atmospheric NO_x inputs, which have very high $\delta\text{N}^{18}\text{O}_3^-$ at low $\delta^{15}\text{NO}_3^-$ (Kendall, 1998). Such an input, if it is not immediately assimilated due to phosphate limitation, would introduce nitrate with low $\delta^{15}\text{NO}_3^-$ and high $\delta^{18}\text{O}_3^-$ into the surface mixed layer of the EMS. We have evidence which suggests that NO_x inputs play a relatively larger role in the EMS than elsewhere: Modelled average annual total NO_x inputs in wet and dry deposition to the EMS surface range between 200 and 400 mg N*m⁻²*a⁻¹ with a pronounced N-S gradient (<http://www.emep.int>). An estimated 14-29 mmol N*m⁻²*a⁻¹ of industrial origin are thus supplied annually to the EMS.

The atmospheric deposition on the island of Crete in winter months of 2006/2007 had a mean $\delta^{15}\text{NO}_3^-$ of -2.0‰ (Mara et al., 2009), and likely had a high $\delta\text{N}^{18}\text{O}_3^-$: 13 samples of dry

atmospheric deposition (no rain events recorded) collected on the Island of Crete during June-September 2007 had an average $\delta\text{N}^{18}\text{O}_3^-$ of $67.5 \pm 4.2\text{‰}$ (Mara, unpubl. data). Although this data set does not cover the time of predominantly wet deposition in winter, the values are within the range reported from other environments (Kendall, 1998) and from the nearby northern Red Sea (Wankel et al., 2009). There, $\delta^{15}\text{N}$ values of water-soluble nitrate in aerosol samples ranged from -6.9‰ to $+1.9\text{‰}$ and $\delta^{18}\text{O}$ was found to range from 65.1‰ to 84.9‰ with highest $\delta^{18}\text{O}$ values in the winter. The source of that nitrate were air masses deriving from the Mediterranean Sea and western Europe (Wankel et al., 2009). Thus, although only $<10\%$ of nitrate in the mixed layer of the EMS may have originated from the atmospheric source over 4 months, the effect on average $\delta\text{N}^{18}\text{O}_3^-$ and $\Delta(15,18)$ is largely due to the small amount of nitrate in the mixed layer of the EMS and the high $\delta\text{N}^{18}\text{O}_3^-$ of atmospheric inputs.

We used the isotopic signatures of internal (recycling) and external (N_2 fixation and NO_x) inputs together with an estimate of N export flux in a conceptual steady-state mass and isotope balance model to explore the effects of externally and internally supplied N on $\Delta(15,18)$. The model is the same as that used in the subtropical SE Atlantic (Bourbonnais et al., 2009), and we refer to that publication for details. We adapted the model to conditions in the EMS by choosing appropriate boundary conditions for the thermocline nitrate isotopic composition (from Table 3.1) and the N-export production in the EMS. We calculated hypothetical $\Delta(15,18)$ for a range of input conditions from 0-40 mmol N from N_2 fixation and 0-40 mmol N of recycled nitrate, both of which acquire their $\delta\text{N}^{18}\text{O}_3^-$ from nitrification and thus have a $\delta\text{N}^{18}\text{O}_3^-$ of 3.4‰ . Nitrate input from N_2 -fixation needs to be $40 \text{ mmol} \cdot \text{m}^{-2} \cdot \text{a}^{-1}$ ($>70\%$ of the $56 \text{ mmol} \cdot \text{m}^{-2} \cdot \text{a}^{-1}$ PN export flux) to create a $\Delta(15,18)$ of around -2‰ ; input of $40 \text{ mmol} \cdot \text{m}^{-2} \cdot \text{a}^{-1}$ of recycled nitrate yielded a $\Delta(15,18)$ of -3.6‰ , which is close to the 3‰ observed. For an assumed NO_x input of only $5 \text{ mmol} \cdot \text{m}^{-2}$, which is well within the known atmospheric NO_x flux, the model calculates a $\Delta(15,18)$ of -5.8‰ .

A number of possible combinations of these external and internal sources can theoretically result in the nitrate isotope anomaly observed in the EMS mixed layer. However, our preferred interpretation of the data is that they represent a mixture of regenerated nitrate and NO_x input, because both are known to be inputs to the mixed layer in the necessary fluxes and isotopic ranges to fully describe the changes observed. We consider significant input from N_2 fixation unlikely for the time of our expedition, both because we sampled a winter situation, and because N_2 fixation measurements across the region sampled here were very low when sampled in June 2007 (Ibello et al., in press). There is ample evidence that primary production in the EMS is supported by regenerated nutrients that are entrained into a microbial loop operating in surface waters (Zohary

and Robarts, 1998; Thingstad et al., 2005). Nutrient budgets (Ribera d'Alcala et al., 2003) and experimental work (Thingstad and Rassoulzadegan, 1999; Thingstad et al., 2005) both imply that surface productivity is to a significant extent supported by regenerated nitrate. In addition, recent genetic investigations suggest that ammonia-oxidizing *Archaea* in mesopelagic waters of the Eastern EMS may have a central role in nitrification of ammonium liberated from particulate N (De Corte et al., 2009). Our data are in agreement with the important role of recycled nitrate, but we again stress that atmospheric NO_x inputs to the EMS must be taken into account in mass-based (Krom et al., 2004) and isotope-based (Mara et al., 2009) budgets of the N-cycle in the EMS.

3.4.6. Is TRN involved in N-cycling?

TRN is the largest pool of reactive N in the mixed layer and after nitrate the second largest in the entire water column of the EMS (Table 3.3). Because ammonia levels are low in the EMS, the major constituent of TRN in our samples is likely to be dissolved organic nitrogen, which is a by-product of N_2 -fixation or of heterotrophy in the mixed layer (Berman and Bronk, 2003). It has been discussed as a possible substrate for phytoplankton assimilation or ammonification and nitrification processes (Bronk et al., 2007), and its isotopic composition should reflect TRN cycling (Knapp et al., 2005). In a previous study from the Sargasso Sea, the small concentration and $\delta^{15}\text{DON}$ differences between the surface and subsurface waters suggested that DON there is recalcitrant and the data indicated only limited DON turnover in that area (Knapp et al., 2005). Although our data is somewhat limited, we see a trend of decreasing concentrations and increasing $\delta^{15}\text{TRN}$ between surface and deep-water samples that imply active participation of TRN in reactive N turnover. Our interpretation of the similar trends in $\delta^{15}\text{N}$ composition of PN and TRN (except in the intermediate water mass, where our data are scarce; Tables 3.1 and 3.3) suggest they are closely coupled, and that both reflect ^{15}N enrichment in the course of mineralisation to produce ^{15}N depleted nitrate in the deep water mass, and most likely even more intensely in the intermediate water mass. There is supporting direct evidence of nitrification at the nutricline based on observed nitrite peaks (Krom et al., 2005a).

The similarity of $\delta^{15}\text{PN}$ and $\delta^{15}\text{TRN}$ in the mixed layer is likely to reflect heterotrophy, where DON is a by-product of PN recycling. The low $\delta^{15}\text{TRN}$ found in the surface layer of the EMS is in accord with rapid grazing and recycling of nutrients during the winter bloom. At pelagic sites, the stable seasonal thermocline had developed prior to our expedition, and had caused the winter phytoplankton bloom to cease, a condition typically reached at NIS sites in March/April. As a result, phytoplankton in the surface layers of the EMS is N- and P-co-limited by May (Zohary et al., 2005). According to current understanding, active grazing of small phytoplankton populations

persisting on recycled nitrate continues in the mixed layer (Krom et al., 2005a; Thingstad et al., 2005), with the result that over time the residual nitrate is converted into DON. This DON may not directly be bioavailable to the phytoplankton, but is consumed largely by heterotrophic bacteria (Bronk, 2002; Thingstad et al., 2005). No isotopic measurements have been made of PN and DON in summer in the EMS, but we would predict that the PN and DON should be isotopically enriched compared to values obtained in this study of a winter situation.

3.5. Conclusions

The total pool of reactive nitrogen (nitrate, dissolved total reduced nitrogen, and particulate nitrogen) of the eastern Mediterranean Sea is unusually depleted in ^{15}N compared to the global ocean. This must to a large extent be due to the isolation and anti-estuarine circulation of the EMS that prevents communication with the global deep-water nitrate pool that is very homogeneous at $\delta^{15}\text{NO}_3^- \sim 5\text{‰}$ / $\delta\text{N}^{18}\text{O}_3^- \sim 2\text{‰}$ (Sigman et al., 2009). The low level of $\delta^{15}\text{N}$ of the EMS reflects the dominance of an isotopically depleted N-source, because processes that enrich ^{15}N in nitrate of other oceans (such as mid-water denitrification) are not acting in the EMS. The low $\delta^{15}\text{NO}_3^-$ in the deep water contrasts with high $\delta^{15}\text{N}$ in TRN (mainly DON) and suspended PN. It is inferred that this is due to extensive and efficient mineralisation of the rapidly sinking fresh PN (sampled in sediment traps) in the ultra-oligotrophic system. We hypothesize that the $\delta^{15}\text{NO}_3^-$ in the deep water may be decreasing with time in response to the depleted (mainly anthropogenic) external supply of NO_x , although the data set is too sparse as yet to be conclusive. The data in this study were collected in the winter of 2006/2007, which coincided with a typical winter bloom at the stations in the northern Ionian basin and with an (unusually early) mature thermocline at maximum depth in the remaining pelagic stations. Using a Rayleigh-closed system approach, it was concluded that it was not possible to explain the isotopic distribution of NO_3^- , TRN and PN only by partial N uptake caused by the extant P-limited phytoplankton bloom. It requires in addition a source of isotopically distinct nitrate, which may be internal (recycled nitrate) or external (N_2 fixation or NO_x input). Possible ranges for the nitrate isotope anomaly $\Delta(15,18)$ in the mixed layer calculated by a simple model point towards nitrification and/or a relatively small (and realistic) contribution of atmospheric nitrate with characteristically low $\delta^{15}\text{N}$ and high $\delta^{18}\text{O}$ as the most likely sources of additional nitrate. It is known that the EMS receives a significant supply of anthropogenic NO_x , which together with known recycling processes adequately describes the isotope distribution. These patterns could also be caused by extensive N_2 fixation, but that would require high rates of diazotrophy in winter, when there are insignificantly low levels measured in the region even in summer, and would be in conflict with our knowledge on the amount and isotopic composition of anthropogenic NO_x input to the EMS.

4. Diagenetic Control of Nitrogen Isotope Ratios in Holocene Sapropels and Recent Sediments from the Eastern Mediterranean Sea

Abstract

The enhanced accumulation of organic matter in Eastern Mediterranean sapropels and their unusually depleted $\delta^{15}\text{N}$ values have been attributed to either enhanced nutrient availability which led to elevated primary production and carbon sequestration or to enhanced organic matter preservation under anoxic conditions. In order to evaluate these two hypothesis we have determined Ba/Al ratios, amino acid composition, N and organic C concentrations and $\delta^{15}\text{N}$ on sinking particles, surface sediments, eight spatially distributed core records of the youngest sapropel S1 (10-6 kyr) and older sapropels (S5, S6) from two locations. These data suggest that (i) temporal and spatial variations in $\delta^{15}\text{N}$ of sedimentary N are driven by different degrees of diagenesis at different sites rather than by changes in N-sources or primary productivity and (ii) that present day TOC export production would suffice to create a sapropel like S1 under conditions of deep-water anoxia. This implies that both enhanced TOC accumulation and $\delta^{15}\text{N}$ depletion in sapropels were due to the absence of oxygen in deep waters. Thus preservation plays a major role for the accumulation of organic-rich sediments enhanced primary production is not needed for sapropel formation in the Mediterranean.

4.1. Introduction

In the Eastern Mediterranean Sea (EMS) paleoceanographic record, the ratio of stable N isotopes $^{15}\text{N}/^{14}\text{N}$ ($\delta^{15}\text{N}$) of organic-rich sediment layers (sapropels) has often been used to understand mechanisms and environmental conditions leading to past black shale formation in a region which is at present an extreme nutrient desert. In a commonly accepted model, recurrent Mediterranean sapropel formation is attributed to a stratified water column and anoxic deep water conditions that developed as a consequence of enhanced fresh water inputs (Ryan, 1972; Cita et al., 1977; Rossignol-Strick et al., 1982; Rohling, 1994; Emeis et al., 2000). The youngest sapropel – termed S1 – formed between 9,800 and 5,700 years ago (de Lange et al., 2008) at water depths below 400 m (Anastasakis and Stanley, 1986) with inferred deep-water anoxia everywhere below 1800 m water depth (de Lange et al., 2008). The sedimentary total organic carbon concentration (%TOC) reaches more than 30% in some Pliocene sapropels (Emeis et al., 1996) and is approximately 2% in S1 (Murat and Got, 2000). Present-day pelagic surface sediments have a range of %TOC from 0.2- 0.6% only (see below). The higher TOC content (which is associated with faunal, floral, and geochemical changes) of sapropels has been attributed to either greatly enhanced surface productivity, which would suggest a different nutrient regime compared to recent conditions (Calvert et al., 1992; Kemp et al., 1999; Mercone et al., 2001), or to a better preservation of organic matter under oxygen-deficient bottom-water conditions at approximately equal productivity rates (Cheddadi and Rossignol-Strick, 1995; Sachs and Repeta, 1999; Moodley et al., 2005) or some combination of both. Based on stoichiometric calculations several authors recently proposed that there is a causal link between anoxia and enhanced productivity via the enhanced recycling of phosphate from sediments/and sinking particles in the water column under anoxic conditions increasing N_2 - fixation (Tyrrell, 1999; Wallmann, 2003). This model combines increased productivity during S1 deposition with enhanced preservation (Struck et al., 2001; Slomp et al., 2002; Arnaboldi and Meyers, 2006; Emeis and Weissert, 2009).

A key argument for this hypothesis are the uncharacteristically low values of $\delta^{15}\text{N}$ in all sapropels, ranging from -5.1‰ to 2‰, whereas surrounding hemipelagic sediments that are poor in organic carbon always have $\delta^{15}\text{N} > 4‰$ (Milder and Montoya, 1999; Struck et al., 2001; Meyers and Bernasconi, 2005; Arnaboldi and Meyers, 2006). The $\delta^{15}\text{N}$ in non-sapropel sediments thus are similar to pelagic sediments world wide that range from 5 to 15‰ (Holmes et al., 1996; Holmes et al., 1997; Gaye-Haake et al., 2005). These $\delta^{15}\text{N}$ of sediments integrate the isotopic composition of the assimilated nitrate source, biological fractionation, foodweb dynamics, and isotope fractionation during sediment diagenesis (McClelland and Valiela, 1998; Voss et al., 2005; Altabet, 2007; Fry, 2007; Dähnke et al., 2008). As a paleoceanographic tool, $\delta^{15}\text{N}$ is widely used

to reconstruct the reactive nitrogen regime of the oceans over geological time scales (Altabet, 2007; Farrell et al., 1995; Ganeshram et al., 2002; Garvin et al., 2009; Jenkyns et al., 2001; Kuypers et al., 2004).

The fact that $\delta^{15}\text{N}$ in sapropels is lower than in the hemipelagic carbonates has originally been attributed to incomplete assimilation of excess nitrate from enhanced reactive N supply to the euphotic zone by either river discharge or upwelling (Calvert et al., 1992). Other authors attributed massive addition of fixed nitrogen to intense P-recycling from anoxic sediments (Struck et al., 2001), or to a compensation for nitrate loss by denitrification at suboxic interfaces between surface and deep waters (Arnaboldi and Meyers, 2006). Interestingly, present-day surface sediments, suspended matter, sinking particles and deep-water nitrate in the EMS all have light $\delta^{15}\text{N}$ that are similar to the $\delta^{15}\text{N}$ of sapropel S1. Assuming that this indicates significant N_2 -fixation in the modern EMS, (Sachs and Repeta, 1999) proposed that the S1-situation was similar to the present-day situation, and that the low $\delta^{15}\text{N}$ in S1 is due to the preservation of the original $\delta^{15}\text{N}$ signature of sedimenting newly fixed N. Preservation may play an important role because sedimentary $\delta^{15}\text{N}$ is known to become enriched during OM degradation resulting from preferential loss of ^{15}N depleted compounds (Altabet, 1996; Freudenthal et al., 2001; Gaye-Haake et al., 2005). Although exact mechanisms remain unknown, kinetic isotope fractionation during protein hydrolysis (Bada et al., 1989; Silfer et al., 1992) and deamination (Macko and Estep, 1984) very likely cause this enrichment.

The recent EMS nutrient and productivity regime appears to be an improbable setting for black shale (aka sapropel) deposition, even if preservation of OM was enhanced by anoxia. The EMS presently has a highly oligotrophic nutrient regime where the carbon export flux (6-12 g $\text{C}\cdot\text{m}^{-2}\cdot\text{y}^{-1}$; Bethoux, 1989) is half of that of the Sargasso Sea. However, both modes of the EMS (the modern nutrient desert and the sapropel mode) have the strikingly low $\delta^{15}\text{N}$ values in common: As shown in Figure 4.1, surface sediments in the EMS presently have $\delta^{15}\text{N}$ -values between 5‰ and 3.5‰ with an eastward decreasing gradient. This is explained by either preferential assimilation of $^{14}\text{NO}_3^-$ (Struck et al., 2001) caused by an excess of nitrate over phosphate in surface waters of the EMS (Krom et al., 2005), or by an eastward increasing supply of fixed N (Pantoja et al., 2002). Although until recently fixed N_2 was the strongest candidate to explain the low modern $\delta^{15}\text{N}$ levels, the observational evidence for significant diazotrophic N_2 fixation is scarce and ambiguous (Mara et al., 2009). New data on the $\delta^{15}\text{N}$ of NO_x input from the atmosphere suggest that the present-day N-cycle of the EMS may recently have been anthropogenically changed: $\delta^{15}\text{N}$ in nitrate in both dry and wet atmospheric deposition have consistently negative $\delta^{15}\text{N}$ compared to air N_2 , implying a strongly ^{15}N -depleted atmospheric

source that contributes >50% of external nitrate inputs with a weighted annual $\delta^{15}\text{N}$ of -3.1‰ (Mara et al., 2009). These authors propose that assimilation of the ^{15}N -depleted atmospheric nitrate in the surface mixed layer and subsequent particle flux and mineralisation in the deep water over the last 40-50 years accounts for the unusually low $\delta^{15}\text{N}$ ratios found in deep-water NO_3^- without the need of any significant N_2 fixation. The nitrogen cycle in the EMS of today, thus, is not likely to be in a natural state, and the similarity of modern and S1 $\delta^{15}\text{N}$ values is due to the fact that the dominant anthropogenic source today ($\delta^{15}\text{N} = -3.1\text{‰}$) and the postulated N_2 -fixation source during S1 (-2 to 1‰ ; Minagawa and Wada, 1986) produce similar ^{15}N depleted sedimentary $\delta^{15}\text{N}$ values.

But what could explain the low $\delta^{15}\text{N}$ values in S1 sediments with regard to input and cycling of reactive N during sapropel deposition? It is essential that the signal encoded in $\delta^{15}\text{N}$ is not affected by post-depositional alterations, or that the diagenetic influence is known and can be corrected for. Determinations of pristine $\delta^{15}\text{N}$, not affected by early diagenetic enrichment, have been achieved by analyzing $\delta^{15}\text{N}$ in diatom frustules (Sigman et al., 1999), foraminifer shells (Ren et al., 2009) and biomarkers (Sachs and Repeta, 1999). In the case of the EMS and S1, data shown in Moodley et al. (2005) already suggested a strong post-depositional enrichment in $\delta^{15}\text{N}$ (by 4-5‰) associated with continued and progressive re-oxygenation of the uppermost section of the S1 sapropel (“burndown”). This appears to be a pervasive feature in oxic water columns (Saino and Hattori, 1980; Altabet, 1988; Sachs and Repeta, 1999), implying that diagenesis under conditions of variable bottom-water oxygenation would most seriously compromise the reliability of $\delta^{15}\text{N}$ as a proxy in environments with low sedimentation rates such as the Mediterranean Sea (Jung et al., 1997).

The aim of this study is to quantify the mechanisms influencing $\delta^{15}\text{N}$ during S1 sapropel deposition and to identify post-depositional alteration. This is possible by using paired data of $\delta^{15}\text{N}$, biological productivity (Ba/Al-ratios) (Dymond et al., 1992; Francois et al., 1995), concentrations of bulk organic carbon and total nitrogen, as well as an index of organic matter preservation based on amino acid composition. To decide if the isotopic signature is more related to diagenesis/preservation or indeed reflects the nutrient regime at the sea surface (including sources, availability and utilization of nitrate), we examined the S1 sapropel time slice at six locations in different basins and at different water depths of the EMS. Data from sinking material intercepted by sediment traps and surface sediments of the EMS are also examined for the impact of early diagenetic alterations on $\delta^{15}\text{N}$ during particle sinking and at the sediment surface. These data and additional data from the Pleistocene S5 and S6 sapropels enable us to distinguish between time slice specific and general tendencies in the behavior of $\delta^{15}\text{N}$. Specifically, they

permit us to answer the following questions: Is $\delta^{15}\text{N}$ in sapropels closely linked to preservation? Were there spatial gradients in $\delta^{15}\text{N}$ during S1 sapropel times, and were these gradients the same as today?

4.2. Methods

Sinking particulate nitrogen (SPN) has been collected at the MID-station (Mediterranean Ierapetra Deep) by sediment traps during three periods covering three to seven months from early 1999 to summer 2007. The traps used in this study were Mc Lane Mark VII and Kiel K/MT 234 type with a collection area of 0.5 m². Sampling intervals varied between 3.5 and 14 days, and the traps were deployed in water depths between 1508 m and 2720 m. Detailed information about trap position, depth and sampling intervals is given in Table 4.1.

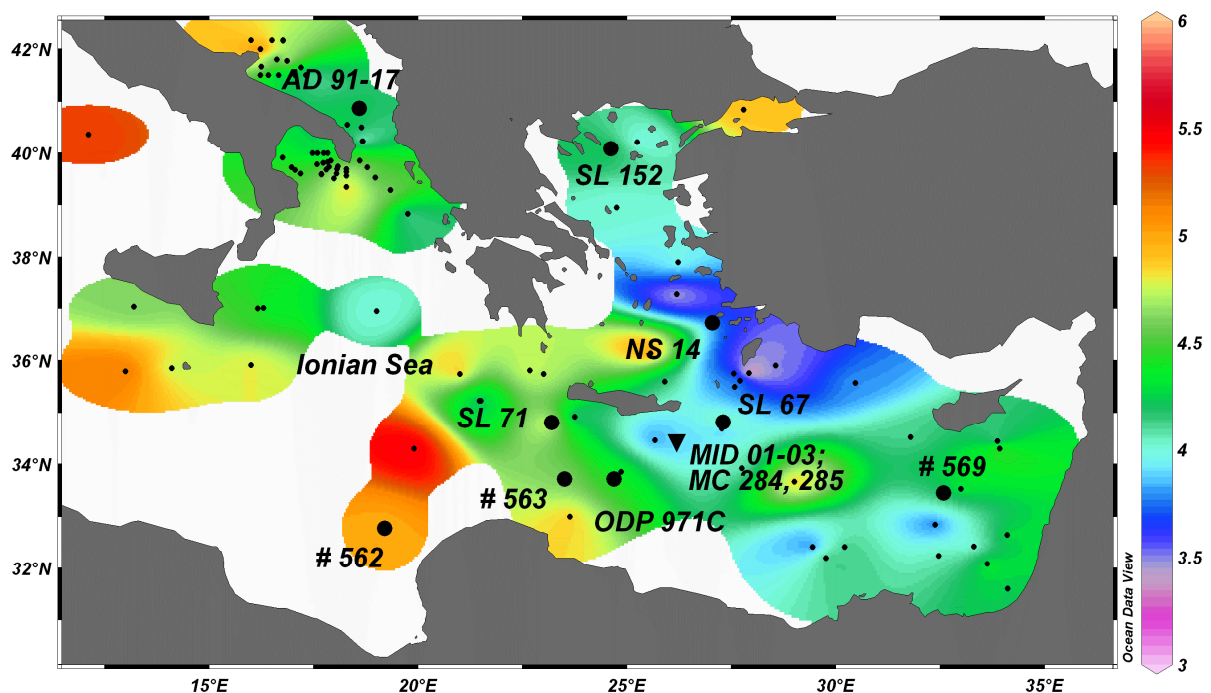


Figure 4.1: Sampling sites in the Eastern Mediterranean Sea. Large dots: Sediment cores; Triangle: Ierapetra Deep sediment traps and multicores; small dots: surface sediment samples. The color shading is $\delta^{15}\text{N}$ (‰) in surface sediments based on this study and Struck et al. (2001). The map is produced by using Ocean Data View (Schlitzer, 2009).

Sediment samples were taken during Meteor cruises M 40/4, M 44/4, M 51/3 as well as RV Minerva AD91 cruise (Giunta et al., 2003) and RV Aegeo cruise (Triantaphyllou et al., 2009) as multicores and gravity cores. ODP 971C is an Ocean Drilling Program core recovered during Leg 160. Further details are given in Table 4.2. Core locations and the sediment trap deployments are shown in Figure 4.1, superimposed are contours of present-day surface sediment $\delta^{15}\text{N}$ in ‰.

Table 4.1: Sediment trap moorings in the Ierapetra Deep: Position, water depth, sampling depth, deployment period and trap type.

Mooring	Longitude (°E)	Latitude (°N)	Water depth (m)	Sampling depth (m)	Deployment period dd.mm.yy	Trap type
MID 01	26.1792	34.4317	3750	2720	30.01.99 - 13.04.99	Mark VII
MID 02	26.1900	34.4417	3600	2560	05.11.01 - 01.04.02	Mark VII
MID 03 SH	26.1930	34.4438	3620	1508	30.01.07 - 22.08.07	Mark VII
MID 03 DP	26.1930	34.4438	3620	2689	30.01.07 - 22.08.07	Kiel K/MT 234

Table 4.2: Sediment sampling locations and sample types: MC = Multicore, GC = Gravity Core, ODP = Ocean Drilling Program Core.

Cruise	Core	Core type	Long. (°E)	Lat. (°N)	Waterdepth (m)
M 51/3	# 562	MC	19.191	32.774	1390
M 51/3	# 563	MC	23.499	33.718	1881
M 51/3	# 569	MC	32.576	33.452	1294
M 51/3	SL 152	GC	24.611	40.087	978
M 40/4	SL 67	GC	27.296	34.814	2158
M 40/4	SL 71	GC	23.194	34.811	2788
M 44/4	MC 284	MC	26.097	34.415	4263
M 44/4	MC 285	MC	26.179	34.432	3702
RV Ageo	NS 14	GC	27.047	36.725	505
RV Minerva	AD 91-17	GC	18.586	40.870	844
ODP 160	ODP 971C	ODP	24.683	33.717	2141

4.2.1. Analytical methods: organic carbon and nitrogen

Total carbon, organic carbon and total nitrogen were measured in duplicate by a Carlo Erba 1500 CNS Analyser (Milan, Italy). The precision of this method is 0.01% for total carbon and 0.002% for nitrogen. Organic carbon was analysed after removal of CaCO₃ by 1N hydrochloric acid (three times) with a precision of 0.02%.

4.2.2. Stable nitrogen isotopic ratio ($\delta^{15}\text{N}$)

The ratio of the two stable isotopes of nitrogen (¹⁵N/¹⁴N) is expressed as $\delta^{15}\text{N}$ after determining the abundance of the two isotopes in samples (after combustion and reduction of NO_x to N₂) by mass spectrometry:

$$\delta^{15}\text{N} (\text{‰}) = \frac{(R_{\text{sample}} - R_{\text{standard}})}{R_{\text{standard}}} * 1000 \quad R = \frac{{}^{15}\text{N}}{{}^{14}\text{N}} \quad (4.1)$$

The standard is atmospheric N₂, defined as $\delta^{15}\text{N} = 0\text{‰}$.

$\delta^{15}\text{N}$ values were determined using a Finnigan MAT 252 gas isotope mass spectrometer after high-temperature flash combustion in a Carlo Erba NA-2500 elemental analyzer at 1100°C. Pure tank N_2 calibrated against the reference standards IAEA-N-1 and IAEA-N-2 of the International Atomic Energy Agency and a sediment standard was used as a working standard. $\delta^{15}\text{N}$ is given as the per mil deviation from the N-isotope composition of atmospheric N_2 . Analytical precision was better than 0.1‰ based on replicate measurements of a reference standard. Duplicate measurements of samples resulted in a mean standard deviation of 0.19‰.

4.2.3. Amino acids

Total hydrolysable amino acids were analysed with a Biochrom 30 Amino Acid Analyser after hydrolysis of 3-40 mg of sediments with 6 N HCl for 22 hours at 110°C. After separation with a cation exchange resin, the individual monomers were detected fluorometrically. Duplicate analysis according to this method results in a relative error of 4% for total amino acids. Further analytical details are given elsewhere (Jennerjahn and Ittekkot, 1999; Lahajnar et al., 2007).

Ratios and indices derived from the monomeric distribution of amino acid are used to estimate the state of organic matter decomposition. The degradation index DI statistically evaluates relative abundances of the 14 most common proteinogenic amino acids (Dauwe et al., 1999). The data matrix used for a principal component analysis was the amino acid composition of 28 samples, representing a wide range of environmental settings and degradation states from living plankton to Pleistocene sediments. First axis factor scores derived from this analysis were taken as the DI (Dauwe et al., 1999). To apply this index to our datasets, the molar percentages of individual amino acids were inserted as var_i into the following formula:

$$\text{DI} = \sum_i \left[\frac{\text{var}_i - \text{AVG var}_i}{\text{STD var}_i} \right] * \text{fac.coef}_i \quad (4.2)$$

where the deviation of the molar percentage of each amino acid from an average value (AVG) is multiplied by an individual coefficient (fac.coef). AVG, fac.coef and STD (standard deviation) are those given in the original publication (Dauwe et al., 1999). The sum of all operations yields the DI of a given sample. Typical DI values range from 2 in well preserved samples (e.g. fresh OM and sapropels) to -1.5 in highly degraded sediments.

4.2.4. X-ray fluorescence

Concentrations of aluminum and barium were analyzed on fused (600 mg of sample diluted with 3600 mg of lithium tetraborate) discs in an automated x-ray fluorescence spectrometer MagixPRO (Panalytical) that is equipped with a Rh-anode. Loss on ignition was determined at 110°C and at 1000°C. Concentrations of major and trace elements were calculated based on a calibration against international standards. Ratios of Ba/Al were calculated as weight ratios of the elements barium and aluminum in the samples.

4.3. Results

4.3.1. Sediment traps

Mean fluxes of TOC and TN in the sediment traps at Ierapetra mooring MID varied between 0.57 and 0.81 $\text{mg}\cdot\text{m}^{-2}\cdot\text{d}^{-1}$ TOC (0.06 to 0.08 $\text{mg}\cdot\text{m}^{-2}\cdot\text{d}^{-1}$ TN) in the deep traps and 3.57 $\text{mg}\cdot\text{m}^{-2}\cdot\text{d}^{-1}$ TOC in the shallow trap (0.37 $\text{mg}\cdot\text{m}^{-2}\cdot\text{d}^{-1}$ TN) and followed the decrease of total flux (Table 4.3) during particle sinking in the water column. On the other hand $\delta^{15}\text{N}$, TOC% and DI show no depth dependence. Mean values of $\delta^{15}\text{N}$ in SPN are between 0.76 and 2.17‰ (Table 4.3) whereas TOC contents and DI range from 2.50 to 2.76% and from -0.21 to 0.32, respectively.

Table 4.3: Sediment trap moorings in the Ierapetra Deep: Mean values of $\delta^{15}\text{N}$, DI, TOC and total flux.

Mooring	$\delta^{15}\text{N}$ (‰)	DI	TOC (%)	Total flux ($\text{mg}\cdot\text{m}^{-2}\cdot\text{d}^{-1}$)
MID 01	2.17	-0.21	2.67	24.64
MID 02	1.19	-0.01	2.76	44.38
MID 03 SH	0.90	0.32	2.50	178.54
MID 03 DP	0.76	0.21	2.52	44.27

4.3.2. Surface sediments

The $\delta^{15}\text{N}$ values of surface sediments are between 3.5 and 5.0‰ (Figure 4.1, Table 4.4) and thus are significantly enriched over the sinking material intercepted by the sediment traps. However, the general level of $\delta^{15}\text{N}$ is low in comparison to values reported for other surface sediments overlain by oxygenated deep waters (Holmes et al., 1996; Holmes et al., 1997; Gaye-Haake et al., 2005). Low TOC contents (0.26 to 0.75%) and poor preservation reflected by DI

values that range from -0.99 to 0.47 are characteristic for the hemipelagic, well oxygenated open marine sediments of the EMS.

Table 4.4: $\delta^{15}\text{N}$, DI and TOC values of recent surface sediments as well as from S1, S5 and S6 sapropel interval (¹)= estimated values; ²)= mean values of entire sapropel).

Core	Time equivalent	$\delta^{15}\text{N}$ (‰)	DI	TOC (%)
# 562		5.00	-0.47	0.26
# 563		4.50	-0.71	0.40
# 569		3.50	-0.48	0.36
SL 152	recent surface sediments	4.30	-0.99	0.75
SL 67		4.40	-0.79	0.44
SL 71		5.00	-0.64	0.45
NS 14		3.90 ¹)	n.a.	n.a.
AD 91-17		4.30 ¹)	n.a.	n.a.
# 562		1.74	0.62	1.74
# 563		0.52	n.a.	1.94
# 569		1.34	0.70	1.64
SL 152	S1 sapropel ²)	2.81	0.24	1.37
SL 67		1.25	n.a.	n.a.
SL 71		1.57	0.96	2.29
NS 14		2.3	0.46	0.86
AD 91-17		3.56	n.a.	n.a.
SL 71	S5 sapropel ²)	-1.01	2.33	7.11
ODP 971C		-0.69	2.43	4.47
SL 71	S6 sapropel ²)	0.17	2.00	2.8

4.3.3. Downcore variations

The insert in Figure 4.2 displays DI and $\delta^{15}\text{N}$ in the upper 10 cm of two multicores retrieved from the Ierapetra Deep close to the trap location. Both cores show a downward enrichment in $\delta^{15}\text{N}$, which is most pronounced in the uppermost 1.5 cm (MC 284 from 2.3 to 4.8‰; MC 285 from 3.5 to 4.6‰) and which goes in concert with an increase in amino acid degradation. Downcore plots of analytical results for multicore #569 from Eratosthenes Seamount in the eastern Levantine Basin that includes the S1 are shown in Figure 4.3a. The %TOC ranges from 1.2 to 2.0% between 22 and 30 cm core depth and indicates the extant sapropel S1 (dark shaded). Above S1, %TOC ranges from 0.18 to 0.37%, below S1 we measured 0.58 to 0.76% in the so-called protosapropel (McCoy, 1974; Anastasakis and Stanley, 1984). A high Ba/Al ratio (seen as the strongest argument for elevated productivity during S1 formation) (Thomson et al., 1999), outlines the original extent of the sapropel in a bell-shaped maximum centered at 22 cm. In the interval from 13 - 22 cm core depth, divergence of Ba/Al and TOC curves marks the burndown zone above the visible S1 (light shaded), where downward progression of oxygen eradicated the

high TOC concentrations, but did not affect Ba/Al (Thomson et al., 1995). The DI curve follows that of TOC contents and displays a well preserved sapropel (DI = 0.4 to 0.9); OM is highly degraded above the sapropel and especially so in the burndown zone (-1.7 to -0.5). In the protosapropel, organic matter is less preserved than in the sapropel directly above (DI = -0.2 to -0.1). The $\delta^{15}\text{N}$ pattern is a mirror image of %TOC and DI curves with values between 4 and 5‰ above the sapropel (an exception is the low value of 3.5‰ of surface sediment), relatively light $\delta^{15}\text{N}$ (0.6 to 2‰) in the sapropel, and intermediate values (2.6 to 3.3‰) in the proto-sapropel. Cores #562 and #563 (Figure 3.3b and 3.3c) show more or less the same patterns in %TOC, $\delta^{15}\text{N}$ and Ba/Al as core #569 and confirm it as typical examples of sapropel S1.

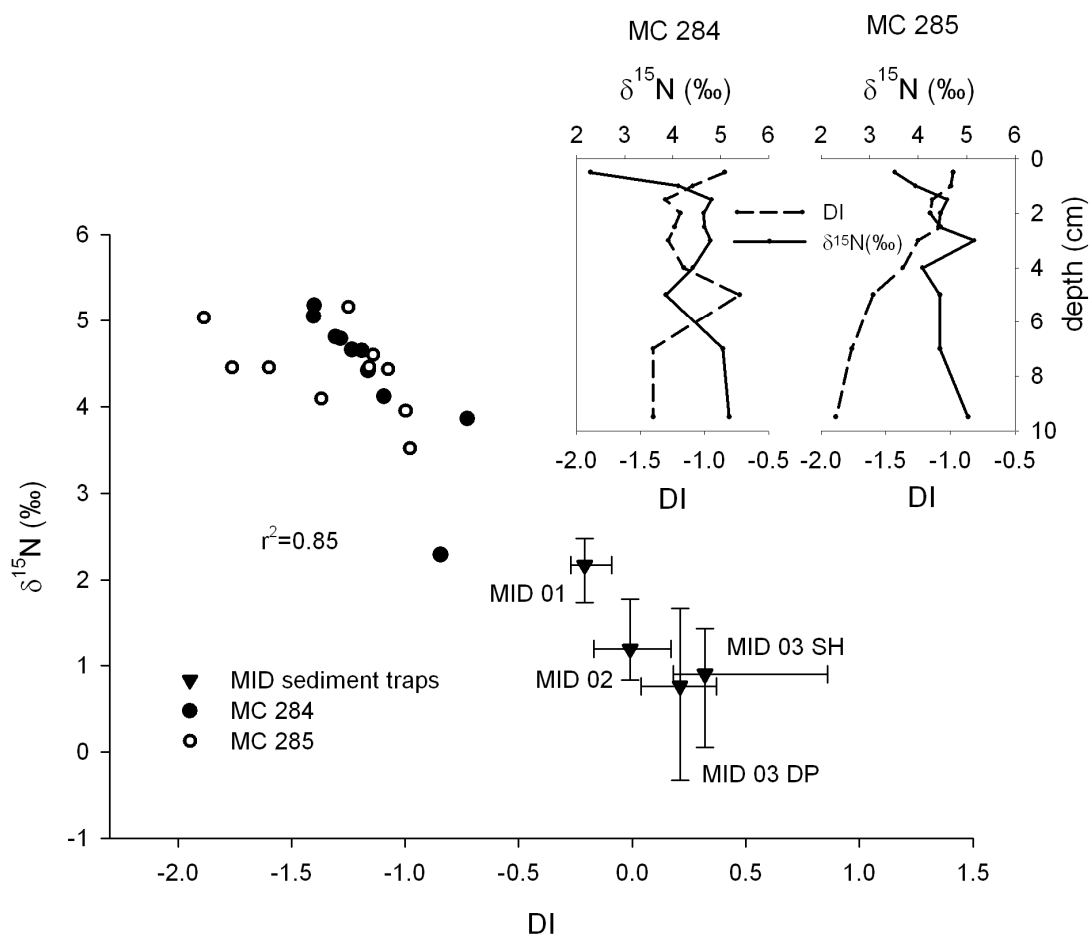


Figure 4.2: $\delta^{15}\text{N}$ vs. degradation index (DI) in cores MC 284/285 from Ierapetra Deep and mean values from MID sediment traps. Insert: High resolution records of $\delta^{15}\text{N}$ and DI of multicores MC 284 and MC 285.

Mean values of $\delta^{15}\text{N}$, DI, TOC for the S1 sapropel at the eight locations examined and for the recent surface sediments at these sites are listed in Table 4.4 (see Table 4.2 for locations and water depths). Average $\delta^{15}\text{N}$ in the S1 range from 0.52‰ in core #563 to 3.56‰ in core AD 91-17. The DI indicates best preservation of amino acids in core SL 71 south of Crete (DI 0.96) and poorest preservation in SL 152 in the northern Aegean Sea (DI 0.24). %TOC in S1 ranges from an

average of 0.96% in NS 14 (Aegean Sea) to 2.29% in SL 71. Unfortunately, DI and TOC data are not available for S1 in core SL 67, and DI data are lacking for cores AD91-17 and #563. The S5 (deposited after 127 kyr) and S6 sapropels (deposited after 176 kyr) from cores SL 71 and ODP 971 C (Table 4.4) have highest organic carbon concentrations (2.8 to 7.1%) and best amino acid preservation, whereas $\delta^{15}\text{N}$ is most depleted in these two older sapropels ($\delta^{15}\text{N} = 0.17$ to -1.01%).

4.4. Discussion

Although the modern N-cycle of the EMS may not be in a natural state due to anthropogenic inputs of atmospheric nitrate that currently dominates external N-inputs (Mara et al., 2009), this reactive N has a $\delta^{15}\text{N}$ of approximately -3% (Mara et al., 2009) and thus is very similar to fixed N (-2 to 1% ; Minagawa and Wada, 1986) that most likely has been the prevailing N source to the EMS in pre-industrial times (Sachs and Repeta, 1999). This coincidence in the $\delta^{15}\text{N}$ of the dominant N source is fortuitous, but it permits us to track the effects of diagenesis from the water column to the sediment record.

4.4.1. Alteration of amino acids and $\delta^{15}\text{N}$ in the water column and in surface sediments

Enrichment of $\delta^{15}\text{N}$ during sinking of particles through an oxygenated water with increasing water depth and at oxygenated sea floors is well known from other studies. Surface sediments commonly show an enrichment of 3- 4‰ over material in the oceanic mixed layer and sinking particles (Altabet, 1996; Gaye-Haake et al., 2005). Increasing $\delta^{15}\text{N}$ together with progressive amino acid degradation in the two multicores from Ierapetra Deep (Figure 4.2) illustrate an enrichment of sedimentary $\delta^{15}\text{N}$ during early diagenesis in the uppermost cm (which is still affected by sea water) as observed in the Eastern Atlantic (Freudenthal et al., 2001). A plot of $\delta^{15}\text{N}$ vs. DI (Figure 4.2) highlights the close relationship between $\delta^{15}\text{N}$ and degradation state for sinking material (mean values and ranges from Ierapetra Deep sediment trap long term moorings MID 01 – 03) and sediments. The linear regression ($r^2 = 0.85$) for the entire data set is highly significant and indicates an enrichment of 3 to 4‰ in $\delta^{15}\text{N}$ during OM decomposition from the water column to the sediment in the modern EMS. Pronounced differences in preservation and relative OM content are not evident between shallow and deep traps, contrasting with differences between traps and surface sediments. This implies that degradation during particle sinking in the water column (few days or weeks) has a much smaller effect than degradation at the oxic seafloor, where organic matter is exposed for decades and centuries due to low sedimentation and sealing rates. The observed decrease in total flux (the deep trap captured only one quarter of the shallow

trap) thus reflects disaggregation and disintegration of sinking material without compound-specific fractionation.

4.4.2. The record of S1

The systematic variations in OM preservation and $\delta^{15}\text{N}$ in the modern EMS help us to interpret the $\delta^{15}\text{N}$ record of core #569 (Figure 4.3a). A plot of DI versus $\delta^{15}\text{N}$ for samples from this core (Figure 4.4) again indicates a highly linear relationship between the $\delta^{15}\text{N}$ and OM preservation. The well preserved and isotopically depleted sapropel S1 (core interval from 22 to 31 cm) defines one end of a slope at good preservation state and low $\delta^{15}\text{N}$ that ends with strongly degraded and ^{15}N enriched (burndown and post sapropel) sediments of the upper core section. Recent surface sediment (0- 1 cm) and the protosapropel are moderately preserved and moderately enriched in $\delta^{15}\text{N}$. In this plot, average values from sediment trap material plot close to protosapropel and sapropel samples. This implies that the $\delta^{15}\text{N}$ of primary produced organic matter probably was similar during sapropel deposition as today because data from sediment traps show that relatively fresh OM sinking through the water column today has an isotopic signature similar to that of sapropels. This has already been postulated by (Sachs and Repeta, 1999), but possibly for the wrong reason: The $\delta^{15}\text{N}$ today is determined by atmospheric nitrate inputs, whereas the S1 inputs must have been N_2 fixation.

What is most important is the fact that major temporal fluctuations in the core record appear to be largely controlled by OM preservation (as indicated by the DI) and not by reactive N sources: ^{15}N enrichment in sedimentary N unambiguously occurs as an enrichment of ^{15}N in residual OM during progressive mineralization (ammonification) in the sediment as shown by the insert in Figure 4.4. This matches experimental evidence of changes in $\delta^{15}\text{N}$ in algal material exposed to oxic degradation (Lehmann et al., 2002). The sapropel deposited during anoxic conditions at the seafloor or in the water column below 1800 m water depth (de Lange et al., 2008), when decay was inhibited, retained the $\delta^{15}\text{N}$ of primary production. The protosapropel that developed under suboxic conditions is slightly degraded and slightly enriched in $\delta^{15}\text{N}$ over the sapropel base level. The $\delta^{15}\text{N}$ of the burn-down zone above the visible sapropel originally must have been equally low as in the visible sapropel but became enriched during re-oxygenation of the sediment. Interestingly, recent sinking material from sediment traps is somewhat more degraded and enriched in ^{15}N in comparison to the material in the S1 sapropel. It may not reflect the original $\delta^{15}\text{N}$ of primary produced OM because the traps sampling at depths of 1508 to 2720 m intercept material that has already been slightly degraded and thus isotopically enriched.

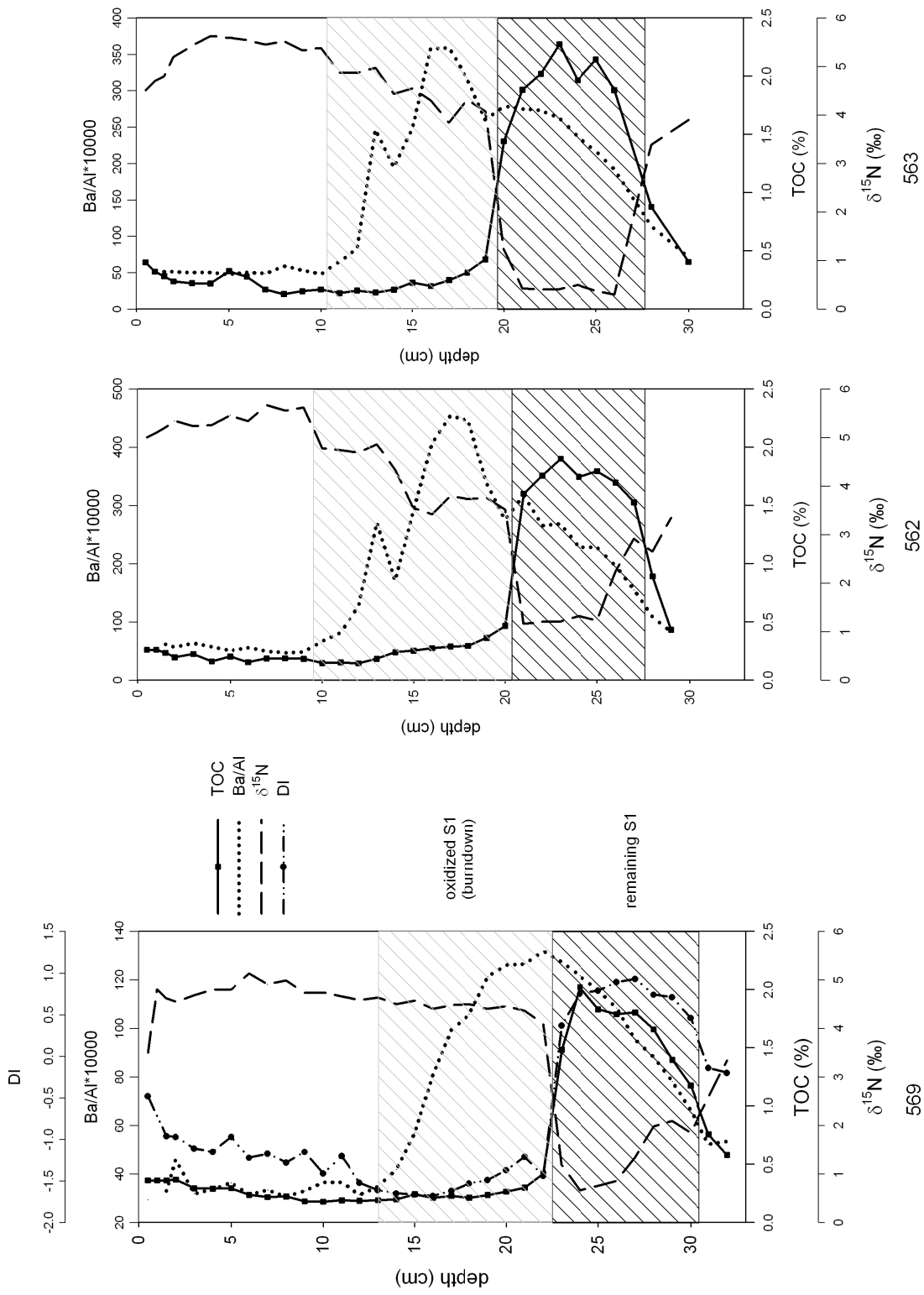


Figure 4.3: Downcore plots of total organic carbon (%TOC), barium to aluminum ratios, degradation index (DI) and $\delta^{15}\text{N}$ in multicores #569 (a), #562 (b) and #563 (c). S1 sapropel intervals and the burn-down zone above S1 are marked.

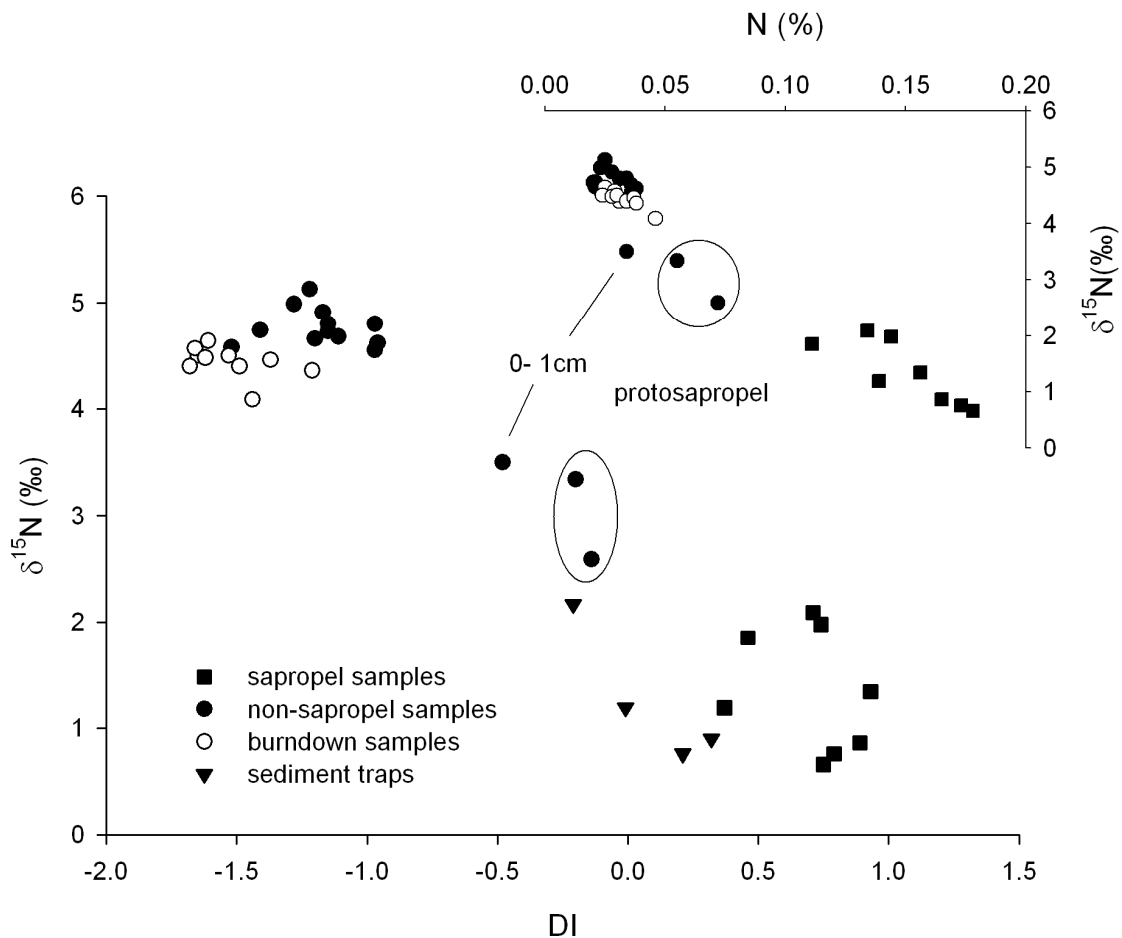


Figure 4.4: $\delta^{15}\text{N}$ vs. DI in core #569 and mean values from MID sediment traps. Insert: $\delta^{15}\text{N}$ vs. N (%) in core #569. Residual N becomes isotopically enriched during remineralization. Surface sediments and protosapropel are marked in both plots.

Can the data help to reconstruct the $\delta^{15}\text{N}$ of primary produced OM in pre-industrial times, i.e. between the S1 sapropel and the recent sediment surface that may be contaminated with NO_x ? In core #569, the pre-industrial interval (from 1 to 13 cm) has $\delta^{15}\text{N}$ values between 4 and 5‰. According to the slope of $\delta^{15}\text{N}$ versus DI (Figure 4.4) and extrapolating to well-preserved OM (DI between 0.5 and 1.0), we reconstruct an original $\delta^{15}\text{N}$ of 0 to 2‰ in fresh OM produced at that time, even though the modern atmospheric source was not yet in operation. This requires that either (1) nitrogen fixation was significant in the pre-industrial EMS or that (2) other isotopically sources with low $\delta^{15}\text{N}$, such as terrestrial/riverine N, were the major inputs. We speculate that the EMS has been N-limited since millennia, and N-fixation occurred regardless of sapropel stages or “normal” stages until the 20th century. During the last decades, atmospheric inputs of industrial NO_x replaced N-fixation as an N-source in a smooth transition – and the EMS became P-limited due to excess external N loads. Because N-fixation and NO_x both result in $\delta^{15}\text{N}$ depleted OM, the transition is not visible in the core record. One could argue that downcore enrichment in ^{15}N in several EMS core tops (MC 284, MC 285, #562, #563 and #569) *reflects* the transition to the

more depleted source of reactive N. However, the simultaneous increase of amino acid degradation strongly suggests that the enrichment must be due to diagenesis.

4.4.3. Spatial gradients during the S1 sapropel time slice

Comparing the mean values of $\delta^{15}\text{N}$ in S1 sapropels at eight locations in the EMS shows that $\delta^{15}\text{N}$ is not spatially homogeneous during the S1 sapropel timeslice; this is in contrast with records for S5 (Struck et al., 2001) that all originated from deep basins. Five cores from the Levantine Basin and the Ionian Sea (M40-4 67, M40-4 71 and M51-3 562, 563 and 569) are relatively more depleted in ^{15}N compared to nearshore locations in the Adriatic and in the Aegean Sea (AD 91-17, NS 14 and SL 152). In line with the hypotheses formulated above, we also attribute this gradient to preservational effects: The northern Mediterranean sub-basins have been suboxic, but not anoxic, during S1 deposition, as is indicated by benthic foraminiferal assemblages and abundances (Kuhnt et al., 2008; Kuhnt et al., 2007). Somewhat higher $\delta^{15}\text{N}$, less well preserved amino acids, and lower %TOC than in S1 from the deep basins probably result from stronger degradation during particle settling through the suboxic water column and at the suboxic seafloor. Average $\delta^{15}\text{N}$ and DI values of samples from the S1 time slice (insert Figure 4.5) follow the same linear relationship between OM preservation and nitrogen isotope composition as was found for recent samples from Ierapetra Deep (MC 284, MC 285, MID 01 – 03) and the paleo record from Eratosthenes Seamount (M51-3 #569). But even if the trend is highly linear, some influence of different nitrate sources/utilization may be present: Extremely ^{15}N depleted OM in cores from the deep basins may have been contributed mainly by nitrogen fixing cyanobacteria, whereas locations closer to land may have been more influenced by terrestrial/riverine OM inputs that are somewhat less depleted in ^{15}N (0 to 5‰, Mayer et al., 2002; Voss et al., 2006). Possibly due to the dominant atmospheric source today, recent Eastern Mediterranean surface sediments display a more or less homogeneous pattern in $\delta^{15}\text{N}$ without pronounced gradients from open marine to nearshore environments or from north to south (see Figure 4.1).

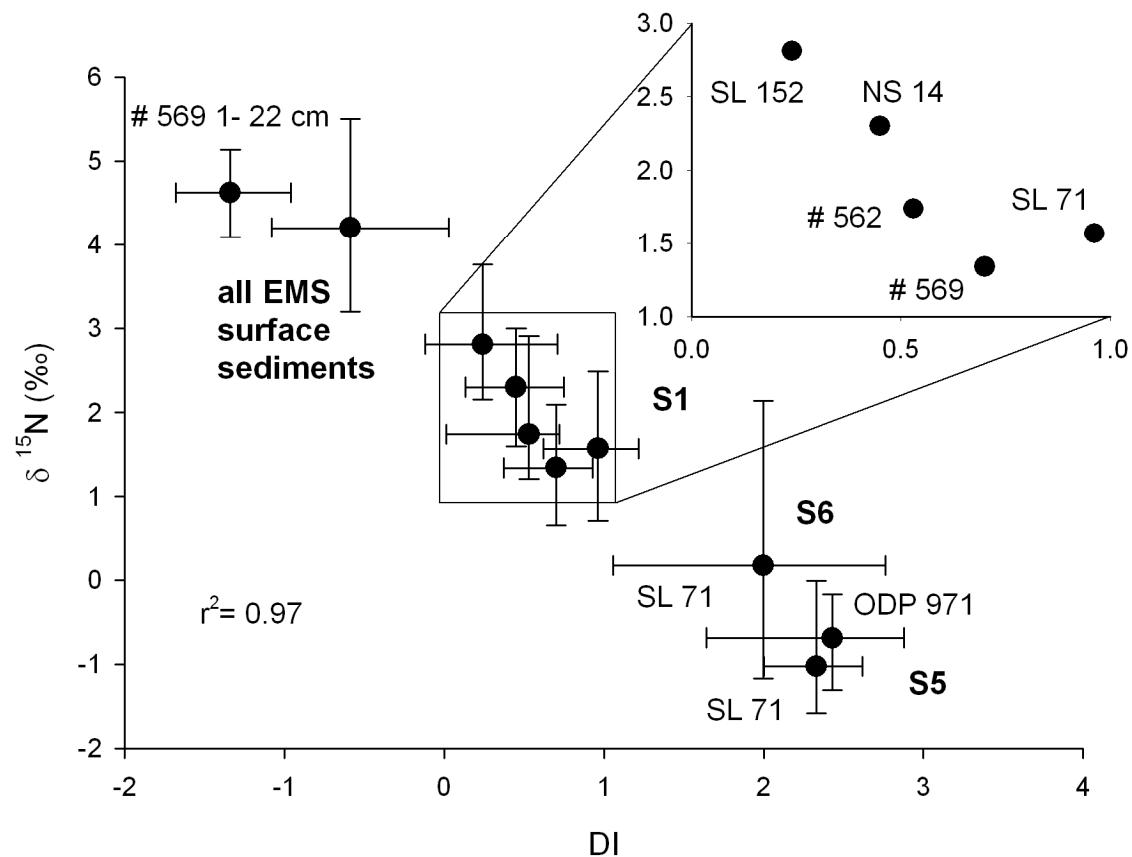


Figure 4.5: $\delta^{15}\text{N}$ vs. DI for S1, S5 and S6 sapropels, core #569 and all Eastern Mediterranean surface samples. Mean values.

4.4.4. The S5 and S6 sapropel

The older sapropels S6 and in particular the S5 have even higher organic carbon contents, better preservation of amino acids, lower $\delta^{15}\text{N}$ values, and greater thickness than the S1 sapropel, and $\delta^{15}\text{N}$ and DI for these layers in cores ODP 971C and SL 71 extend the linear relationship between preservation and $\delta^{15}\text{N}$ (Figure 4.5). This implies a similar isotopic signature of primary produced PN for all sapropels, and also suggests that the PN produced during S5 was uncharacteristically depleted ($< -1\text{‰}$). As in surface sediments and S1, the differences between the sapropels must be due to differences in organic matter preservation that may have been caused by variable degrees of anoxia during deposition: The depth of the oxycline and hence the oxygen exposure time of the sinking material has been variable for each sapropel interval as indicated by biomarker records. For the S5 sapropel (which has best preservation and lowest $\delta^{15}\text{N}$), molecular fossils of anaerobic, photolithotrophic green sulphur bacteria (*Chlorobiaceae*) evidence a relatively shallow oxic/anoxic interface at 150 to 300 m water depth (Rohling et al., 2006), whereas during S1 sapropel deposition the interface has been at ~ 1800 m (de Lange et al., 2008).

4.4.5. Alternative explanations for ^{15}N depletion in sapropels

The negative $\delta^{15}\text{N}$ in S5 is unusual even if N_2 -fixation and/or incomplete nitrate utilization occurred, and we speculate that another source of isotopically light nitrogen may have contributed to sedimentary N: Recent studies in the Black Sea, which is permanently anoxic at depth and thus may be a suitable analogue for the S5 situation in the EMS, revealed that appreciable amounts of depleted particulate N must be produced by chemoautotrophic bacteria at the transition from suboxic to anoxic waters (Fry et al., 1991; Coban-Yildiz et al., 2006). This production is sustained by either assimilation of ammonia (Fry et al., 1991; Coban-Yildiz et al., 2006) or may derive from chemoautotrophic fixation of N_2 (McCarthy et al., 2007; Fuchsman et al., 2008) and N_2O (Westley et al., 2006) that has been released by denitrification or anammox. Water column profiles of suspended organic $\delta^{15}\text{N}$ (SPON) (Coban-Yildiz et al., 2006) show a slight enrichment from ca. 4‰ in the upper mixed layer to up to 8‰ at the oxycline, as expected during early stages of OM decomposition in an oxygenated water column. Below the oxycline in the Black Sea, however, $\delta^{15}\text{N}$ values shift dramatically to extremely depleted values (-8‰) at the top of the anoxic water body. A simultaneous increase in the mass of total SPON implies that ^{15}N -depleted OM must be newly produced. This was attributed to newly produced OM by the biomass of chemoautotrophic bacteria utilizing NH_4^+ as their dominant N source (Coban-Yildiz et al., 2006). Estimated fractionation factors for bacterial ammonia assimilation are between 11 and 14‰ (Hoch et al., 1992; Voss et al., 1997), explaining the extremely low $\delta^{15}\text{N}$ values of bacterial biomass.

A second mechanism leading to negative $\delta^{15}\text{N}$ in S5 may have been the fixation of ^{15}N depleted N_2 and N_2O that was released by denitrification and anammox. An unusual isotopomeric composition of N_2O in the suboxic zone of the Black Sea suggested that there has been consumption and hence assimilation of depleted N (Westley et al., 2006), and N_2 fixation has been observed in samples from the suboxic water layer during incubation experiments (McCarthy et al., 2007).

Considering the recent Black Sea as an analog of the EMS in its sapropel mode (i.e. anoxic deepwater, stratification, reduced surface water salinity, low ^{15}N values, TOC-rich sediments), it appears plausible that similar processes also occurred at the redox boundary in mid-water during sapropel S5 formation. The extremely low ^{15}N values in the S5 sapropel and as low as -5‰ in older Pliocene sapropels (Arnaboldi and Meyers, 2006) are difficult to explain by either N_2 -fixation from cyanobacteria or by the preferential uptake of $^{14}\text{N}\text{-NO}_3^-$ as a result of NO_3^- excess alone, but instead suggest a highly fractionating N-pathway such as chemoautotrophic NH_4^+ assimilation.

Interestingly, $\delta^{15}\text{N}$ values of recent deep Black Sea sediments (2-3‰; Reschke, 1999) are in the high range of Mediterranean sapropels (-5 to 3‰). The reason may lie in the fact that main sources of bioavailable N in the Black Sea are terrestrial and riverine inputs (McCarthy et al., 2007), whereas fixation of atmospheric N_2 probably was the main N-source during times of sapropel formation in the Mediterranean Sea.

4.4.6. Higher than modern productivity during S1 deposition?

There is a long-standing debate on whether TOC enrichment in Mediterranean sapropels may be solely due to better preservation under anoxic deepwater conditions, or whether it requires enhanced primary production (Howell and Thunell, 1992; Cheddadi and Rossignol-Strick, 1995). When comparing reconstructed TOC accumulation rates in the S1 sapropel with TOC fluxes in the sediment traps, we found that the modern flux rates would indeed suffice to produce a sapropel under appropriate preservation conditions: Sediment traps recorded a TOC-flux of 207 to 294 $\text{mg}\cdot\text{m}^{-2}\cdot\text{y}^{-1}$ in the deeper traps, and 1300 $\text{mg}\cdot\text{m}^{-2}\cdot\text{y}^{-1}$ in the shallow trap. On the other hand, the TOC accumulation rate for the S1 sapropel of core #569 is roughly 450 $\text{mg}\cdot\text{m}^{-2}\cdot\text{y}^{-1}$, which agrees with accumulation rates calculated for a larger set of S1 by de Lange et al. (2008). Not only is the accumulation rate similar, but also %TOC of sinking material is in the range known from the S1 sapropel (see Table 4.3 and Table 4.4). The EMS was suboxic in waters deeper than 400 m (Anastasakis and Stanley, 1986) and anoxic below 1800 m during S1 time (de Lange et al., 2008). Assuming a distinctly reduced or even inhibited decay of OM under anoxic conditions, and considering that OM in the traps has been already degraded during passage of the oxic water column, present-day export production in the EMS would suffice to create an S1 sapropel of the correct $\delta^{15}\text{N}$.

Enhanced primary productivity during S1 has mainly been inferred from elevated Ba/Al ratios (Thomson et al., 1999; de Lange et al., 2008), whereby the formation and enrichment of barite crystals occurs in predominantly siliceous detritus during particle sinking through the water column (Bishop, 1988; Dymond et al., 1992; Francois et al., 1995), and newly formed barite crystals are imbedded in a matrix of organic particles. In line with our findings on $\delta^{15}\text{N}$ and TOC we consider it possible that the accumulation of biogenic barium in sapropels may also be controlled by OM preservation. During particle disaggregation, intense OM remineralization and cell lysis during particle sinking in the water column under normal oligotrophic conditions, barite crystals become exposed to and dissolve in sea water (Dehairs et al., 1980; Dehairs et al., 1990). This affects more than 70 % of the particulate Ba flux in the recent Southern Atlantic Ocean (Dehairs et al., 1980). On the other hand, if OM is less degraded and remineralized during passage

through a suboxic or anoxic water column where OM decay is inhibited, barite is shielded in more or less intact detritus and accumulates in higher relative amounts in the sediments. This may have been the case during Mediterranean sapropel formation and may explain the high Ba contents without the need of enhanced organic carbon flux rates.

In the oxidized upper part of S1, however, Ba concentrations are decoupled from organic carbon. Whereas OM is respired to CO_2 and NH_4^+ during diagenesis, elevated barium concentrations remain as a relatively inert trace of former OM rich layers (Thomson et al., 1995) that outline the original extent of sapropels.

4.5. Conclusions

We have shown that variations of $\delta^{15}\text{N}$ in Eastern Mediterranean sediment records are closely tied to OM preservation and do not reflect the isotopic composition of the reactive nitrogen source or nitrate utilisation. Diazotrophic nitrogen fixation very likely has been the dominant N source at least during the Holocene and probably since the Pleistocene – regardless of whether the Mediterranean Sea was in sapropel or non-sapropel mode. Spatial patterns in $\delta^{15}\text{N}$ of S1 can also be attributed to variable degrees of OM preservation due to differences in water column oxygenation at different sites. TOC accumulation rates in long-term sediment trap moorings from the EMS are the same as those calculated for sapropel S1, so that present day primary production levels would be sufficient to create a S1 analog under conditions of deep water anoxia. The strongest argument for elevated organic carbon export fluxes from the ocean surface during sapropel times are elevated Ba/Al records, which also may be affected by water column oxygenation.

5. Influence of Diagenesis on Sedimentary $\delta^{15}\text{N}$ in the Arabian Sea Over the Last 130 kyr

Abstract

We determined the ratio of stable nitrogen isotopes $^{15}\text{N}/^{14}\text{N}$ ($\delta^{15}\text{N}$) and amino acid composition in coeval sediments from Ocean Drilling Program (ODP) Hole 722 B in the central Arabian Sea and from Hole 724 C situated on the Oman Margin in the western Arabian Sea coastal upwelling area. The records span the last 130 kyr and include two glacial-interglacial cycles. These new data are used in conjunction with data available for surface sediments and other cores from the northern and eastern Arabian Sea to explore spatial variations in the isotopic signal and to evaluate effects of water depth, sedimentation rates and oxygen content at the sea floor on the isotopic signal. All core records have similar patterns through time, but different average values for $\delta^{15}\text{N}$ at each core location. All records show a positive correlation of $\delta^{15}\text{N}$ and with an amino-acid derived Reactivity Index (RI; Jennerjahn and Ittekkot, 1997) that indicates the relative degradation state of organic matter. The data confirm that changes in the isotopic source signal of nitrate, commonly attributed to variations in the intensity of denitrification in the regional mid-water oxygen minimum zone (OMZ), covary with enhanced productivity, but also with enhanced organic matter preservation. Different accumulation rates of the cores apparently have minor effect on amino acid reactivity and $\delta^{15}\text{N}$. Hence, parallel but offset trends in $\delta^{15}\text{N}$ and the RI at the different core locations through time are interpreted to reflect the isotopic signature of source nitrate; these original $\delta^{15}\text{N}$ are altered during early diagenetic degradation of N-bearing organic matter and can be normalized by using the RI. An evaluation of two preservation indexes based on amino acid composition (RI and the Degradation Index, DI; Dauwe et al., 1999) in both recent sediments and core samples suggests that the RI is more suitable than the DI in estimating the state of organic matter degradation in older sediments.

5.1. Introduction

The isotope ratio $^{15}\text{N}/^{14}\text{N}$ in sediment records, expressed as $\delta^{15}\text{N}$, is a commonly used proxy to reconstruct changes in the oceanic nitrogen cycle and to evaluate past ocean productivity (Farrell et al., 1995; Ganeshram et al., 2002; Altabet, 2007). The $\delta^{15}\text{N}$ of sediments reflects nitrogen sources (dissolved inorganic nitrogen, DIN) (Sweeney and Kaplan, 1980), as well as transformation processes in the ocean that cause isotopic fractionation during cycling of nitrogen (Altabet, 2006). Nitrate - the major DIN species - has an average $\delta^{15}\text{N}$ value of about $5.0\pm 0.5\text{‰}$ in deep waters of the modern global ocean (Sigman et al., 2000), which may have been different in the geological past in response to different source and sink terms (Brandes and Devol, 2002; Deutsch et al., 2004). Nitrate in modern intermediate water masses has more variable isotopic signatures than the deep reservoir which can be due to denitrification in oxygen-depleted subsurface waters that enriches the residual nitrate in ^{15}N up to above 15‰ (e.g., Naqvi et al., 1998; Voss et al., 2001; Thunell et al., 2004) or to the more recently discovered anammox process that probably also enriches residual $^{15}\text{NO}_3^-$ (Ward et al., 2009). Assimilation of such an enriched source entering the euphotic zone leads to $\delta^{15}\text{N}$ values of particulate organic matter and sediments far above 5‰ (Naqvi et al., 1998; Altabet et al., 1999a; Voss et al., 2001). Isotopically depleted $\delta^{15}\text{N}$ values, on the other hand, often occur in sediments with a strong imprint of relatively pristine terrestrial nitrogen supply (Gaye-Haake et al., 2005; Voss et al., 2005) or in areas of N_2 -fixation, which regionally or seasonally introduces depleted $\delta^{15}\text{N}$ that has the isotopic signal of air ($\sim 0\text{‰}$; Mariotti, 1984; Karl et al., 2002).

Isotopic fractionation during biological DIN uptake also has an effect on $\delta^{15}\text{N}$ of sediments. Lateral gradients of $\delta^{15}\text{N}$ in particulate N assimilated from an isotopically homogeneous DIN source are caused by “Rayleigh”-type fractionation during progressive DIN uptake by phytoplankton. The initial products are isotopically depleted over the nitrate pool, whereas later products are enriched over the original substrate (Altabet and Francois, 1994). This process can explain increases of $\delta^{15}\text{N}$ in sediments with increasing distance from nitrate sources such as river mouths and upwelling areas (Holmes et al., 1997; Pichevin et al., 2005). Incomplete nitrate utilization has been invoked to explain varying $\delta^{15}\text{N}$ in sedimentary archives (Calvert et al., 1992; Farrell et al., 1995).

Due to the short residence time of nitrogen in the ocean, the nitrogen cycle responds to perturbations on very short time-scales (Tyrrell, 1999; Deutsch et al., 2004). Variations of $\delta^{15}\text{N}$ values in late Quaternary sediment records of the Arabian Sea have been interpreted as signals of a response of the nitrogen cycle to climatic oscillations. Climatic changes led to changes in ocean

circulation and induce changes in denitrification rates, assimilation rates, nutrient limitations, or nitrogen fixation (Suthhof et al., 2001; Altabet et al., 2002; Ganeshram et al., 2002).

However, quantitative reconstructions of the global or regional N-cycles from geological records are generally hampered by early diagenetic overprinting of the original $^{15}\text{N}/^{14}\text{N}$ ratio. Offsets in $\delta^{15}\text{N}$ by 3-5‰ between particles in the water column and surface sediments have been observed in open ocean sediments (Francois et al., 1992; Francois et al., 1997; Gaye-Haake et al., 2005) and have been related to the intensity of degradation as reflected in the reactivity of amino acid (AA) mixtures in sediments (Gaye-Haake et al., 2005). Although exact mechanisms remain unknown, kinetic isotope fractionation during protein hydrolysis (Bada et al., 1989; Silfer et al., 1992) and deamination (Macko and Estep, 1984), resulting in the preferential loss of ^{15}N depleted compounds during organic matter (OM) degradation, very likely causes this enrichment.

Decomposition of particulate OM in aquatic environments follows different pathways and occurs in various steps. The main controlling factors are water column oxygenation, duration of particle sinking as a consequence of water depth and particle size as well as the sealing efficiency driven by sedimentation rates (e.g., Müller and Suess, 1979; Libes, 1992) that influence the residence time of OM at the sediment water interface. In contrast, sedimentary degradation after burial in the sediment is mediated by other microbial assemblages/communities than in the water column and, depending on the depth of burial and sequestration time, by kinetic/thermal decay ending in catagenesis (e.g., Tissot and Welte, 1978). Indexes of organic matter quality derived from AA composition, such as the Reactivity Index RI (Jennerjahn and Ittekkot, 1997) and the Degradation Index DI (Dauwe et al., 1999), are sensitive to degradation of OM in the water column and at the sediment water interface and have often been used to estimate organic matter quality (e.g., Unger et al., 2005; Kaiser and Benner, 2009); the extent to which they are overprinted by late-stage diagenesis upon burial during several thousand years after sedimentation has not been studied.

Our aim is to quantify diagenetic influences on sedimentary $\delta^{15}\text{N}$. We investigate surface sediments that were deposited in a wide range of water depths and oxygen contents in bottom waters, and sediment cores with variable sedimentation rates over the last 130 kyr from the Arabian Sea. The main goal of our study is to quantify potential influences on sedimentary $\delta^{15}\text{N}$ other than source nitrate $\delta^{15}\text{N}$ composition to permit an unbiased reconstruction of nitrate isotopic composition in this key area of the global N-cycle (Altabet et al., 2002). For this we produced paired data of $\delta^{15}\text{N}$ and of indices of organic matter degradation based on AA composition (Cowie and Hedges, 1992; Jennerjahn and Ittekkot, 1997; Dauwe and Middelburg, 1998; Dauwe et al., 1999). To test the two indexes RI and DI for suitability in studies of OM degradation over

geological periods we use statistical methods on data of amino acid composition in samples from ODP cores 722 B and 724 C and derive an index that captures OM degradation in sediment cores better than previously used indexes.

5.2. Study Sites

The data set of 46 surface sediments from the Arabian Sea north of 15° N and deeper than 250 m water depth published by Gaye-Haake et al. (2005) is our basis for estimating the effects of water depth and bottom-water oxygen contents on both the degradation of amino acids and $\delta^{15}\text{N}$. Oxygen contents in deep waters were interpolated for the sampling sites from the climatology of Gouretski and Koltermann (2004).

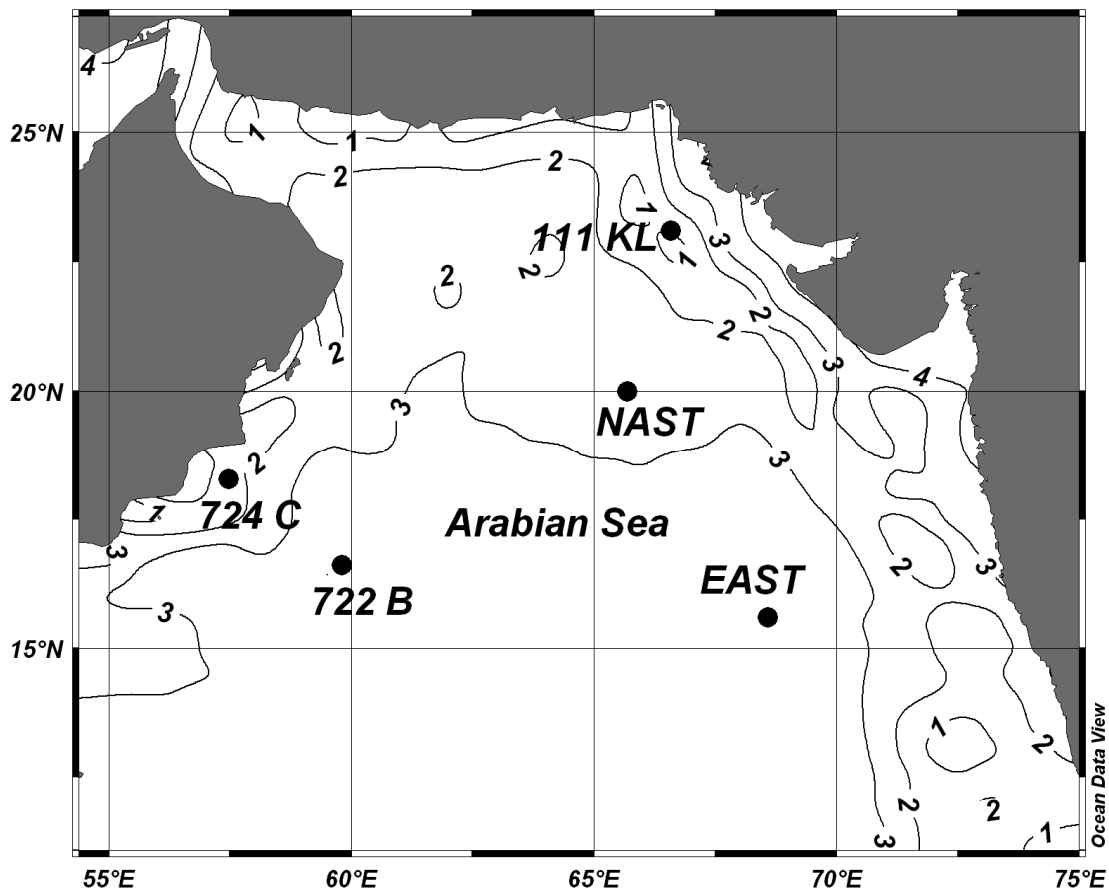


Figure 5.1: Oxygen concentrations (ml/l) in bottom water of the Arabian Sea (Gouretski and Koltermann, 2004) and locations of sites referred to in the text. This map is produced by using Ocean Data View (Schlitzer, 2009).

New data were raised from 2 Ocean Drilling Program (ODP) Sites (722 B and 724 C) in the western Arabian Sea; additional core data are from cores 111 KL, NAST and EAST in the northern and central Arabian Sea (Suthhof et al., 2001; Ivanova et al., 2003) (Figure 5.1 and Table 5.1). Site 722 is located on the Owen Ridge at a water depth of 2028 m ($16^{\circ}37'\text{N}$; $059^{\circ}48'\text{E}$), i.e. below the oxygen minimum zone of the Arabian Sea. Due to low detrital and biogenic particle fluxes in this offshore setting, the bulk sediment accumulation rates (BAR) calculated from linear sedimentation rates (based on the age model and on determinations of dry-bulk densities given in Prell et al. (1989)) on the Owen Ridge are lower than at the Oman margin Site 724. Site 724 is located on the upper slope of the Oman margin at a water depth of about 600 m ($18^{\circ}17'\text{N}$; $057^{\circ}28'\text{E}$), i.e. within the oxygen minimum layer. Sediments at Site 724 have higher organic carbon contents as well as higher accumulation rates compared to those at Site 722. Age models for Holes 722 B and 724 C are based on oxygen isotope stratigraphies of Clemens and Prell (1991) and Zahn and Pedersen (1991) and have been adjusted to visually fit the high-resolution $\delta^{15}\text{N}$ record in core NAST.

Core NAST was taken in the northern central Arabian Sea at $19^{\circ}59.9'\text{N}$ and $065^{\circ}41.0'\text{E}$ from a water depth of 3170 m; core EAST was raised at $15^{\circ}35.5'\text{N}$ and $068^{\circ}34.9'\text{E}$ at 3820 m water depth. Further details on these two cores are given in Suthhof et al. (2001), Ivanova et al. (2003) and Guptha et al. (2005). $\delta^{15}\text{N}$ of the NAST core older than 60 ky and the entire EAST core are published here for the first time. The Pakistan margin core 111 KL was retrieved from $23^{\circ}05.8'\text{N}$ and $066^{\circ}29.0'\text{E}$ at a water depth of 775 m and was described in Suthhof et al. (2001).

Table 5.1: Geographical position, water depth, and bottom water oxygenation (BWO) as well as examined depth interval (downcore from seafloor in m) and time equivalent (kyr) of examined cores.

Core	Latitude ($^{\circ}\text{N}$)	Longitude ($^{\circ}\text{E}$)	Bottom depth (m)	Core length (m)	Time interval (kyr)	BWO (ml/l)
ODP 722 B	$16^{\circ}37'$	$059^{\circ}48'$	2028	5.23	7.1- 130.1	2.78
ODP 724 C	$18^{\circ}17'$	$057^{\circ}28'$	603	12.26	5.6- 143.9	0.18
111KL	$23^{\circ}06'$	$066^{\circ}29'$	775	14.00	5.3- 60.8	0.09
EAST	$15^{\circ}36'$	$068^{\circ}35'$	3820	5.00	0.2- 132.9	3.39
NAST	$20^{\circ}00'$	$065^{\circ}41'$	3170	5.60	0.1- 132.8	2.89

5.3. Methods

5.3.1. Organic carbon and nitrogen

Total carbon and nitrogen were measured by a Carlo Erba elemental analyser 1500 (Milan, Italy). The precision of this method is 0.2% for carbon and 0.02% for nitrogen. Carbonate percentages were determined by a Wösthoff Carmograph 6 (Bochum, Germany). The relative error of carbonate analyses is 1%. Total organic carbon (TOC) was calculated as the difference between total and carbonate carbon.

5.3.2. Stable nitrogen isotopic ratio ($\delta^{15}\text{N}$)

The ratio of the two stable isotopes of nitrogen ($^{15}\text{N}/^{14}\text{N}$) is expressed as $\delta^{15}\text{N}$ after determining the abundance of the two isotopes in samples (after combustion and reduction of NO_x to N_2) by mass spectrometry:

$$\delta^{15}\text{N}_{\text{sample}} (\text{‰}) = (\text{R}_{\text{sample}}/\text{R}_{\text{standard}} - 1) * 1000 \quad \text{R} = ^{15}\text{N}/^{14}\text{N} \quad (5.1)$$

The standard is atmospheric N_2 ($\delta^{15}\text{N} = 0\text{‰}$).

$\delta^{15}\text{N}$ values were determined using a Finnigan MAT 252 gas isotope mass spectrometer after high-temperature flash combustion in a Carlo Erba NA-2500 elemental analyzer at 1100°C . Pure tank N_2 calibrated against the reference standards IAEA-N-1 and IAEA-N-2 of the International Atomic Energy Agency as well as a sediment standard that was used as a working standard. Analytical precision was better than 0.1‰ based on replicate measurements of a reference standard. Duplicate measurements of samples resulted in a mean standard deviation of 0.19‰ (Bahlmann et al., 2009).

5.3.3. Amino acids

Total hydrolysable AA were analysed with a Biochrom 30 Amino Acid Analyser after hydrolysis of 30-40 mg of sediments with 6 N HCl for 22 hours at 110°C . After separation with a cation exchange resin, the individual monomers were detected fluorometrically. Duplicate analysis according to this method results in a relative error of 4% for total AA. A list of AAs analyzed and the abbreviations used is given in Table 5.2. Further analytical details are given by Jennerjahn and Ittekkot (1999).

Table 5.2: Amino acids analyzed in this study, their abbreviations and occurrence in indexes. DI = Degradation Index; RI = Reactivity Index; PCA = Principal Component Analysis.

Protein amino acids	Abbrev.	DI	RI	PCA
cysteic acid	Cya			x
taurine	Tau			x
aspartic acid	Asp	x		x
threonine	Thr	x		x
serine	Ser	x		x
glutamic acid	Glu	x		x
glycine	Gly	x		x
alanine	Ala	x		x
valine	Val	x		x
methionine	Met	x		x
iso-leucine	Ile	x		x
leucine	Leu	x		x
tyrosine	Tyr	x	x	x
phenylalanine	Phe	x	x	x
histidine	His	x		x
tryptophane	Trp			x
lysine	Lys			x
arginine	Arg	x		x
Non-protein amino acids				
ornithine	Orn			x
β -alanine	β -Ala		x	x
γ -aminobutyric acid	γ -Aba		x	x

Ratios and indices derived from the monomeric distribution of AA are used to estimate the state of AA degradation:

Reactivity Index (RI)

The aromatic AAs tyrosine (Tyr) and phenylalanine (Phe) are concentrated in cell plasma and are therefore most labile during cell lysis and decay processes (Hecky et al., 1973). Non-protein β -alanine (β -Ala) and γ -aminobutyric acid (γ -Aba) occur only in trace amounts in living tissue but become enriched as metabolic end-members during microbial decay (Cowie and Hedges, 1992). Hence, the ratio of aromatic to non-protein AAs (the RI) reflects the relative degradation state of OM (Jennerjahn and Ittekkot, 1997):

$$\text{RI} = \frac{\text{Tyr} + \text{Phe}}{\beta\text{-Ala} + \gamma\text{-Aba}} \quad (5.2)$$

Poorest OM preservation is indicated by values close to 0; living marine plankton ranges between 4 and 6 (Jennerjahn and Ittekkot, 1997).

Degradation Index (DI)

The DI (Dauwe et al., 1999) statistically evaluates relative abundances of the 14 most common protein AAs (see Table 5.2). Dauwe et al. (1999) used the AA composition of 28 samples, representing a wide range of environmental settings and degradation state from living plankton to Pleistocene sediments, as the data matrix for a principal component analysis (PCA). The first PC factor scores derived from the analysis were considered to be the DI. To apply this index to other datasets, the molar percentages of individual AAs have to be inserted as var_i into the following formula:

$$\text{DI} = \sum_i \left[\frac{\text{var}_i - \text{AVG var}_i}{\text{STD var}_i} \right] * \text{fac.coef}_i \quad (5.3)$$

where the deviation of the molar percentage of each AA from an average value (AVG) is multiplied by an individual coefficient (fac.coef). AVG, fac.coef and STD (standard deviation) are given by Dauwe et al. (1999). The sum of all operations yields the DI of a given sample; higher values indicate better preservation than lower values. This approach has been successfully applied to determine different stages of early OM decomposition in aquatic environments (e.g. Ingalls et al., 2003; Gaye-Haake et al., 2005).

5.4. Results**5.4.1. Surface sediments**

RI and DI show the same patterns in surface sediments but the DI was used for the same data set by Gaye-Haake et al. (2005) to study the relationship between organic matter preservation and the $\delta^{15}\text{N}$. Here we use the RI as it is more applicable for cores studies (see below) and correlate it with $\delta^{15}\text{N}$, water depths, and oxygen in deep waters for the set of 46 surface sediments from the earlier study of Gaye-Haake et al. (2005). The RI is significantly negatively correlated at the 99.9% significance level with both water depth ($r^2 = 0.82$) (Figure 5.2a) and oxygen in bottom waters ($r^2 = 0.61$) (Figure 5.2c). Also, the correlation of $\delta^{15}\text{N}$ with both water depth ($r^2 = 0.67$) (Figure 5.2b) and oxygen ($r^2 = 0.65$) (Figure 5.2d) are statistically significant at the 99.9% level. Similar correlations can be obtained by using the DI.

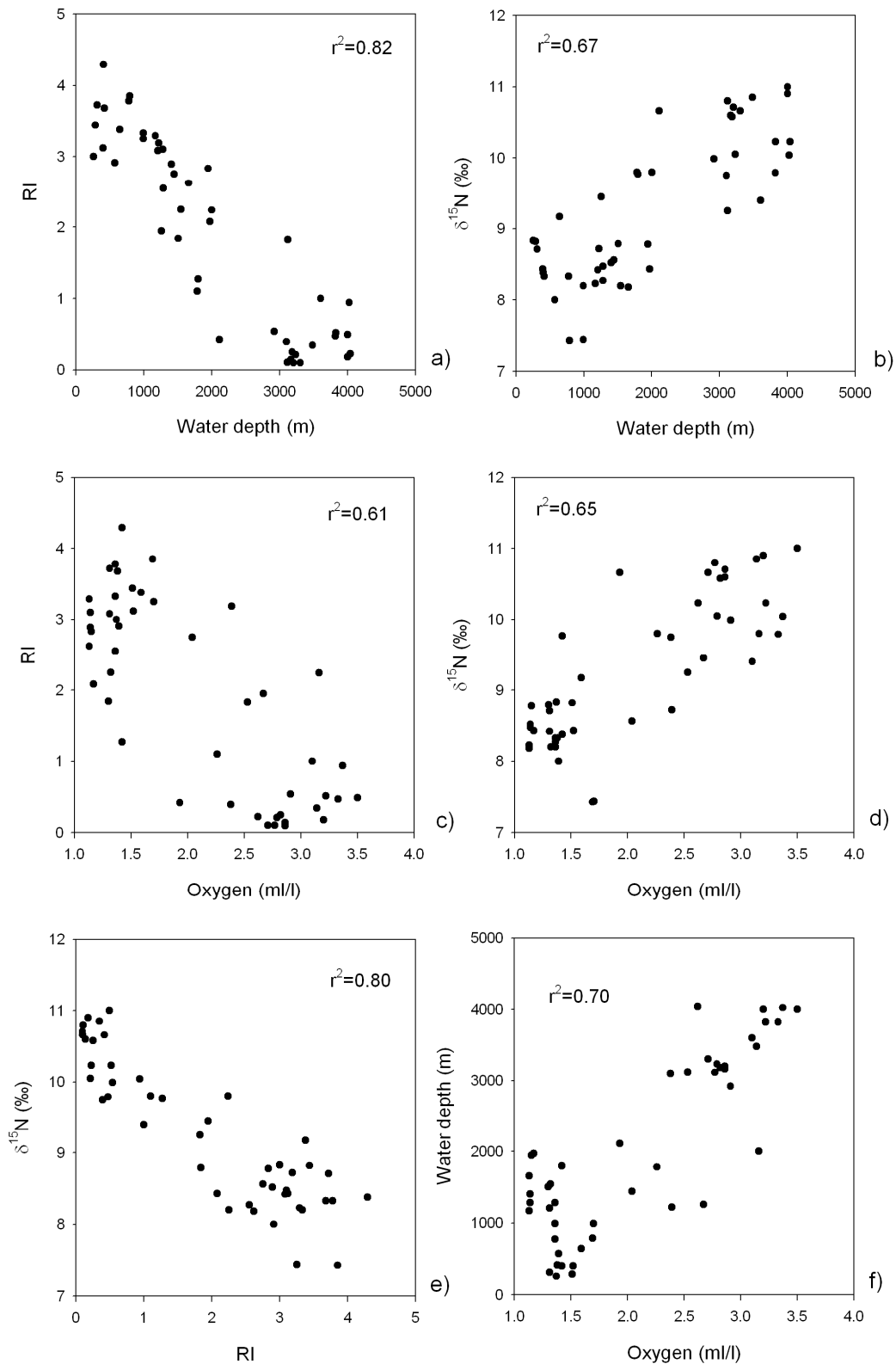


Figure 5.2: Amino acid Reactivity Index (RI) and $\delta^{15}\text{N}$ (‰) vs. water depth and bottom water oxygenation (ml/l) in a set of 46 surface sediments. RI/ water depth (a), $\delta^{15}\text{N}$ / water depth (b), RI/ bottom water oxygenation (c), $\delta^{15}\text{N}$ / bottom water oxygenation (d), $\delta^{15}\text{N}$ / RI (e), water depth/ bottom water oxygenation (f).

5.4.2. Core data

The TOC contents at ODP Site 722 are between 0.3% in the older core section and 1.3% for the youngest samples of an age of about 7 kyr. Total nitrogen ranges between 0.03 and 0.14%. The accumulation rate at this site varied between 2.5 and 13.5 g*cm⁻²*kyr⁻¹ over the last 130 kyr, and the entire sequence analyzed has been deposited under oxygenated bottom water. The RI ranges between 0.6 and 2.0 (Figure 5.3) and indicates poor to moderate preservation of amino acids. The $\delta^{15}\text{N}$ values are between 5.5 and 9.0‰ (Figure 5.3) and do not vary systematically with either sediment accumulation rates or isotopic stage boundaries. Organic carbon contents in sediments of Site 724 are between 0.1% and 2.7% and thus are higher than at Site 722 in the core section younger than about 50 kyr and similar to Site 722 in the older core sections. TN concentrations are between 0.03 and 0.3% with $\delta^{15}\text{N}$ values between 3.8 and 8.0‰. Amino acid concentrations are between 0.2 and 5.6 mg g⁻¹ and track variations in TOC concentrations. The RI varies between 1.3 and 3.6 (Figure 5.3), indicating moderate to good preservation. Two values in RI are considered to be outliers (1.29 in Marine Isotope Stage (MIS) 1 and 3.34 in MIS 3) and are excluded in later correlations. As in samples of Site 722, there is no systematic relationship of $\delta^{15}\text{N}$ with either sediment accumulation rates or isotopic stage boundaries. The average $\delta^{15}\text{N}$ over the last 130 kyr is 5.5‰ compared to 7.2‰ at Site 722. This offset of 1.7‰ is more or less uniform through time between the two locations, with exceptional phases in the Holocene and during MIS 3 when $\delta^{15}\text{N}$ at Site 724 varies with large amplitude and the $\delta^{15}\text{N}$ levels at the two sites converge.

Variations in $\delta^{15}\text{N}$ through time in NAST, EAST and 111 KL are very similar to those of ODP 722 B and 724 C series (Figure 5.4). $\delta^{15}\text{N}$ ranges from 5.4‰ (NAST) and 5.7‰ (EAST) up to 10.6‰ and 10.2‰, respectively, so that the amplitudes of change are similar to that of 724 C, but at a higher level of enrichment in ¹⁵N. Core 111 KL (Suthhof et al., 2001) only covers the last 60 kyr; here, at the Pakistan continental margin, $\delta^{15}\text{N}$ varies between 4.2 and 9.8‰.

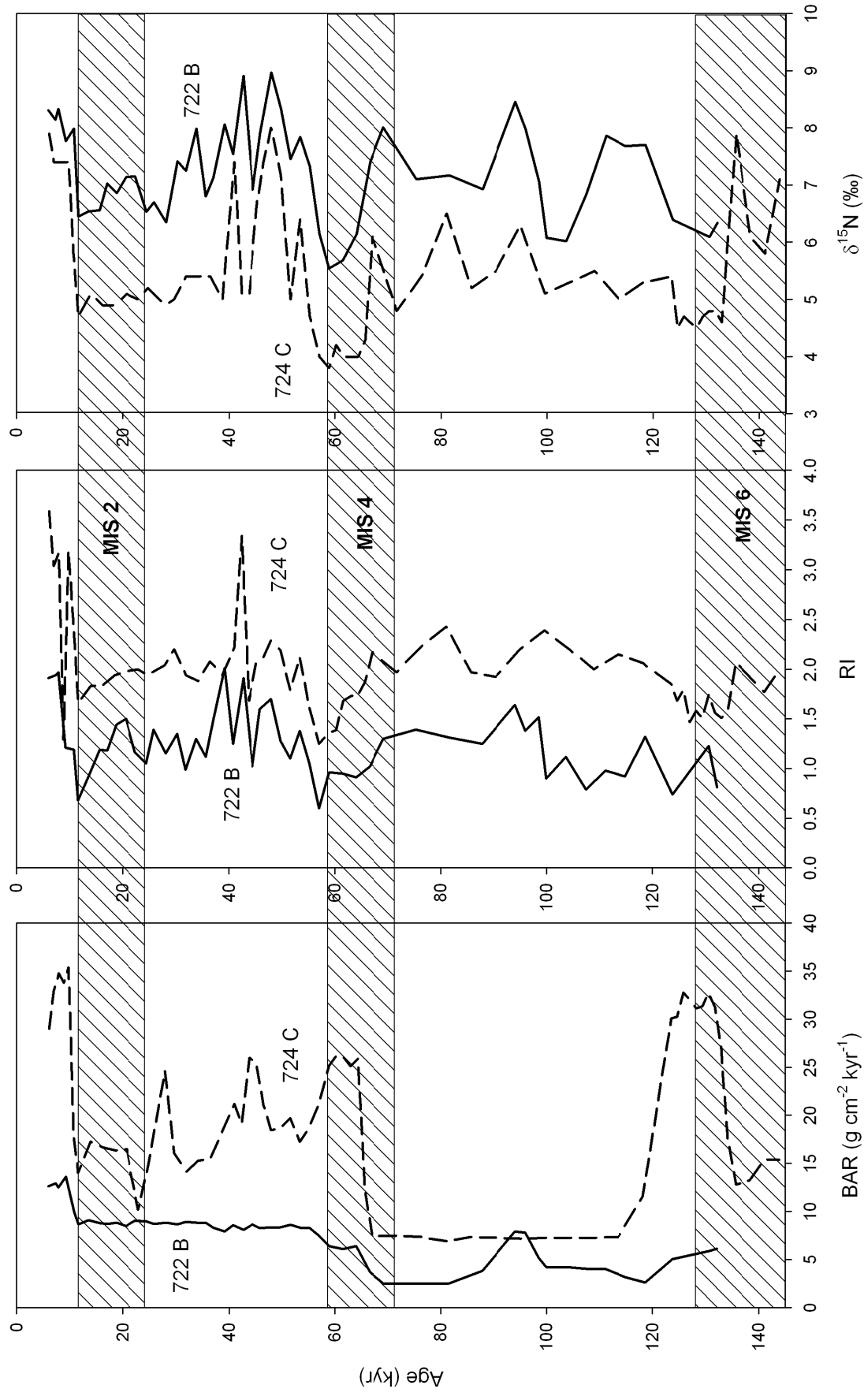


Figure 5.3: Bulk sediment accumulation rates (BAR), RI, and $\delta^{15}\text{N}$ (‰) of samples from site 722 B (solid) and 724 C (dashed). MIS= Marine Isotope Stage; shaded are glacials.

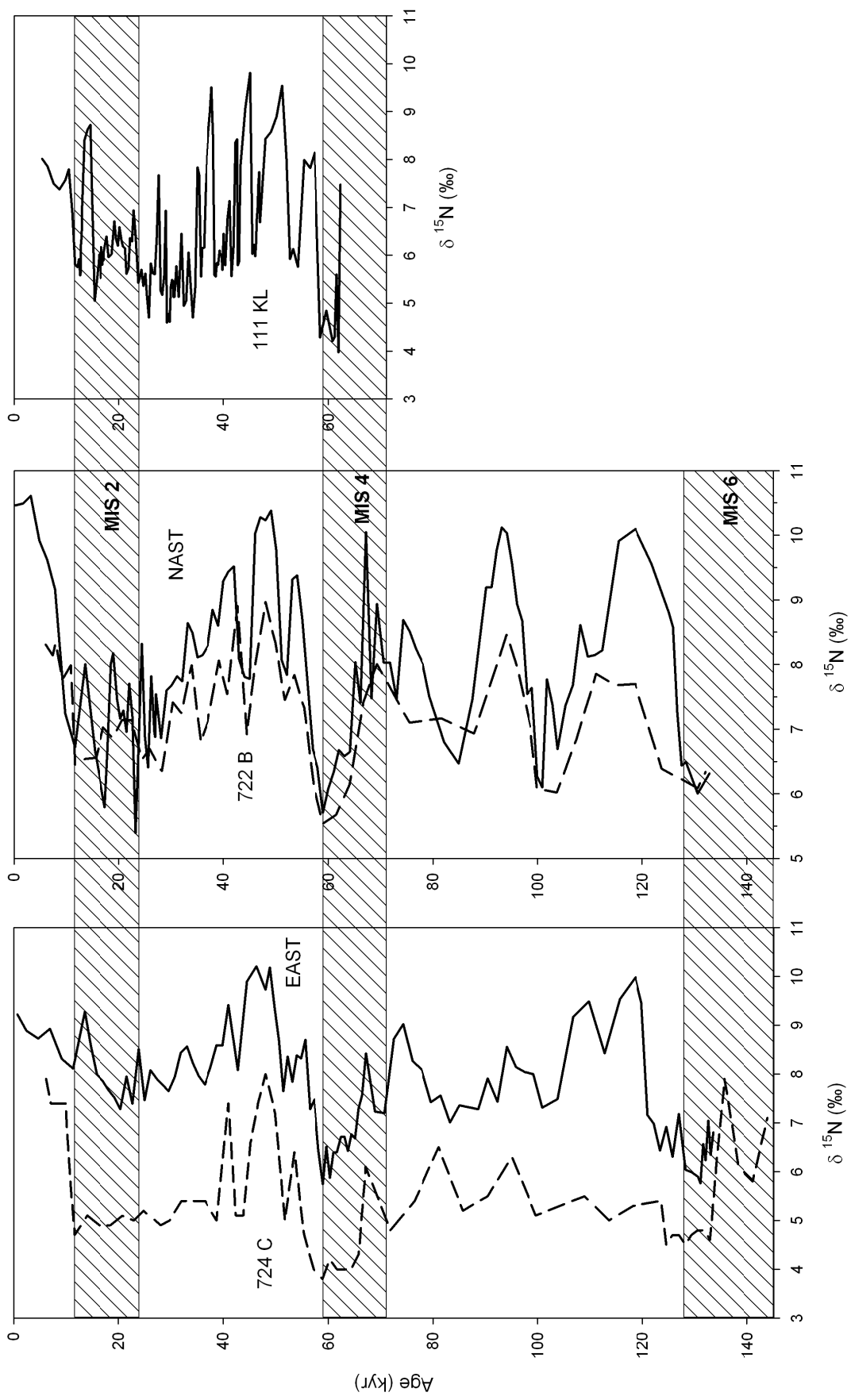


Figure 5.4: $\delta^{15}\text{N}$ (‰) of samples from Hole 724 C (dashed) and core EAST (solid) and Hole 722 B (dashed) and core NAST (solid) plus 111 KL (Suthhof et al., 2001).

5.4.3. Comparison of amino acid indexes in the core studies

DI and RI diverge in samples from ODP 722 B (not shown) and 724 C from the Oman Margin (Figure 5.5). While the RI traces the $\delta^{15}\text{N}$ record, the relationship between $\delta^{15}\text{N}$ and the DI is ambiguous: The DI indicates the poorest preservation in the youngest samples, followed by a continuous downcore increase towards a supposedly better preservation in the oldest samples. To obtain independent biogeochemical indicators to the data set created here, we carried out a PCA on amino acid data of core 722 B and 724 C using the mole-% values of all 21 individual AAs analyzed (Table 5.2). The PCA yielded two factors explaining about 55% of the total variance. The scores of the first factor plotted versus depth show an exponential downcore increase, whereas the scores of the second factor oscillate in concert with the $\delta^{15}\text{N}$ record (Figure 5.6). This parallel trend in $\delta^{15}\text{N}$ and the second factor score of AA data is evident in both data sets, but whereas the correlation is highly significant (at the 99% level) for samples from 724 C, it is not in 722 B.

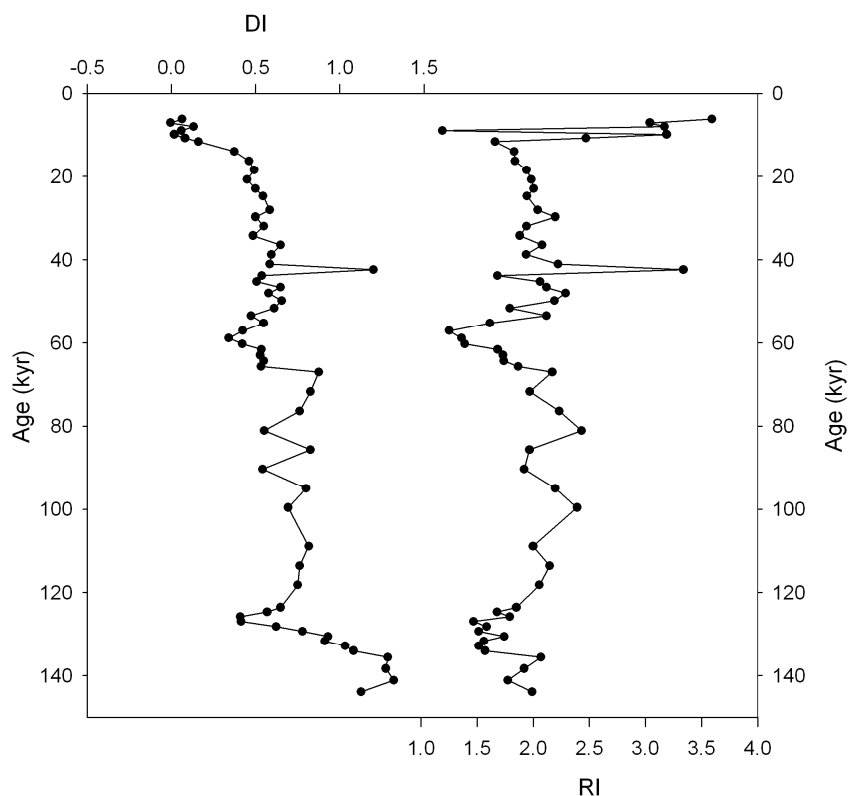


Figure 5.5: AA derived Degradation Index (DI) and Reactivity Index (RI) in ODP core 724 C show little congruence in indication. For both indices higher values indicate better preservation than lower values.

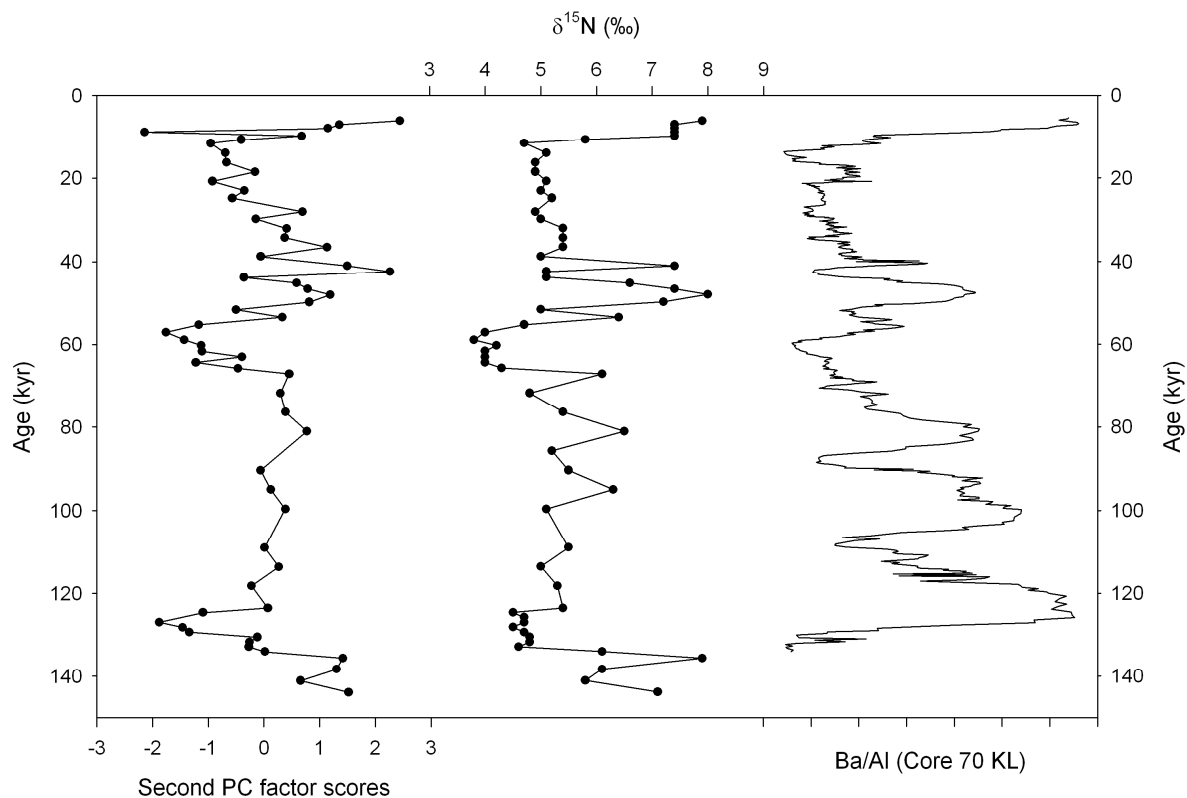


Figure 5.6: Variations in second PC factor scores (left plot) of AA PCA are similar to millennial scale oscillations in $\delta^{15}\text{N}$ (mid plot) and Ba/Al (data from Leuschner and Sirocko, 2003; right plot).

5.5. Discussion

5.5.1. Applicability of amino acid indexes in sediment cores

The fact that the RI and DI are comparable in surface sediments but diverge in core profiles suggests that degradation processes differ depending on sediment age. Whereas microbial degradation processes and subsequent physical segregation dominate in the water column and at the sediment water interface, long-term abiotic processes (related to temperature, equilibrium- and kinetic processes) in sediment cores alter the AA composition in a different way. Glycine (Gly) and Threonine (Thr) are enriched during water column degradation as a result of their initially high concentration in cell walls, preferentially accumulating in a more resistant OM fraction (Lee and Cronin, 1984). For this reason, their enrichment is an indicator of OM degradation as expressed in the DI. During degradation in the sediment column, when proteins are further degraded and monomers are incorporated into geopolymers, these two AAs are depleted relative to bulk AA content (Figure 5.7, Thr not shown). On the other hand, Phe and Glutamic acid (Glu) (concentrated in cell plasma; Hecky et al., 1973) tend to be depleted during degradation in the

water column and in surface sediments as a consequence of cell break-down (Lee and Cronin, 1984), but are relatively enriched downcore (Figure 5.7, Glu not shown).

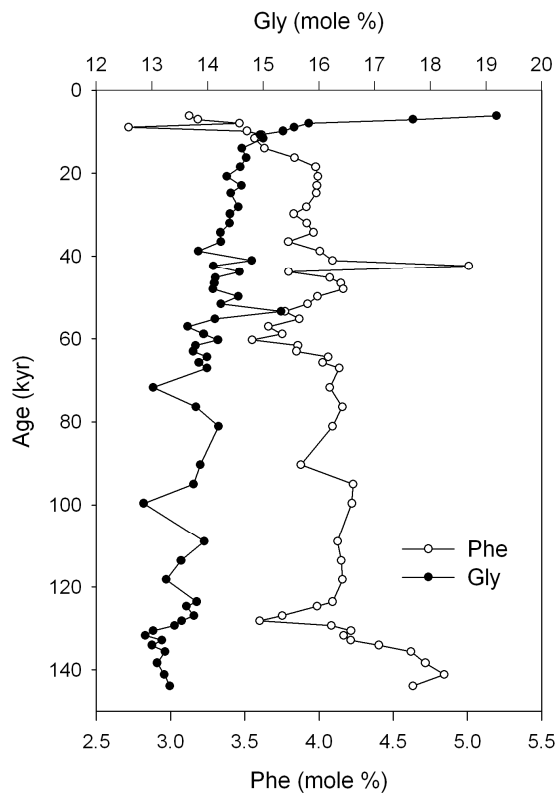


Figure 5.7: Molar percentages of protein AA glycine (Gly) and phenylalanine (Phe) in ODP core 724 C. Relative abundance of both amino acids due to depth and time is opposite as expected from water column decay processes.

The relative abundance of Gly is schematically shown in Figure 5.8: after initial enrichment in the water column, its relative contribution to total AA rapidly decreases in the sediments. This may reflect preferential degradation by microbes utilizing AAs of low molecular weight, so that larger AAs (such as Phe) may be relatively enriched over Gly in the course of degradation. The later stage diagenetic effects are not captured by the DI. The index was derived from a broad suite of surface sediments of different sedimentation and productivity regimes, but only few older sediments from cores, mostly sapropels and turbidites (Dauwe et al., 1999) that possibly do not represent undisturbed and continuous sedimentary degradation. This explains why the state of degradation in sediments that have undergone downcore diagenesis may be not well reflected in the DI; in our assessment, the DI is less applicable to characterize the state of degradation in the sediment sequence from Hole 724 C.

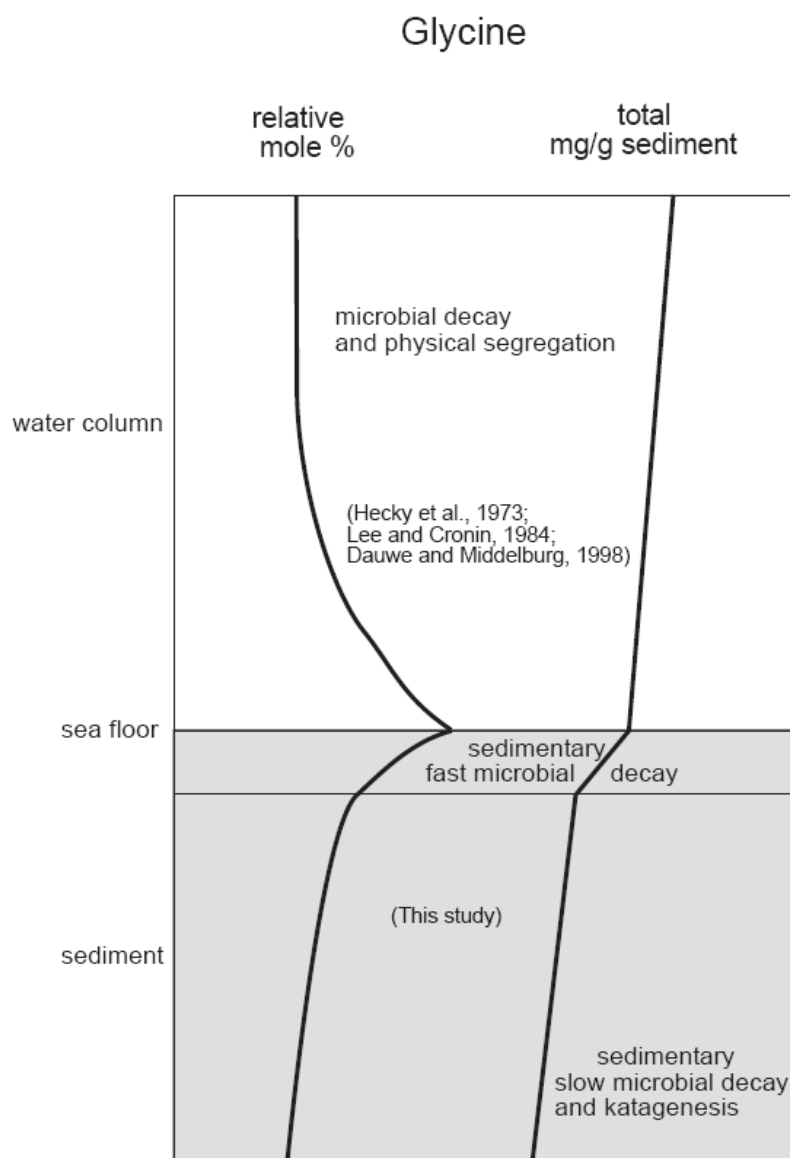


Figure 5.8: Schematic of Gly decay from the water column to the deeper sediment. In the water column and at the sediment-water interface, Gly (as a cell wall constituent) becomes relatively enriched in a more stable OM fraction. In the sediment Gly is rapidly consumed by benthic microorganisms due to its easy metabolization and high availability. Further decay in the deeper sediment is achieved by slow microbial uptake and katagenesis.

Advanced degradation also affects the AAs used for the RI equation. In the water column the non-protein AAs β -Ala and γ -Aba are relatively enriched over the aromatic AAs which has been explained by the fact that non-protein AAs are either not utilizable for metabolism or are decarboxylation products of aspartic acid and Glu, respectively, and are therefore accumulating during diagenesis (Lee and Cronin, 1982). Non-protein AAs are thus enriched over the most labile aromatic AAs Tyr and Phe (Jennerjahn and Ittekkot, 1997). In our cores, both non-protein and total aromatic AAs show significant downcore enrichment relative to the other AAs. Tyr and Phe, however, behave very differently. Whereas Phe gets twice as much enriched as β -Ala and γ -Aba,

Tyr gets depleted close to the detection limit. These processes evidently lead to a conservation of the RI originally achieved after degradation in the water column and at the sediment water interface. As the RI of both ODP cores is correlated with the $\delta^{15}\text{N}$ record (see Section 5.5.4.) and with the Ba/Al record (as a proxy for paleoproductivity or preservation) from core KL 70 (Leuschner and Sirocko, 2003) located close to 722 C (Figure 5.6) we consider this indicator to be more suitable for organic matter preservation in the water column and in surface sediments than the DI, which appears to be overprinted by late stage OM degradation in sediment cores. In other core studies, however, the DI appears to be robust (Chapter 4) highlighting the significance of environment specific conditions on decay processes.

5.5.2. The relationship between organic matter preservation and $\delta^{15}\text{N}$: Influence of water depth, bottom water oxygen concentrations and sediment accumulation rates

The paired data on AA preservation (RI) and $\delta^{15}\text{N}$ of 46 surface sediments (Figures 5.2 a-f) suggest a significant influence of water depth and oxygen concentrations on the degradation state of organic matter and the N-isotope composition of sediments. This may reflect protein degradation during passage of fresh organic matter through the water column and at the sediment water interface where the degradation rates are high (Honjo et al., 1982; Cole et al., 1987). Recent deep-sea sediments deposited in an oxic environment reveal the largest $\delta^{15}\text{N}$ increase over sinking particles (3-4‰; Francois et al., 1992; Francois et al., 1997; Altabet et al., 1999a), whereas $\delta^{15}\text{N}$ in sediments from suboxic continental margins only increase by <1‰ (Holmes et al., 2002; Thunell et al., 2004; Gaye-Haake et al., 2005).

The change in organic matter composition with increasing water depth may reflect an interplay of processes that are related to the distance to the coast. Near coastal environments are characterized by higher productivity, shorter food chains and higher export production than pelagic environments (Eppley and Peterson, 1979). The allochthonous supply of detritus from land further enhances sedimentation and mass accumulation rates and thus promotes a relatively fast sealing of organic matter in the sediment that reduces the period of intensive degradation at the sediment-water boundary. Higher sinking speeds, induced by higher total fluxes and mineral ballast, also reduce the time for degradation in the water column (Sirocko and Ittekkot, 1992). More distal environments in contrast have lower primary production and bulk sedimentation rates that are usually located in areas with a deeper water column. The decreasing productivity and increasing degradation contribute to a gradient in organic matter flux away from land and with increasing water depth (for a detailed discussion, including parts of this dataset see Suthhof et al. (2000)). This general tendency is strengthened by the specific situation in the Arabian Sea. Bottom water oxygen concentrations are lowest where the OMZ impinges on the shelf and slope.

This additional effect of low oxygen levels further enhances organic matter preservation at relatively shallow water depths and amplifies the differences in composition between shallow and deep stations.

A comparison of average $\delta^{15}\text{N}$ for the last 60 kyr between cores 722 B, 724 C, 111 KL, NAST and EAST implies a slight increase with water depth converging to a $\delta^{15}\text{N}$ value of about 8‰ below 3000 m depth (Figure 5.9).

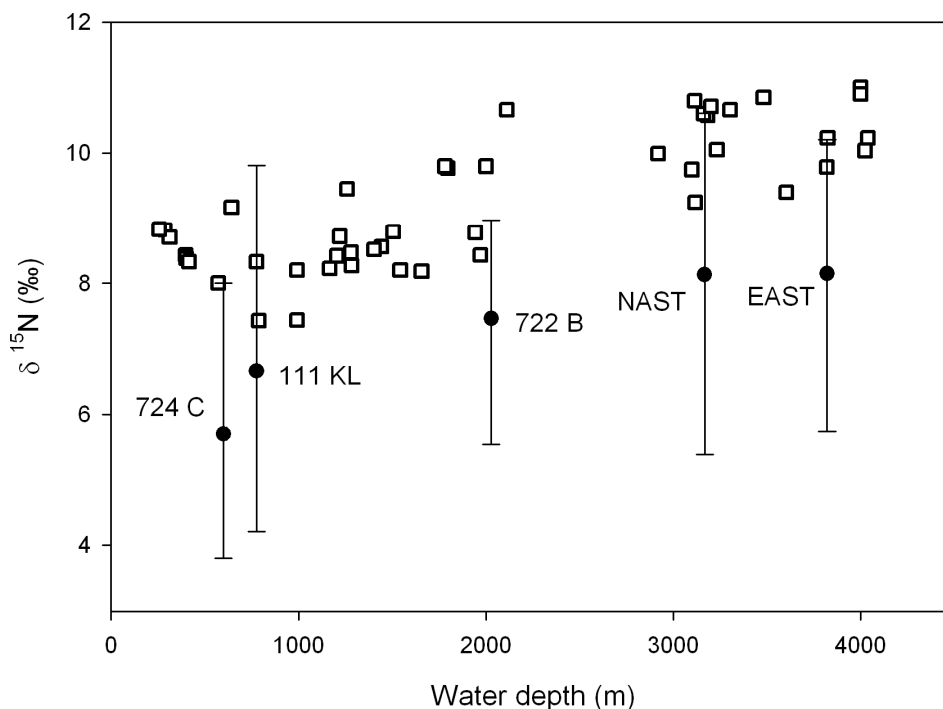


Figure 5.9: Average $\delta^{15}\text{N}$ (‰) of the study sites over the last 60 kyr versus water depth. Squares: recent surface sediments. Both datasets show ^{15}N enrichment due to increasing water depth.

In agreement with our findings on surface sediments, we interpret the increase in average $\delta^{15}\text{N}$ of cores with water depth as a result of (i) increased bottom water oxygenation from the slope to the deep sea; (ii) effects related to the distance from land such as gradients in sedimentation rates and primary production; and (iii) early diagenetic alterations related to the duration of particle passage through the oxic water column. In contrast to Pichevin et al. (2007) our data do not reveal a negative correlation of average sedimentation rates and the arithmetic mean of $\delta^{15}\text{N}$ which may be due to the much smaller range of sedimentation rates in our data set. Similarly, we do not find a very significant relationship between sedimentary $\delta^{15}\text{N}$ and RI with bulk accumulation rates (BAR) over core records at ODP sites 722 B and 724 C (Figure 5.3). This may also be due to a small range of BAR so that sealing effects on organic matter preservation may be masked by other processes having a much stronger imprint on $\delta^{15}\text{N}$. Oxygen concentrations may probably have

been more important for organic matter preservation in the sediment record, similar to the findings in surface sediments (see above).

5.5.3. Other reasons for different $\delta^{15}\text{N}$ values among the cores

A comparison of the $\delta^{15}\text{N}$ record of 724 C with the deep-sea cores NAST and EAST shows a constant offset of 2.4‰ in $\delta^{15}\text{N}$ (as seen in surface sediments) over much of the Holocene and late Pleistocene record (Figures 5.3 and 5.4). The $\delta^{15}\text{N}$ values analyzed in core 722 B also correspond very well to those at stations NAST and EAST, with similar values at $\delta^{15}\text{N}$ minima and slightly lower (1.5 to 2.5‰) for the maxima at these sites. Little offsets between the deep-sea cores may result from different intensities in early diagenesis as discussed above. Generally, values of 722 B are intermediate between the slope (111 KL, 724 C) and deep-sea cores (EAST, NAST). The smaller amplitude in $\delta^{15}\text{N}$ can be attributed to sedimentary winnowing effects that discriminate smaller grain sizes (that usually are rich in OM) due to its elevated position on the Owen Ridge.

Recent studies indicate that the $\delta^{15}\text{NO}_3$ of subsurface nitrate of the Arabian Sea is $\sim 7\text{--}7.5\text{‰}$ (Altabet et al., 1999b; Nagel et al., in prep.) and is generally homogenous in the entire basin. While cores 722 B, EAST and NAST have significant fluctuations in $\delta^{15}\text{N}$ in sediments older than 80 kyr and track the insolation record and millennial scale climatic fluctuations, the Oman Margin record of Site 724 C displays uniformly low values. The generally lower $\delta^{15}\text{N}$ in core 724 C compared to present-day nitrate and the other cores, as well as the uniformly depleted values in the lower part of core 724 C (Figure 5.4), can be explained by isotopic fractionation due to incomplete nitrate assimilation since the location is situated in the Oman coastal upwelling zone where nitrate is seldom exhausted.

5.5.4. Variations of denitrification and organic matter preservation over the last 130 kyr

Millennial scale oscillations of $\delta^{15}\text{N}$ in the core records (Figures 5.3 and 5.4) confirm results of earlier investigations on the same cores (Altabet et al., 1999b; Higginson and Altabet, 2004), and are similar to other records from the region (Altabet et al., 1995; 2002; Suthhof et al., 2001). Because of insufficient temporal resolution our data set aliases high-frequency variability seen in other records - but clearly elevated $\delta^{15}\text{N}$ characterize interglacial periods, whereas low $\delta^{15}\text{N}$ prevails during glacial periods and shorter cooling periods such as the Younger Dryas and Heinrich events. This general pattern has been attributed to changes in denitrification intensity which affects the isotopic composition of source nitrate (Altabet et al., 1995). Higher productivity during enhanced monsoon-driven upwelling in conjunction with reduced ventilation of the intermediate water masses is thought to have intensified the oxygen minimum zone, expanding

the area and amount of denitrification, and thus raising the $\delta^{15}\text{N}$ of sub-euphotic zone nitrate due to a more intense denitrification (Altabet et al., 1995). Assimilation of this enriched nitrate pool upon upwelling or after convection resulted in generally higher $\delta^{15}\text{N}$ values of sediments deposited during warm climatic stages. Temporal variation in $\delta^{15}\text{N}$ in sediment cores thus mainly reflects changes in the Arabian Sea nitrogen inventory (Altabet et al., 1995).

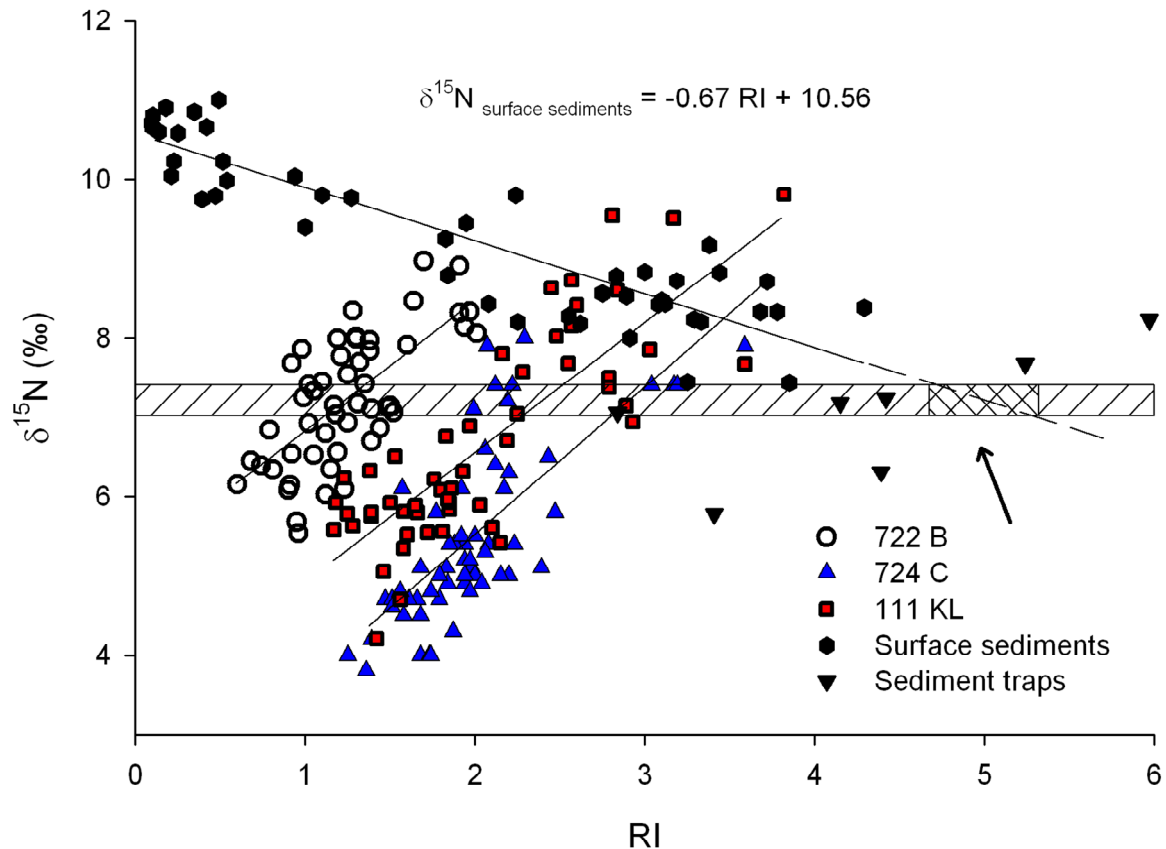


Figure 5.10: $\delta^{15}\text{N}$ (‰) in comparison with amino acid reactivity (RI) in samples of Holes 722 B (n=51), Hole 724 C (n=58), 111 KL (n=52) (Suthhof et al., 2001), surface sediments (n=46) and sediment traps (n=6; mean values). The shaded rectangle indicates the recent subsurface $\delta^{15}\text{NO}_3$ of 7 to 7.5‰. Note that RI and $\delta^{15}\text{N}$ are positively correlated in core records but negatively correlated in surface sediments.

Exactly the same temporal patterns are evident in the second factor score of amino acid PCA and in the RI of core 724 C as well as in the Ba/Al record of core 74 KL (Figure 5.6). Together, the data imply that denitrification intensity (and $\delta^{15}\text{N}$ of nitrate at the base of the mixed layer) is closely coupled to higher primary production (providing substrate organic matter) and/or organic matter preservation. In consequence, the relationship of $\delta^{15}\text{N}$ and the RI in core samples is opposite to the trend in surface samples - better preservation of organic matter is accompanied by enriched $\delta^{15}\text{N}$ (Figure 5.10). The same positive relationship in $\delta^{15}\text{N}$ and RI also characterizes core 111 KL from the oxygen-deficient Pakistan margin environment (Suthhof et al., 2001) (Figure 5.10). Because the RI in surface sediments increases with decreasing bottom water oxygen concentrations, the positive correlation between $\delta^{15}\text{N}$ and RI found for each individual core seems

to reflect changes in source nitrate composition rather than in degradation. We interpret the positive correlation of RI and $\delta^{15}\text{N}$ as a result of residual nitrate enrichment in ^{15}N due to the intensity of denitrification. At the same time preservation becomes enhanced as a consequence of contemporaneous oxygen limitation and higher primary production. Although the individual data sets show some scatter, the regression lines of RI and $\delta^{15}\text{N}$ for the three cores (Figure 5.10) have approximately the same slopes determined by source nitrate isotopic composition, which in turn is determined by denitrification intensity. The offsets between the three regression lines may be caused by either differences in preservation or in the degree of nutrient utilization at the three locations (see above). Highest $\delta^{15}\text{N}$ and RI of the core records are in the range of values of recent surface sediments and represent phases of intense denitrification.

The values for RI and $\delta^{15}\text{N}$ in material from sediment traps (Figure 5.10) extend the trend of surface sediments to fresh OM and are in the same range as the intersection of the slope of recent PN (surface sediments and traps) with the $\delta^{15}\text{N}$ of subsurface NO_3^- .

5.5.5. Estimating source nitrate isotopic composition

According to our considerations about processes that modulate spatial and temporal patterns in the $\delta^{15}\text{N}$ and RI of sediments in the Arabian Sea we suggest the following schematic summary (Figure 5.11): (1) The $\delta^{15}\text{N}$ of source nitrate is determined by the intensity of denitrification and nutrient utilization in the euphotic zone, as well as by external inputs. This $\delta^{15}\text{N}$ is transferred into the particulate organic matter pool by assimilation. Spatial differences in particulate and settling organic matter $\delta^{15}\text{N}$ within the basin are produced when nutrients are incompletely utilized. (2) There is a systematic relationship between the intensity of water column denitrification that determines the $\delta^{15}\text{N}$ of source nitrate and the preservation of organic matter in the core record of the recent geological history. This is reflected by the typically positive correlation of $\delta^{15}\text{N}$ and the AA-derived biogeochemical indicator RI. (3) Diagenetic enrichment of the original $\delta^{15}\text{N}$ of the assimilated nitrate increases with water depth, bottom water oxygenation and other basin effects, as indicated by a negative correlation of the RI and $\delta^{15}\text{N}$ in surface sediments.

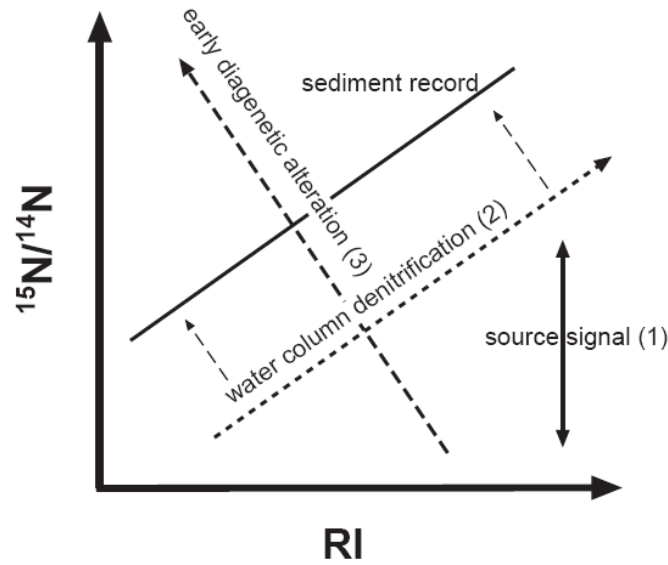


Figure 5.11: Schematic interpretation of the relationship between sedimentary $\delta^{15}\text{N}$ and RI in the Arabian Sea as shown in figure 10: External sources, the intensity of denitrification and the degree of NO_3^- assimilation determine the general setting of $\delta^{15}\text{N}$ (1). Water column denitrification leads to an enrichment in ^{15}N and contemporaneous better preservation (2). During progressive OM decay (expressed by decrease in RI) $\delta^{15}\text{N}$ becomes enriched (3). The offset between the dashed arrow “water column denitrification (2)” and the solid “sediment record” represents the early diagenetic enrichment of the examined sediment cores.

In earlier studies the proportion of diagenetic enrichment on sedimentary $\delta^{15}\text{N}$ has been quantified by analyzing the $\delta^{15}\text{N}$ preserved in diatom frustules (Sigman et al., 1999), foraminifer shells (Ren et al., 2009) and biomarkers resistant to diagenesis (Sachs and Repeta, 1999). Here we suggest a reconstruction of the pristine diagenetically non altered $\delta^{15}\text{N}$ under the assumption of a linear relationship between ^{15}N enrichment and OM degradation as reflected in AA composition. The diagenetic increase (labelled 3 in Figure 5.11) depicts the relative trends caused by different processes that affect $\delta^{15}\text{N}$ and RI as seen in surface sediments. This diagenetic offset should be applicable to any other time slice in core records from the Arabian Sea. Assuming that the slope of the regression has not changed significantly, we may use the $\delta^{15}\text{N}$ -RI correlation obtained for surface sediments (Figure 5.10) to reconstruct the $\delta^{15}\text{N}$ of primary produced OM: Each $\delta^{15}\text{N}$ value ($\delta^{15}\text{N}_{\text{sample}}$) is corrected by the slope of $\delta^{15}\text{N}$ vs. RI in surface sediments ($\delta^{15}\text{N} = -0.67 \text{ RI} = m_{\text{surf.sed.}}$; Figure 5.10) to an assumed RI value before diagenetic enrichment of $\delta^{15}\text{N}$ ($\text{RI}_{\text{original}}$) by the equation:

$$\delta^{15}\text{N}_{\text{original}} = \delta^{15}\text{N}_{\text{sample}} + (m_{\text{surf.sed.}} * \Delta\text{RI}_{\text{original-sample}}) \quad (5.4)$$

According to the intersection of surface sediments and sediment traps slope with the $\delta^{15}\text{N}$ of 7 to 7.5‰ in recent subsurface NO_3^- we assign the RI of newly produced, isotopically non altered

OM to ~ 5 (Figure 5.10, arrow). This value is in good agreement with data for living marine plankton from Jennerjahn and Ittekkot (1997).

The main uncertainty of this reconstruction is the assumption that the slope of the RI- $\delta^{15}\text{N}$ regression has been stable over the geological history. A study carried out on recent sediments from the South China Sea suggests that the slope is less steep under more oligotrophic conditions (Gaye et al., 2009).

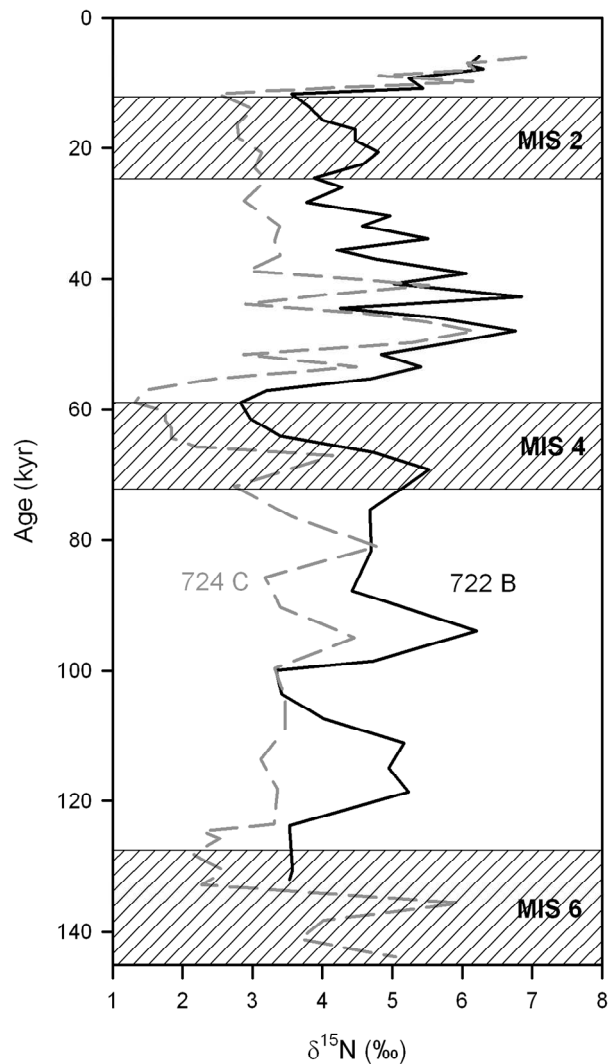


Figure 5.12: Reconstructed $\delta^{15}\text{N}$ record for primary produced OM in cores 722 B (gray dashed) and 724 C (black). Compare to Figure 3, right plot. The reconstructed records show significant lower values and records converge by 0.5‰ on average.

Despite these uncertainties we reconstructed the presumed pre-diagenetic $\delta^{15}\text{N}$ of cores 724 C and 722 B that generally have lower $\delta^{15}\text{N}$ values, but larger amplitudes than the uncorrected time series (Figure 5.12). The means of reconstructed $\delta^{15}\text{N}$ -records converge by 0.5‰ and values are almost the same during phases of intense denitrification. The calculated $\delta^{15}\text{N}$ for isotopically enriched interstadial sediments remain in a similar order of magnitude as recent NO_3^- (maximum 6.9‰ in both cores). However, for sediments deposited during glacial stages and Younger Dryas/Heinrich events, reconstructed $\delta^{15}\text{N}$ values show a significant offset between both cores (minima

in $\delta^{15}\text{N}$ = 1.3‰ for 724 C and 2.7‰ for 722 B). Generally, these very low values suggest intense N_2 fixation by cyanobacteria. This is feasible as enhanced inputs from Tibet supplied Fe/Mo (Karl et al., 2002) as a consequence of a strengthened NE-monsoon during glacial stages (Tamburini et al., 2003).

5.6. Conclusions

The fluctuations in $\delta^{15}\text{N}$ in the sediment cores investigated in this study are not primarily driven by diagenesis but by differences in $\delta^{15}\text{N}$ of the assimilated nitrogen. The intensified OMZ during the warm phases such as the Holocene and Interstadials is reflected by enriched $\delta^{15}\text{N}$ values, and this organic matter is less degraded than the material deposited during the colder stadials, especially during the Younger Dryas and Heinrich events. Near shore cores (724 C, 111 KL) show similar pattern as deep Arabian Sea cores (722 B, NAST, EAST). However, the absolute $\delta^{15}\text{N}$ records are enriched by about 0.6-3.0‰ during both cold and warm stages in deep sea cores compared to shallow cores. This offset is caused by (i) basin effects as there are gradients in sedimentation rate, primary production, water depth and bottom water oxygenation that lead to gradients in early diagenetic alterations in $\delta^{15}\text{N}$ and (ii) higher fractionation during NO_3^- uptake in the upwelling environment of core 724 C.

Established AA indices RI and DI diverge and are not comparable in the examined cores. We suspect that the reason for this discrepancy lies in different pathways or rates of AA decomposition in older sediments compared to decay in the water column and at the sediment water interface; this difference is inherent in the calculation of AA quality by the RI, but is not captured in the DI. A normalization of $\delta^{15}\text{N}$ in core records to diagenetic non altered values of primary produced OM by using the RI seems possible but vague. This reconstruction suggests that the interstadial conditions were comparable to the recent late Holocene whereas cold stages were characterized by significant nitrogen fixation stimulated by enhanced dust supply from the Tibetan Plateau.

6. Conclusions and Outlook

6.1. Conclusions

This thesis successfully uses $\delta^{15}\text{N}$ as a tracer of reactive N sources in the present-day Mediterranean Sea and investigates factors determining the $\delta^{15}\text{N}$ of particulate OM as well as the applicability of $\delta^{15}\text{N}$ as a proxy for N sources in sediment cores from the Mediterranean Sea and the Arabian Sea.

Unusually depleted ^{15}N values in all compartments of reactive N in the EMS are indicative for the isolation of the basin from the global ocean. The low level of $\delta^{15}\text{N}$ reflects the dominance of isotopically depleted N sources and the lack of processes that enrich nitrate in ^{15}N . Isotopic enrichment of TRN and suspended PN over NO_3^- and model data as well as the nitrate isotope anomaly $\Delta(15,18)$ suggest that N-remineralisation and atmospheric deposited NO_x are important contributors of ^{15}N depleted reactive N to the mixed layer. Atmospheric input (mainly anthropogenic) of ^{15}N depleted NO_x possibly decreases the $\delta^{15}\text{NO}_3^-$ in deepwater during the last decades.

Large scale variations in sedimentary $\delta^{15}\text{N}$ -records of the Eastern Mediterranean during the Holocene (including sapropel S1) are mainly driven by preservation, and not by the isotopic composition of the reactive N source, or the degree of nitrate utilization. The enhanced accumulation of OM in sapropel S1 can be explained by better preservation as a consequence of deep water anoxia, without the need of elevated primary production.

Both studies will be important contributions to the long standing debates about the origin of Mediterranean sapropels as well as the applicability of $\delta^{15}\text{N}$ as a proxy, and in the evaluation of current anthropogenic impacts on marine ecosystems.

Results of the Arabian Sea study, however, are less conclusive. Although my data confirm a strong early diagenetic imprint on $\delta^{15}\text{N}$, and imply that the RI can be used to reconstruct the primary produced $\delta^{15}\text{N}$, conclusions about the N inventory and utilization during the investigated period are less clear. Opposed to the Mediterranean Sea study, variations in $\delta^{15}\text{N}$ in the sediment records from the Arabian Sea appear to be primarily driven by differences in $\delta^{15}\text{N}$ of the assimilated nitrate. Warm phases, such as the Holocene and Interstadials, are reflected by enriched $\delta^{15}\text{N}$ values and well preserved OM as a consequence of an intensified oxygen minimum zone in intermediate water masses. Core records show similar basin-wide millennial-scale oscillations in $\delta^{15}\text{N}$ with an offset from one location to the next that I attribute to different degrees of early diagenetic enrichment in $\delta^{15}\text{N}$ and differences in NO_3^- availability at each core location.

EMS and Arabian Sea cores are both archives of late Pleistocene to Holocene climate variability in the monsoon system. They both show millennial-scale oscillations in TOC accumulation and $\delta^{15}\text{N}$ that are driven by monsoon intensity and follow Milankovitch cycles. The signal in $\delta^{15}\text{N}$ and its relationship to OM preservation, however, has an opposite sign in these two settings, because better OM preservation goes in concert with depleted $\delta^{15}\text{N}$ values in the EMS, but with enriched $\delta^{15}\text{N}$ in the Arabian Sea. This is because different environmental settings force different processes that in the end determine the records. This opposite behavior illustrates that single data of $\delta^{15}\text{N}$ can be easily misinterpreted – but in conjunction with other proxies, $\delta^{15}\text{N}$ is a highly potent proxy.

6.2. Outlook

While studies performed towards this Ph.D.-thesis gave many fascinating results and some answers, they also pose new questions and suggest further research and different approaches:

The monitoring of deep water NO_3^- isotopic composition in the Mediterranean Sea should be continued to further investigate the current trend of ^{15}N depletion. Based on a broader data set local models of Northern Ionian Sea stations and pelagic stations could be extended to a regional Eastern Mediterranean isotope budget. An improvement of analytical techniques to determine isotopic composition of small amounts of nitrate may allow to investigate the NO_3^- starved surface layer in more detail, thus closing the gap between atmospheric deposition and the deep-water nitrate pool to better trace nitrification in the nutrient-starved surface layer and the input of anthropogenic reactive N. In my opinion, the EMS is an ocean basin (albeit a small one) where (an as yet undefined) natural N-cycle is currently being flooded by anthropogenic reactive nitrogen. But to fully understand only the present-day N-cycle in the EMS, we need additional insights from inter-annual time-series of N-export flux, which currently are discontinuous, and preferably from depths immediately below the thermocline at several stations. I also speculate that TRN, which was ^{15}N depleted in our samples, should have a distinct seasonal cycle with characteristic enrichment in summer months. The largest issue to date is the presence or absence of significant N_2 fixation, whether near the surface or in the enigmatic deep chlorophyll maximum, and its true magnitude. And a nagging questions remains: If atmospheric inputs are indeed large and have been delivering excess nitrate in the last decades, and if these inputs have high (~50) N:P ratios as suggested by measurements, why have N:P ratios in deep water not been rising?

Further investigations on OM decomposition and N-isotope fractionation will be conclusive in order to substantiate the findings of Chapter 4: Planktonic foraminifer shells in Eastern Mediterranean sediments probably retain the original, primary produced $\delta^{15}\text{N}$ signal in their proteinaceous linings (Ren et al., 2009) and may (or may not) verify the DI-normalized values presented in this study. An undisturbed sediment core from a permanently anoxic brine basin of the EMS should reflect relative changes in the $\delta^{15}\text{N}$ of primary produced OM that are not overprinted by the diagenetic enrichment occurring today at the sediment-water-interface (e.g. core #569); if there were changes in sedimentary $\delta^{15}\text{N}$ deposited during the last decades it should be due to anthropogenic perturbations but not to a diagenetic overprint. Studies on sinking material and sediment cores from the Black Sea (as an analogue to Mediterranean sapropel conditions) can in addition clarify the relationship of OM accumulation, N-isotope distribution and Ba/Al ratios to preservation.

The evident linear to logarithmic relationship of $\delta^{15}\text{N}$ and N (%) in core #569 and other Mediterranean cores suggests an isotopic enrichment of the residual fraction during N-removal in the sediments following a Rayleigh type fractionation. Assuming that variations of $\delta^{15}\text{N}$ in Mediterranean sediments of the Holocene were solely driven by differences in degradation from the same amount of N with a similar $\delta^{15}\text{N}$ by ammonification, it should be possible to calculate the fractionation factor $^{15}\epsilon$ of ammonification in sediments. Results from coupled analyses of $\delta^{15}\text{N}$ in pore water ammonium and nitrate as well as organic N can be used to verify results of such calculations.

The Arabian Sea study revealed that knowledge about amino acid decay under differing environmental conditions and during progressive diagenesis is scarce and needs further research. If the approach of correcting sedimentary $\delta^{15}\text{N}$ for diagenetic increase by using amino acid spectra to determine preservation is validated by other studies from areas with variable OMZs, modelled estimates for the extent of water column denitrification and hence the rates for removal of reactive N from the global ocean and emissions of N_2O can be improved for older geological time. Again, a comparison to $\delta^{15}\text{N}$ records from planktonic foraminifer shells from sampling locations in different water depths would be conclusive. Another interesting question arises from the current debate whether denitrification or anammox is the main actor of N removal in the Arabian Sea (Ward et al., 2009): Is the systematic relationship between OM preservation and ^{15}N enrichment the same for both, denitrification and anammox? And if it is not, can we distinguish the proportion of both in core records via different slopes in the relationships between $\delta^{15}\text{N}$ and amino acid preservation indexes?

Acknowledgements

I would like to thank Prof. Dr. Kay-Christian Emeis for the supervision of my thesis; for his open mind regarding new ideas and for valuable discussions. I further thank for organizing four years of financial support and for the opportunity to participate in numerous conferences where I could smell the breath of international science.

I thank Dr. Birgit Gaye for co-supervision, and together with Dr. Andrea Wieland and Prof. Dr. Gerhard Schmiedl for endless scientific discussions that resulted in new ideas and encouragement.

Many thanks to laboratory security agent Dr. Niko Lahajnar for never losing his patience about my chaotic lab management, for scientific discussions and for support whenever I needed.

A special thank goes to Marc Metzke and Frauke Langenberg for their great support in sample preparation, management and analyses.

Thanks to Andreas Neumann for scientific discussions and the nice office atmosphere.

Thanks to Birgit Nagel for supervision and support in the GKSS labs.

I would like to acknowledge the nice working and social atmosphere: Thanks to all my colleagues of the IfBM, GKSS, the MERF project and during three research cruises!

Finally I thank my parents, brothers and sisters, my flat sharing in St. Georg and all my friends who made my life easier during the past four years by giving me support or diversion.

Figure Captions

Figure 1.1: The marine nitrogen cycle

Figure 1.2: Rayleigh fractionation during NO_3^- assimilation in a closed system

Figure 3.1: Map of stations occupied in the Eastern Mediterranean Sea during r/v Meteor cruise 71-3 (January-February, 2007). NIS stations referred to in the text are stations H07 to H12. The black square SE of Crete (water columns sampling station Ier1) marks the location of the sediment trap deployment station (MID).

Figure 3.2: Profiles of fluorescence (a; arbitrary units), nitrate (b) and phosphate (c) concentrations in the upper 400 m at 2 stations representative of NIS (H07) and pelagic stations (Her03) show stratification between 80 and 230 m water depth and indicate the biologically active mixed layer. An ongoing phytoplankton bloom in the northern Ionian Sea (at station H07) is sustained by nitrate and phosphate provided from ongoing regional thermocline deepening, whereas station Her03 illustrates the mature and thick mixed layer with very low nutrient concentrations at pelagic sites.

Figure 3.3: Concentrations of nitrate (a), phosphate (b), TRN (c) and particulate N in total suspended solids (d) plotted against water depth for all stations.

Figure 3.4: Isotopic composition $\delta^{15}\text{NO}_3^-$ (a), $\delta\text{N}^{18}\text{O}_3^-$ (b), $\delta^{15}\text{TRN}$ (c), and $\delta^{15}\text{PN}$ (d) plotted against water depth for all stations.

Figure 3.5: Composite seasonal diagram of SPN fluxes (squares) and $\delta^{15}\text{SPN}$ (circles) and their standard deviations at 2600 m water depth at station Ierapetra ($34^\circ 26' \text{N}$, $26^\circ 11' \text{E}$, water depth 3750 m). Fluxes (squares, black line and s.d. in red) and $\delta^{15}\text{SPN}$ (circles, grey line, s.d. in blue) for three deployment periods (MID-1: 01/30/1999 to 04/13/1999), MID-2: 11/05/2001 to 04/01/2002 and MID-3: 01/30/2007 to 09/05/2007) at 2700 m water depth have been assembled in a surrogate annual cycle.

Figure 3.6: Plots of log-normal nitrate concentrations (X-axis) versus $\delta^{15}\text{NO}_3^-$ (a) and $\delta\text{N}^{18}\text{O}_3^-$ (b) found in samples in and above the nitraclines for individual station. The solid regression line in Figure 6a is for samples in the northern Ionian Sea (NIS) where

Figure captions

nitrate is replenished from thermocline deepening ($r^2=0.89$). In these samples, ^{15}N in nitrate is enriched in the course of ongoing nitrate assimilation with an apparent separation factor $^{15}\epsilon$ close to -3‰ . In samples from the open Ionian Sea and Herodotus Basin (pelagic stations), where the mixed layer was thick and nitrate poor at the time of sampling, $\ln(\text{nitrate})$ and $\delta^{15}\text{NO}_3^-$ are uncorrelated. In Figure 3.6b, the correlation between $\ln(\text{nitrate})$ and $\delta\text{N}^{18}\text{O}_3^-$ for NIS samples is also significant ($r^2=0.78$), with an apparent separation factor $^{18}\epsilon$ close to -5‰ . There is no significant correlation in samples from pelagic stations and from the northern Aegean station.

Figure 3.7: Depth plot of $\Delta(15,18)$ of nitrate for different station sets in the upper 500 m of the water column.

Figure 4.1: Sampling sites in the Eastern Mediterranean Sea. Large dots: Sediment cores; Triangle: Ierapetra Deep sediment traps and multicores; small dots: surface sediment samples. The color shading is $\delta^{15}\text{N}$ (‰) in surface sediments based on this study and Struck et al. (2001). The map is produced by using Ocean Data View (Schlitzer, 2009).

Figure 4.2: $\delta^{15}\text{N}$ vs. degradation index (DI) in cores MC 284/285 from Ierapetra Deep and mean values from MID sediment traps. Insert: High resolution records of $\delta^{15}\text{N}$ and DI of multicores MC 284 and MC 285.

Figure 4.3: Downcore plots of total organic carbon (%TOC), barium to aluminum ratios, degradation index (DI) and $\delta^{15}\text{N}$ in multicores #569 (a), #562 (b) and #563 (c). S1 sapropel intervals and the burn-down zone above S1 are marked.

Figure 4.4: $\delta^{15}\text{N}$ vs. DI in core #569 and mean values from MID sediment traps. Insert: $\delta^{15}\text{N}$ vs. N (‰) in core #569. Residual N becomes isotopically enriched during remineralization. Surface sediments and protosapropel are marked in both plots.

Figure 4.5: $\delta^{15}\text{N}$ vs. DI for S1, S5 and S6 sapropels, core #569 and all Eastern Mediterranean surface samples. Mean values.

Figure 5.1: Oxygen concentrations (ml/l) in bottom water of the Arabian Sea (Gouretsky and Koltermann, 2004) and locations of sites referred to in the text. This map is produced by using Ocean Data View (Schlitzer, 2009).

Figure 5.2: Amino acid Reactivity Index (RI) and $\delta^{15}\text{N}$ (‰) vs. water depth and bottom water oxygenation (ml/l) in a set of 46 surface sediments. RI/ water depth (a), $\delta^{15}\text{N}$ / water depth (b), RI/ bottom water oxygenation (c), $\delta^{15}\text{N}$ / bottom water oxygenation (d), $\delta^{15}\text{N}$ / RI (e), water depth/ bottom water oxygenation (f).

Figure 5.3: Bulk sediment accumulation rates (BAR), RI, and $\delta^{15}\text{N}$ (‰) of samples from site 722 B (solid) and 724 C (dashed). MIS= Marine Isotope Stage; shaded are glacials.

Figure 5.4: $\delta^{15}\text{N}$ (‰) of samples from Hole 724 C (dashed) and core EAST (solid) and Hole 722 B (dashed) and core NAST (solid) plus 111 KL (Suthhof et al., 2001).

Figure 5.5: AA derived Degradation Index (DI) and Reactivity Index (RI) in ODP core 724 C show little congruence in indication. For both indices higher values indicate better preservation than lower values.

Figure 5.6: Variations in second PC factor scores (left plot) of AA PCA are similar to millennial scale oscillations in $\delta^{15}\text{N}$ (mid plot) and Ba/Al (data from Leuschner and Sirocko, 2003; right plot).

Figure 5.7: Molar percentages of protein AA glycine (Gly) and phenylalanine (Phe) in ODP core 724 C. Relative abundance of both amino acids due to depth and time is opposite as expected from water column decay processes.

Figure 5.8: Schematic of Gly decay from the water column to the deeper sediment. In the water column and at the sediment-water interface, Gly (as a cell wall constituent) becomes relatively enriched in a more stable OM fraction. In the sediment Gly is rapidly consumed by benthic microorganisms due to its easy metabolization and high availability. Further decay in the deeper sediment is achieved by slow microbial uptake and katagenesis.

Figure 5.9: Average $\delta^{15}\text{N}$ (‰) of the study sites over the last 60 kyr versus water depth. Squares: recent surface sediments. Both datasets show ^{15}N enrichment due to increasing water depth.

Figure captions

Figure 5.10: $\delta^{15}\text{N}$ (‰) in comparison with amino acid reactivity (RI) in samples of Holes 722 B (n=51), Hole 724 C (n=58), 111 KL (n=52) (Suthhof et al., 2001), surface sediments (n=46) and sediment traps (n=6; mean values). The shaded rectangle indicates the recent subsurface $\delta^{15}\text{NO}_3^-$ of 7 to 7.5‰. Note that RI and $\delta^{15}\text{N}$ are positively correlated in core records but negatively correlated in surface sediments.

Figure 5.11: Schematic interpretation of the relationship between sedimentary $\delta^{15}\text{N}$ and RI in the Arabian Sea as shown in figure 10: External sources, the intensity of denitrification and the degree of NO_3^- assimilation determine the general setting of $\delta^{15}\text{N}$ (1). Water column denitrification leads to an enrichment in ^{15}N and contemporaneous better preservation (2). During progressive OM decay (expressed by decrease in RI) $\delta^{15}\text{N}$ becomes enriched (3). The offset between the dashed arrow “water column denitrification (2)” and the solid “sediment record” represents the early diagenetic enrichment of the examined sediment cores.

Figure 5.12: Reconstructed $\delta^{15}\text{N}$ record for primary produced OM in cores 722 B (gray dashed) and 724 C (black). Compare to Figure 3, right plot. The reconstructed records show significant lower values and records converge by 0.5‰ on average.

Table Captions

Table 1.1: Fractionation factors ϵ for major transformation processes in the marine N-cycle. ^{14}N preference is expressed by negative values.

Table 1.2: Isotopic signatures of selected N-pools.

Table 3.1: Comparison of averages in water above, in and below the nitracline for samples taken in stations of the Northern Ionian Sea (6 stations, Table 3.1a), at pelagic stations (10 stations, Table 3.1b) and at one station in the northern Aegean Sea (Table 3.1c) in the EMS in January/February 2007 during Meteor expedition 71-3.

Table 3.2: Composite seasonal course of N-flux and $\delta^{15}\text{N}$ of sinking particulate matter at station MID (Ierapetra), water depth 2700 m. Data are from three separate and discontinuous deployment periods starting in 1999 and ending in 2007, as explained in the text.

Table 3.3: Estimate of reactive N-inventories of the EMS in different depth intervals and mass-weighted $\delta^{15}\text{N}$ of the different components (nitrate, particulate nitrogen PN, and total reduced nitrogen, TRN). We calculated inventories (given in gigamol N) based on interval water volumes for the EMS without Adriatic and Aegean sub-basins (R. Grimm, pers. comm., 2009) and weight $\delta^{15}\text{N}$ values by average concentrations found during our cruise. The last column is the integrated and mass-weighted $\delta^{15}\text{N}$ over all components of reactive N for each interval, the last line are the integrated inventories and $\delta^{15}\text{N}$ of the entire water column.

Table 3.4: Calculation of the isotopic composition of residual nitrate ($\delta^{15}\text{N}$ and $\delta^{18}\text{O}$) and instantaneous and accumulated products of nitrate assimilation expected from Rayleigh-fractionation in closed systems (NIS and pelagic mixed layers) with starting concentrations and isotopic compositions corresponding to thermocline nitrate from Table 3.1. Note that the permil fractionation factors $^{15}\epsilon$ and $^{18}\epsilon$ have been set to -5%. Results of measurements are also shown.

Table 4.1: Sediment trap moorings in the Ierapetra Deep: Position, water depth, sampling depth, deployment period and trap type.

Table captions

Table 4.2: Sediment sampling locations and sample types: MC = Multicore, GC = Gravity Core, ODP = Ocean Drilling Program Core.

Table 4.3: Sediment trap moorings in the Ierapetra Deep: Mean values of $\delta^{15}\text{N}$, DI, TOC and total flux.

Table 4.4: $\delta^{15}\text{N}$, DI and TOC values of recent surface sediments as well as from S1, S5 and S6 sapropel interval (¹=estimated values; ²=mean values of entire sapropel).

Table 5.1: Geographical position, water depth, and bottom water oxygenation (BWO) as well as examined depth interval (downcore from seafloor in m) and time equivalent (kyr) of examined cores.

Table 5.2: Amino acids analyzed in this study, their abbreviations and occurrence in indexes. DI = Degradation Index; RI = Reactivity Index; PCA = Principal Component Analysis.

List of abbreviations

AA = Amino Acid

DI = Degradation Index

DON = Dissolved Organic Nitrogen

ϵ = isotope fractionation factor

EMDW = Eastern Mediterranean Deep Water

EMS = Eastern Mediterranean Sea

GC = Gravity Core

LIW = Levantine Intermediate Water

MAW = Modified Atlantic Water

MC = MultiCore

MID = Mediterranean Ierapetra Deep

NIS = Northern Ionian Sea

OM = Organic Matter

OMZ = Oxygen Minimum Zone

PN = Particulate Nitrogen

R = isotope Ratio

RI = Reactivity Index

SL = gravity core

SPN = Sinking Particulate Nitrogen

SPON = Suspended Organic Nitrogen

TDN = Total Dissolved Nitrogen

TN = Total Nitrogen

TRN = Total dissolved Reduced Nitrogen

TOC = Total Organic Carbon

References

- Altabet, M.A., 1988. Variations in nitrogen isotopic composition between sinking and suspended particles: implications for nitrogen cycling and particle transformation in the open ocean. *Deep Sea Research I*, 535-554.
- Altabet, M.A. and Francois, R., 1994. Sedimentary Nitrogen Isotopic Ratio as a Recorder for Surface Ocean Nitrate Utilization. *Global Biogeochemical Cycles* 8, 103-116.
- Altabet, M.A., Francois, R., Murray, D.W. and Prell, W.L., 1995. Climate-related variations in denitrification in the Arabian Sea from sediment $^{15}\text{N}/^{14}\text{N}$ ratios. *Nature* 373, 506-509.
- Altabet, M.A., 1996. Nitrogen and carbon isotopic tracers of the source and transformation of particles in the deep-sea. In: V. Ittekkot, P. Schafer, S. Honjo and P.J. Depetris (Editors), *Particle Flux in the Ocean*. Wiley, London, pp. 155-184.
- Altabet, M.A., Pilskaln, C., Thunell, R., Pride, C., Sigman, D., Chavez, F. and Francois, R., 1999a. The nitrogen isotope biogeochemistry of sinking particles from the margin of the Eastern North Pacific. *Deep Sea Research I* 46, 655-679.
- Altabet, M.A., Murray, D.W. and Prell, W.L., 1999b. Climatically linked oscillations in Arabian Sea denitrification over the past 1 m.y.: Implications for the marine N cycle *Paleoceanography* 14, 732-743.
- Altabet, M.A., Higginson, M.J. and Murray, D.W., 2002. The effect of millennial-scale changes in Arabian Sea denitrification on atmospheric CO_2 . *Nature* 415, 159-162.
- Altabet, M.A., 2006. Isotopic tracers of the marine nitrogen cycle: Present and past. *Marine Organic Matter: Biomarkers, Isotopes and DNA* 2, 251-293.
- Altabet, M.A., 2007. Constraints on oceanic N balance/imbalance from sedimentary N-15 records. *Biogeosciences* 4, 75-86.
- Anastasakis, G.C. and Stanley, D.J., 1984. Sapropels and organic-rich variants in the Mediterranean: sequence development and classification. In: D.A.W. Stow and D.J.W. Piper (Editors), *Fine-grained Sediments: Deep-water Processes and Facies*. Geological Society, London, pp. 497-510.
- Anastasakis, G.C. and Stanley, D.J., 1986. Uppermost Sapropel, Eastern Mediterranean - *Paleoceanography and Stagnation*. *National Geographic Research* 2, 179-197.
- Antoine, D., Morel, A. and André, J.-M., 1995. Algal pigment distribution and primary production in the eastern Mediterranean as derived from coastal zone color scanner observations. *Journal of Geophysical Research* 100(C8), 16193-16209.
- Arnaboldi, M. and Meyers, P.A., 2006. Patterns of organic carbon and nitrogen isotopic compositions of latest Pliocene sapropels from six locations across the Mediterranean Sea. *Palaeogeography, Palaeoclimatology, Palaeoecology* 235, 149-167.

- Bada, J.L., Schoeninger, M.J. and Schimmelmann, A., 1989. Isotopic Fractionation During Peptide-Bond Hydrolysis. *Geochimica et Cosmochimica Acta* 53, 3337-3341.
- Badr, O. and Probert, S.D., 1993. Environmental Impacts of Atmospheric Nitrous-Oxide. *Applied Energy* 44(3), 197-231.
- Bahlmann, E., Bernasconi, S.M., Bouillon, S., Houtekamer, M., Korntheuer, M., Langenberg, F., Mayr, C., Metzke, M., Middelburg, J.J., Nagel, B., Struck, U., Voß, M. and Emeis, K.-C., Performance evaluation of nitrogen isotope ratio determination in marine and lacustrine sediments: An inter-laboratory comparison. *Organic Geochemistry*, in press, corrected proof.
- Barber, R.T., Marra, J., Bidigare, R.C., Codispoti, L.A., Halpern, D., Johnson, Z., Latasa, M., Goericke, R. and Smith, S.L., 2001. Primary productivity and its regulation in the Arabian Sea during 1995. *Deep Sea Research II* 48, 1127-1172.
- Benitez-Nelson, C.R., 2000. The biogeochemical cycling of phosphorus in marine systems. *Earth-Science Reviews* 51(1-4), 109-135.
- Berman-Frank, I., Yogeve, T., Aharonovich, D. and Beja, O., 2007. Nitrogen fixation in the Eastern Mediterranean Sea, Oral presentation, *IUGG XXIV General Assembly*, Perugia, Italy, PS001.
- Berman, T. and Bronk, D.A., 2003. Dissolved organic nitrogen: a dynamic participant in aquatic ecosystems. *Aquatic Microbial Ecology* 31, 279-305.
- Béthoux, J.P. and Copin-Montegut, G., 1986. Biological fixation of atmospheric nitrogen in the Mediterranean Sea. *Limnology and Oceanography* 31, 1353-1358.
- Béthoux, J.P., 1989. Oxygen-Consumption, New Production, Vertical Advection and Environmental Evolution in the Mediterranean Sea. *Deep Sea Research I* 36, 769-781.
- Bishop, J.K.B., 1988. The barite-opal-organic carbon association in oceanic particulate matter. *Nature* 332, 341-343.
- Böhlke, J.K., Mroczkowski, S.J. and Coplen, T.B., 2003. Oxygen isotopes in nitrate: new reference materials for 18O:17O:16O measurements and observations on nitrate-water equilibration. *Rapid Communications in Mass Spectrometry* 17, 1835-1846.
- Bourbonnais, A., Lehmann, M.F., Waniek, J.J. and Schulz-Bull, D.E., 2009. Nitrate isotope anomalies reflect N₂ fixation in the Azores Front region (subtropical NE Atlantic). *Journal of Geophysical Research* 114, doi:10.1029/2007JC004617
- Brandes, J.A., Devol, A.H., Yoshinari, T., Jayakumar, D.A. and Naqvi, S.W.A., 1998. Isotopic composition of nitrate in the central Arabian Sea and eastern tropical North Pacific: A tracer for mixing and nitrogen cycles. *Limnology and Oceanography* 43(7), 1680-1689.
- Brandes, J.A. and Devol, A.H., 2002. A global marine-fixed nitrogen isotopic budget: Implications for Holocene nitrogen cycling. *Global Biogeochemical Cycles* 16(4), doi:10.1029/2001GB001856.
- Bronk, D.A., 2002. Dynamics of DON. In: D.A. Hansell and C.A. Carlson (Editors), *Biogeochemistry of Marine Dissolved Organic Matter*. Academic Press, New York, pp. 153-247.

References

- Bronk, D.A., See, J.H., Bradley, P. and Killberg, L., 2007. DON as a source of bioavailable nitrogen for phytoplankton. *Biogeosciences* 4, 283-296.
- Calvert, S.E., Nielsen, B. and Fontugne, M.R., 1992. Evidence from nitrogen isotope ratios for enhanced productivity during formation of Eastern Mediterranean sapropels. *Nature* 359, 223-225.
- Canfield, D.E., Thamdrup, B. and Kristensen, E., 2005. The Nitrogen Cycle. In: A.J. Southward, P.A. Tyler, C.M. Young and L.A. Fuiman (Editors), *Aquatic Geomicrobiology. Advances in Marine Biology*. Elsevier Academic Press, Amsterdam, Boston, Heidelberg, London, New York, Oxford, Paris, San Diego, San Francisco, Singapore, Sydney, Tokyo, pp. 205-267.
- Carpenter, E.J., Harvey, H.R., Fry, B. and Capone, D.G., 1997. Biogeochemical tracers of the marine cyanobacterium *Trichodesmium*. *Deep Sea Research I* 44, 27-38.
- Casciotti, K.L., Sigman, D.M., Hastings, M.G., Bohlke, J.K. and Hilkert, A., 2002. Measurement of the oxygen isotopic composition of nitrate in seawater and freshwater using the denitrifier method. *Analytical Chemistry* 74, 4905-4912.
- Casciotti, K.L., Sigman, D.M. and Ward, B.B., 2003. Linking diversity and stable isotope fractionation in ammonia-oxidizing bacteria. *Geomicrobiology Journal* 20, 335-353.
- Casciotti, K.L. and Mc Ilvin, M.R., 2007. Isotopic analyses of nitrate and nitrite from reference mixtures and application to Eastern Tropical North Pacific waters. *Marine Chemistry* 107, 184-201.
- Casciotti, K.L., Trull, T.W., Glover, D.M. and Davies, D., 2008. Constraints on nitrogen cycling at the subtropical North Pacific Station ALOHA from isotopic measurements of nitrate and particulate nitrogen. *Deep Sea Research II* 55, 1661-1672.
- Casciotti, K.L., 2009. Inverse kinetic isotope fractionation during bacterial nitrite oxidation. *Geochimica et Cosmochimica Acta* 73(7), 2061-2076.
- Cheddadi, R. and Rossignol-Strick, M., 1995. Eastern Mediterranean Quaternary Paleoclimates from Pollen and Isotope Records of Marine Cores in the Nile Cone Area. *Paleoceanography* 10(2), 291-300.
- Cita, M.B., Vergnaud-Grazzini, C., Robert, C., Chamley, H., Ciaranfi, N. and d'Onofrio, S., 1977. Paleoclimatic record of a long deep sea core from the eastern Mediterranean. *Quaternary Research* 8(2), 205-235.
- Clemens, S.C. and Prell, W.L., 1991. One million year record of summer monsoon winds and continental aridity from the Owen Ridge (Site722), northwest Arabian Sea. In: W.D. Prell, N. Niitsuma, K.C. Emeis and P.A. Meyers (Editors), *Proceedings of the Ocean Drilling Program, Scientific Results*. Ocean Drilling Program, College Station, pp. 365-388.
- Coban-Yildiz, Y., Altabet, M.A., Yilmaz, A. and Tugrul, S., 2006. Carbon and nitrogen isotopic ratios of suspended particulate organic matter (SPOM) in the Black Sea water column. *Deep Sea Research II* 53, 1875-1892.

- Codispoti, L.A., Brandes, J.A., Christensen, J.P., Devol, A.H., Naqvi, S.W.A., Paerl, H.W. and Yoshinari, T., 2001. The oceanic fixed nitrogen and nitrous oxide budgets: Moving targets as we enter the anthropocene? *Scientia Marina* 65, 85-105.
- Codispoti, L.A., 2007. An oceanic fixed nitrogen sink exceeding 400 Tg Na-1 vs the concept of homeostasis in the fixed-nitrogen inventory. *Biogeosciences* 4(2), 233-253.
- Cole, J.J., Honjo, S. and Erez, J., 1987. Benthic decomposition of organic-matter at a deep-water site in the Panama Basin. *Nature* 327, 703-704.
- Cowie, G.L. and Hedges, J.I., 1992. Sources and Reactivities of Amino-Acids in a Coastal Marine-Environment. *Limnology and Oceanography* 37(4), 703-724.
- Dähnke, K., Bahlmann, E. and Emeis, K.-C., 2008. Nitrogen turnover in the Elbe estuary – assessment by means of stable nitrate isotopes. *Limnology and Oceanography* 53(4), 1504-1511.
- Dähnke, K., Serna, A., Blanz, T. and Emeis, K.C., 2008. Sub-recent nitrogen-isotope trends in sediments from Skagerrak (North Sea) and Kattegat: Changes in N-budgets and N-sources? *Marine Geology* 253, 92-98.
- Dauwe, B. and Middelburg, J.J., 1998. Amino acids and hexosamines as indicators of organic matter degradation state in North Sea sediments. *Limnology and Oceanography* 43(5), 782-798.
- Dauwe, B., Middelburg, J.J., Herman, P.M.J. and Heip, C.H.R., 1999. Linking diagenetic alteration of aminoacids and bulk organic matter reactivity. *Limnology and Oceanography* 44(7), 1809-1814.
- De Corte, D., Yokokawa, T., Varela, M., Agogué, H. and Herndl, G.J., 2009. Spatial distribution of Bacteria and Archaea and amoA gene copy numbers throughout the water column of the Eastern Mediterranean Sea. *The ISME Journal* 3(2), 147-158.
- De Lange, G.J., Thomson, J., Reitz, A., Slomp, C.P., Principato, M.S., Erba, E. and Corselli, C., 2008. Synchronous basin-wide formation and redox-controlled preservation of a Mediterranean sapropel. *Nature Geoscience* 1, doi:10.1038/ngeo283.
- Dehairs, F., Chesselet, R. and Jedwab, J., 1980. Discrete suspended particles of barite and the barium cycle in the open ocean. *Earth and Planetary Science Letters* 49(2), 528-550.
- Dehairs, F., Goeyens, L., Stroobants, N., Bernard, P., Goyet, C., Poisson, A. and Chesselet, R., 1990. On Suspended Barite and the Oxygen Minimum in the Southern Ocean. *Global Biogeochemical Cycles* 4(1), 85-102.
- Deutsch, C., Sigman, D.M., Thunell, R.C., Meckler, A.N. and Haug, G.H., 2004. Isotopic constraints on glacial/interglacial changes in the oceanic nitrogen budget. *Global Biogeochemical Cycles* 18(4), doi:10.1029/2003GB002189.
- Diaz, F. and Raimbault, P., 2000. Nitrogen regeneration and dissolved organic nitrogen release during spring in a NW Mediterranean coastal zone (Gulf of Lions): implications for the estimation of new production. *Marine Ecology Progress Series* 197, 51-65.
- Duce, R.A., LaRoche, J., Altieri, K., Arrigo, K.R., Baker, A.R., Capone, D.G., Cornell, S., Dentener, F., Galloway, J., Ganeshram, R.S., Geider, R.J., Jickells, T., Kuypers, M.M.,

References

- Langlois, R., Liss, P.S., Liu, S.M., Middelburg, J.J., Moore, C.M., Nickovic, S., Oschlies, A., Pedersen, T., Prospero, J., Schlitzer, R., Seitzinger, S., Sorensen, L.L., Uematsu, M., Ulloa, O., Voss, M., Ward, B. and Zamora, L., 2008. Impacts of atmospheric anthropogenic nitrogen on the open ocean. *Science* 320, 893-897.
- Dymond, J., Suess, E. and Lyle, M., 1992. Barium in deep-sea sediments: A geochemical proxy for paleoproductivity. *Paleoceanography* 7, 163-181.
- Emeis, K.C., Robertson, A.H.F., Richter, C. and others, 1996. Proceedings ODP, Initial Reports 160. Ocean Drilling Programm, College Station, TX.
- Emeis, K.-C., Struck, U., Schulz, H.-M., Rosenberg, R., Bernasconi, S., Erlenkeuser, H., Sakamoto, T. and Martinez-Ruiz, F., 2000. Temperature and salinity variations of Mediterranean Sea surface waters over the last 16,000 years from records of planktonic stable oxygen isotopes and alkenone unsaturation ratios. *Palaeogeography, Palaeoclimatology, Palaeoecology* 158, 259-280.
- Emeis, K.C. and Weissert, H., 2009. Tethyan-Mediterranean organic carbon-rich sediments from Mesozoic black shales to sapropels. *Sedimentology* 56, 247-266.
- Eppley, R.W. and Peterson, B.J., 1979. Particulate organic-matter flux and planktonic new production in the deep ocean. *Nature* 282, 677-680.
- Fagerli, H., Legrand, M., Preunkert, S., Vestreng, V., Simpson, D. and Cerqueira, M., 2007. Modeling historical long-term trends of sulfate, ammonium, and elemental carbon over Europe: A comparison with ice core records in the Alps. *Journal of Geophysical Research - Atmospheres* 112, doi:10.1029.2006JD008044
- Farrell, G., Pedersen, T.F., Calvert, S.E. and Nielsen, B., 1995. Glacial-interglacial changes in nutrient utilization in the equatorial Pacific Ocean. *Nature* 377, 514-517.
- Francois, R., Altabet, M.A. and Burckle, L.H., 1992. Glacial to interglacial changes in surface nitrate utilization in the Indian sector of the Southern Ocean as recorded by sediment $\delta^{15}\text{N}$. *Paleoceanography* 7, 589-606.
- Francois, R., Honjo, S., Manganini, S.J. and Ravizza, G.E., 1995. Biogenic Barium Fluxes to the Deep-Sea - Implications for Paleoproductivity Reconstruction. *Global Biogeochemical Cycles* 9(2), 289-303.
- Francois, R., Altabet, M.A., Yu, E.F., Sigman, D.M., Bacon, M.P., Frank, M., Bohrmann, G., Bareille, G. and Labeyrie, L.D., 1997. Contribution of Southern Ocean surface-water stratification to low atmospheric CO_2 concentrations during the last glacial period. *Nature* 389, 929-935.
- Freudenthal, T., Wagner, T., Wenzhöfer, F., Zabel, M. and Wefer, G., 2001. Early diagenesis of organic matter from sediments of the eastern subtropical Atlantic: evidence from stable nitrogen and carbon isotopes. *Geochimica et Cosmochimica Acta* 65, 1795-1808.
- Fry, B., Jannasch, H.W., Molyneaux, S.J., Wirsen, C.O., Muramoto, J.A. and King, S., 1991. Stable Isotope Studies of the Carbon, Nitrogen and Sulfur Cycles in the Black-Sea and the Cariaco Trench. *Deep Sea Research I* 38, 1003-1019.
- Fry, B., 2007. *Stable Isotope Ecology*. Springer-Verlag, Berlin, 308 pp.

- Fuchsman, C.A., Murray, J.W. and Konovalov, S.K., 2008. Concentration and natural stable isotope profiles of nitrogen species in the Black Sea. *Marine Chemistry* 111(1-2), 90-105.
- Galloway, J.N., Aber, J.D., Erisman, J.W., Seitzinger, S.P., Howarth, R.W., Cowling, E.B. and Cosby, B.J., 2003. The nitrogen cascade. *Bioscience* 53(4), 341-356.
- Ganeshram, R.S., Pedersen, T.F., Calvert, S.E. and Francois, R., 2002. Reduced nitrogen fixation in the glacial ocean inferred from changes in marine nitrogen and phosphorus inventories. *Nature* 415, 156-159.
- Garvin, J., Buick, R., Anbar, A.D., Arnold, G.L. and Kaufman, A.J., 2009. Isotopic Evidence for an Aerobic Nitrogen Cycle in the Latest Archean. *Science* 323, 1045-1048.
- Gat, J.R., Shemesh, A., Tziperman, E., Hecht, A., Georgopoulos, D. and Bastürk, O., 1996. *Journal of Geophysical Research* 106(C3), 6441-6451.
- Gaye-Haake, B., Lahajnar, N., Emeis, K.-C., Rixen, T., Unger, D., Schulz, H., Ramaswamy, V., Paropkari, A.L., Guptha, M.V.S. and Ittekkot, V., 2005. Stable nitrogen isotopic ratios of sinking particles and sediments from the northern Indian Ocean. *Marine Chemistry* 96, 243-255.
- Gaye, B., Wiesner, M.G. and Lahajnar, N., 2009. Nitrogen sources in the South China Sea as discerned from stable nitrogen isotopic ratios in rivers, sinking particles, and sediments. *Marine Chemistry* 114, 72-85.
- Giunta, S., Negri, A., Morigi, C., Capotondi, L., Combourieu-Nebout, N., Emeis, K.C., Sangiorgi, F. and Vigliotti, L., 2003. Coccolithophorid ecostratigraphy and multi-proxy paleoceanographic reconstruction in the Southern Adriatic Sea during the last deglacial time (Core AD91-17). *Palaeogeography, Palaeoclimatology, Palaeoecology* 190, 39-59.
- Gouretski, V.V. and Koltermann, K.P., 2004. WOCE Global Hydrographic Climatology. *Berichte des Bundesamtes für Seeschifffahrt und Hydrographie* 35, pp. 52.
- Granger, J., Sigman, D.M., Needoba, J.A. and Harrison, P.J., 2004. Coupled nitrogen and oxygen isotope fractionation of nitrate during assimilation by cultures of marine phytoplankton. *Limnology and Oceanography* 49(5), 1763-1773.
- Grasshoff, K., Ehrhardt, M., Kremling, K. and Anderson, L.G. (Editors), 1999. *Methods of Seawater Analysis*. Verlag Chemie, Weinheim, 632 pp.
- Gruber, N. and Sarmiento, J., 1997. Global patterns of nitrogen fixation and denitrification. *Global Biogeochemical Cycles* 11, 235-266.
- Gruber, N. and Galloway, J.N., 2008. An Earth-system perspective of the global nitrogen cycle. *Nature* 451, 293-296.
- Guptha, M.V.S., Naidu, P.D., Haake, B.G. and Schiebel, R., 2005. Carbonate and carbon fluctuations in the Eastern Arabian Sea over 140 ka: Implications on productivity changes? *Deep Sea Research II* 52, 1981-1993.
- Hecky, R.E., Mopper, K., Kilham, P. and Degens, E.T., 1973. The Amino Acid and Sugar Composition of Diatom Cell-Walls. *Marine Biology* 19, 323-331.

References

- Higginson, M.J. and Altabet, M.A., 2004. Comment on "Sedimentary phosphorus record from the Oman margin: New evidence of high productivity during glacial periods" by F. Tamburini et al.. *Paleoceanography* 19(2). doi:10.1029/2004PA001017.
- Hoch, M.P., Fogel, M.L. and Kirchman, D.L., 1992. Isotope Fractionation Associated with Ammonium Uptake by a Marine Bacterium. *Limnology and Oceanography* 37(7), 1447-1459.
- Holmes, M.E., Muller, P.J., Schneider, R.R., Segl, M., Patzold, J. and Wefer, G., 1996. Stable nitrogen isotopes in Angola Basin surface sediments. *Marine Geology* 134, 1-12.
- Holmes, M.E., Müller, P.J., Segl, M. and Wefer, G., 1997. Reconstruction of past nutrient utilization in the eastern Angola Basin based on sedimentary $^{15}\text{N}/^{14}\text{N}$ ratios. *Paleoceanography* 12(4), 604-614.
- Holmes, E., Lavik, G., Fischer, G., Segl, M., Ruhland, G. and Wefer, G., 2002. Seasonal variability of $\delta^{15}\text{N}$ in sinking particles in the Benguela upwelling region. *Deep Sea Research I* 49, 377-394.
- Honjo, S., Manganini, S.J. and Cole, J.J., 1982. Sedimentation of biogenic matter in the deep ocean. *Deep Sea Research I* 29, 609-625.
- Howell, M.W. and Thunell, R.C., 1992. Organic carbon accumulation in Bannock Basin: Evaluating the role of productivity in the formation of eastern Mediterranean sapropels. *Marine Geology* 103, 461-471.
- Ibello, V., Cantoni, C., Cozzi, S. and Civitarese, G., in press. First basin-wide experimental results on N_2 fixation in the open Mediterranean Sea. *Geophysical Research Letters*.
- Ingalls, A.E., Lee, C., Wakeham, S.G. and Hedges, J.I., 2003. The role of biominerals in the sinking flux and preservation of amino acids in the Southern Ocean along 170 degrees W. *Deep Sea Research II* 50, 713-738.
- Ivanova, E., Schiebel, R., Singh, A.D., Schmiedl, G., Niebler, H.-S. and Hemleben, C., 2003. Primary production in the Arabian Sea during the last 135.000 years. *Palaeogeography, Palaeoclimatology, Palaeoecology* 197, 61-82.
- Jaeschke, A., Hopmans, E.C., Wakeham, S.G., Schouten, S. and Sinninghe Damste, J.S., 2007. The presence of ladderane lipids in the oxygen minimum zone of the Arabian Sea indicates nitrogen loss through anammox. *Limnology and Oceanography* 52(2), 780-786.
- Jenkyns, H.C., Grocke, D.R. and Hesselbo, S.P., 2001. Nitrogen isotope evidence for water mass denitrification during the early Toarcian (Jurassic) oceanic anoxic event. *Paleoceanography* 16(6), 593-603.
- Jennerjahn, T.C. and Ittekkot, V., 1997. Organic Matter in sediments in the mangrove areas and adjacent continental margins of Brazil: I. Amino acids and hexosamines. *Oceanologica Acta* 20(2), 359-369.
- Jennerjahn, T.C. and Ittekkot, V., 1999. Changes in organic matter from surface waters to continental slope sediments off the Sao Francisco River, eastern Brazil. *Marine Geology* 161, 129-140.

- Johannsen, A., Dähnke, K. and Emeis, K., 2008. Isotopic composition of nitrate in five German rivers discharging into the North Sea. *Organic Geochemistry* 39, 1678-1689.
- Jung, M., Ilmberger, J., Mangini, A. and Emeis, K.C., 1997. Why some Mediterranean sapropels survived burn-down (and others did not). *Marine Geology* 141, 51-60.
- Kaiser, K. and Benner, R., 2009. Biochemical composition and size distribution of organic matter at the Pacific and Atlantic time-series stations. *Marine Chemistry* 113, 63-77.
- Karl, D., Michaels, A., Bergman, B., Capone, D., Carpenter, E., Letelier, R., Lipschultz, F., Paerl, H., Sigman, D. and Stal, L., 2002. Dinitrogen fixation in the world's oceans. *Biogeochemistry* 57(1), 47-98.
- Kemp, A.E.S., Pearce, R.B., Koizumi, I., Pike, J. and Rance, S.J., 1999. The role of mat-forming diatoms in the formation of Mediterranean sapropels. *Nature* 398, 57-61.
- Kendall, C., 1998. Tracing nitrogen sources and cycling in catchments. In: Kendall C & McDonnell JJ (Editors) *Isotope Tracers in Catchment Hydrology*. Elsevier, Amsterdam, pp. 521-576.
- Kendall, C., Elliott, E.M. and Wankel, S.D., 2007. Tracing anthropogenic inputs of nitrogen to ecosystems. In: K. Lajtha and R.H. Michener (Editors), *Stable Isotopes in Ecology and Environmental Science*. Blackwell Scientific Publications, Oxford, pp. 375-449.
- Knapp, A.N., Sigman, D. and Lipschultz, F., 2005. N-isotopic composition of dissolved organic nitrogen and nitrate at the Bermuda Atlantic Time-Series study site. *Global Biogeochemical Cycles* 19, doi:10.1029/2004GBC002320.
- Knapp, A., DiFiore, P.J., Deutsch, C., Sigman, D.M. and Lipschultz, F., 2008. Nitrate isotopic composition between Bermuda and Puerto Rico: Implications for N₂ fixation in the Atlantic Ocean *Global Biogeochemical Cycles* 22, doi: 10.1029/2007GB003107
- Koppelman, R., Böttger-Schnack, R., Möbius, J. and Weikert, H., 2009. Trophic relationships of zooplankton in the eastern Mediterranean Sea based on stable isotope measurements. *Journal of Plankton Research* 31, 669-686.
- Kouvarakis, G., Mihalopoulos, N., Tselepides, A. and Stavrakakis, S., 2001. On the importance of atmospheric inputs of inorganic nitrogen species on the productivity of the eastern Mediterranean Sea. *Global Biogeochemical Cycles* 15(4), 805-817.
- Kress, N. and Herut, B., 2001. Spatial and seasonal evolution of dissolved oxygen and nutrients in the Southern Levantine Basin (Eastern Mediterranean Sea): Chemical characterisation of the water masses and inferences on the N: P ratios. *Deep Sea Research I* 48, 2347-2372.
- Krom, M.D., Kress, N., Brenner, S. and Gordon, L.I., 1991. Phosphorus limitation of primary production in the eastern Mediterranean Sea. *Limnology and Oceanography* 36, 424-432.
- Krom, M.D., Groom, S. and Zohary, T., 2003. The Eastern Mediterranean. In: K.D. Black and G.B. Shimmield (Editors), *The Biogeochemistry of Marine Systems*. Blackwell Publishing, Oxford, pp. 91-122.
- Krom, M.D., Herut, B. and Mantoura, R.F.C., 2004. Nutrient budget for the Eastern Mediterranean: Implications for phosphorus limitation. *Limnology and Oceanography* 49(5), 1582-1592.

References

- Krom, M.D., Woodward, E.M.S., Herut, B., Kress, N., Carbo, P., Mantoura, R.F.C., Spyres, G., Thingstad, T.F., Wassmann, P., Wexels-Riser, C., Kitidis, V., Law, C.S. and Zodiatis, G., 2005a. Nutrient cycling in the south east Levantine basin of the eastern Mediterranean: Results from a phosphorus starved system *Deep Sea Research II* 52, 2879–2896.
- Krom, M.D., Thingstad, T.F., Brenner, S., Carbo, P., Drakopoulos, P., Fileman, T.W., Flaten, G.A.F., Groom, S., Herut, B., Kitidis, V., Kress, N., Law, C.S., Liddicoat, M.I., Mantoura, R.F.C., Pasternak, A., Pitta, P., Polychronaki, T., Psarra, S., Rassoulzadegan, F., Skjoldal, E.F., Spyres, G., Tanaka, T., Tselepides, A., Wassmann, P., Wexels Riser, C., Woodward, E.M.S., Zodiatis, G. and Zohary, T., 2005b. Summary and overview of the CYCLOPS P addition Lagrangian experiment in the Eastern Mediterranean Sea. *Deep Sea Research II* 52, 3090-3108.
- Kuhnt, T., Schmiedl, G., Ehrmann, W., Hamann, Y. and Hemleben, C., 2007. Deep-sea ecosystem variability of the Aegean Sea during the past 22 kyr as revealed by Benthic Foraminifera. *Marine Micropaleontology* 64, 141-162.
- Kuhnt, T., Schmiedl, G., Ehrmann, W., Hamann, Y. and Andersen, N., 2008. Stable isotopic composition of Holocene benthic foraminifers from the Eastern Mediterranean Sea: Past changes in productivity and deep water oxygenation. *Palaeogeography, Palaeoclimatology, Palaeoecology* 268,106-115.
- Kullenberg, B., 1952. On the salinity of water contained in marine sediments. *Meddelanden fran Oceanografiska Institutet i Göteborg* 21, 1-38.
- Kuypers, M.M.M., van Breugel, Y., Schouten, S., Erba, E. and Damste, J.S.S., 2004. N₂-fixing cyanobacteria supplied nutrient N for Cretaceous oceanic anoxic events. *Geology* 32, 853-856.
- Lahajnar, N., Wiesner, M.G. and Gaye, B., 2007. Fluxes of amino acids and hexosamines to the deep South China Sea. *Deep Sea Research I* 54, 2120-2144.
- Lascaratos, A., Roether, W., Nittis, K. and Klein, B., 1999. Recent changes in deep water formation and spreading in the eastern Mediterranean Sea: a review. *Progress in Oceanography* 44, 5–36.
- Lee, C. and Cronin, C., 1982. The vertical flux of particulate organic nitrogen in the sea: decomposition of amino acids in the Peru upwelling area and the equatorial Atlantic. *Journal of Marine Research* 40, 227-251.
- Lee, C. and Cronin, C., 1984. Particulate amino acids in the sea: Effects of primary productivity and biological decomposition. *Journal of Marine Research* 42, 1075-1097.
- LeGrande, N.A. and Schmidt, G.A., 2006. Global gridded data set of the oxygen isotopic composition in seawater. *Geophysical Research Letters* 33, doi:10.1029/2006GL026011.
- Lehmann, M.F., Bernasconi, S.M., Barbieri, A. and McKenzie, J.A., 2002. Preservation of organic matter and alteration of its carbon and nitrogen isotope composition during simulated and in situ early sedimentary diagenesis. *Geochimica et Cosmochimica Acta* 66, 3573-3584.

- Lehmann, M.F., Reichert, P., Bernasconi, S.M., Barbieri, A. and McKenzie, J.A., 2003. Modelling nitrogen and oxygen isotope fractionation during denitrification in a lacustrine redox-transition zone. *Geochimica et Cosmochimica Acta* 67, 2529-2542.
- Lehmann, M.F., Sigman, D.M., McCorkle, D.C., Brunelle, B.G., Hoffmann, S., Kienast, M., Cane, G. and Clement, J., 2005. The origin of the deep Bering Sea nitrate deficit - Constraints from the nitrogen and oxygen isotopic composition of water-column nitrate and benthic nitrate fluxes. *Global Biogeochemical Cycles* 19, doi:10.1029/2005GB002508.
- Leuschner, D.C. and Sirocko, F., 2003. Orbital insolation forcing of the Indian Monsoon - a motor for global climate changes? *Palaeogeography, Palaeoclimatology, Palaeoecology* 197, 83-95.
- Li, Q.P., Hansell, D.A. and Zhang, J.Z., 2008. Underway monitoring of nanomolar nitrate plus nitrite and phosphate in oligotrophic seawater. *Limnology and Oceanography - Methods*, 6: 319-326.
- Libes, S.M., 1992. *An Introduction to Marine Biogeochemistry*. John Wiley & Sons, Inc., New York, Chichester, Brisbane, Toronto, Singapore, 734 pp.
- Macko, S.A. and Estep, M.L.F., 1984. Microbial alteration of stable nitrogen and carbon isotopic compositions of organic matter. *Organic Geochemistry* 6, 787-790.
- Mahaffey, C., Michaels, A. and Capone, D.G., 2005. The conundrum of marine nitrogen fixation. *American Journal of Science* 305, 546-595.
- Malanotte-Rizzolli, P. and Bergamasco, A., 1989. The circulation of the eastern Mediterranean, Part 1. *Oceanologica Acta* 12, 335-351.
- Mara, P., Mihalopoulos, N., Gogou, A., Dähnke, K., Schlarbaum, T., Emeis, K.-C. and Krom, M., 2009. Isotopic composition of nitrate in wet and dry atmospheric deposition on Crete in the eastern Mediterranean Sea. *Global Biogeochemical Cycles* 23, doi:10.1029/2008gb003395
- Mariotti, A., Germon, J.C., Hubert, P., Kaiser, P., Letolle, R., Tardieux, A. and Tardieux, P., 1981. Experimental determination of nitrogen kinetic isotope fractionation: some principles; illustration for the denitrification and nitrification processes. *Plant and Soil* 62, 413-430.
- Mariotti, A., 1984. Natural N-15 abundance measurements and atmospheric nitrogen standard calibration. *Nature* 311, 251-252.
- Martin, J.H., Gordon, R.M. and Fitzwater, S.E., 1990. Iron in Antarctic Waters. *Nature* 345, 156-158.
- Mayer, B., Boyer, E.W., Goodale, C., Jaworski, N.A., Van Breemen, N., Howarth, R.W., Seitzinger, S., Billen, G., Lajtha, L.J., Nosal, M. and Paustian, K., 2002. Sources of nitrate in rivers draining sixteen watersheds in the northeastern US: Isotopic constraints. *Biogeochemistry* 57(1), 171-197.
- McCarthy, J.J., Yilmaz, A., Coban-Yildiz, Y. and Nevins, J.L., 2007. Nitrogen cycling in the offshore waters of the Black Sea. *Estuarine, Coastal and Shelf Science* 74, 493-514.

References

- McClelland, J.W. and Valiela, I., 1998. Linking nitrogen in estuarine producers to land-derived sources. *Limnology and Oceanography* 43(4), 577-585.
- McCoy, F.W., 1974. Late Quaternary sediments in the Eastern Mediterranean Sea. Ph.D. thesis, Harvard University, Cambridge, MA.
- Meador, T.B., Aluwihare, L.I. and Mahaffey, C., 2007. Isotopic heterogeneity and cycling of organic nitrogen in the oligotrophic ocean. *Limnology and Oceanography* 52 (3), 934-947.
- Mercone, D., Thomson, J., Abu-Zied, R.H., Croudace, I.W. and Rohling, E.J., 2001. High-resolution geochemical and micropalaeontological profiling of the most recent eastern Mediterranean sapropel. *Marine Geology* 177, 25-44.
- Meyers, P.A. and Bernasconi, S.M., 2005. Carbon and nitrogen isotope excursions in mid-Pleistocene sapropels from the Tyrrhenian Basin: Evidence for climate-induced increases in microbial primary production. *Marine Geology* 220, 41-58.
- Milder, J.C. and Montoya, J.P., 1999. Carbon and nitrogen stable isotope ratios at Sites 969 and 974: interpreting spatial gradients in sapropel properties. In: R. Zahn, M. Comas and A. Klaus (Editors), *Proceedings ODP, Scientific Results*, 161. Ocean Drilling Program, College Station, pp. 401-411.
- Minagawa, M. and Wada, E., 1986. Nitrogen isotope ratios of red tide organisms in the East China Sea: A characterization of biological nitrogen fixation. *Marine Chemistry* 19, 245-249.
- Montoya, J., Carpenter, E. and Capone, D., 2002. Nitrogen fixation and nitrogen isotope abundance in zooplankton of the oligotrophic North Atlantic. *Limnology and Oceanography* 47, 1617– 1628.
- Moodley, L., Middleburg, J.J., Herman, P.M.J., Soetaert, K. and de Lange, G.J., 2005. Oxygenation and organic-matter preservation in marine sediments: Direct experimental evidence from ancient organic carbon-rich deposits. *Geology* 33, 889-892.
- Müller, P.J. and Suess, E., 1979. Productivity, sedimentation rate, and sedimentary organic matter in the oceans-I. Organic carbon preservation. *Deep Sea Research I* 26, 1347-1362.
- Murat, A. and Got, H., 2000. Organic carbon variations of the eastern Mediterranean Holocene sapropel: a key for understanding formation processes. *Palaeogeography, Palaeoclimatology, Palaeoecology* 158, 241- 257.
- Naqvi, S.W.A., 1994. Denitrification Processes in the Arabian Sea. *Proceedings of the Indian Academy of Sciences-Earth and Planetary Sciences* 103(2), 279-300.
- Naqvi, S.W.A., Yoshinari, T., Jayakumar, D.A., Altabet, M.A., Narvekar, P.V., Devol, A.H., Brandes, J.A. and Codispoti, L.A., 1998. Budgetary and biogeochemical implications of N₂O isotope signatures in the Arabian Sea. *Nature* 394, 462-464.
- Pantoja, S., Repeta, D.J., Sachs, J.P. and Sigman, D.M., 2002. Stable isotope constraints on the nitrogen cycle of the Mediterranean Sea water column. *Deep Sea Research I* 49, 1609-1621.

- Pichevin, L., Martinez, P., Bertrand, P., Schneider, R. and Emeis, K.-C., 2005. Nitrogen cycling on the Namibian shelf and slope over the last two climatic cycles: Local and global forcings. *Paleoceanography* 20, doi:10.1029/2006GB002852.
- Pichevin, L., Bard, E., Martinez, P. and Billy, I., 2007. Evidence of ventilation changes in the Arabian Sea during the late Quaternary: Implication for denitrification and nitrous oxide emission. *Global Biogeochemical Cycles* 21, doi:10.1029/2006GB002852.
- Pierre, C., 1999. The oxygen and carbon isotope distribution in the Mediterranean water masses. *Marine Geology* 153, 41-55.
- Prell, W.D., Niitsuma, N. and others, 1989. Proceedings ODP, Initial Reports 117. Ocean Drilling Program, College Station, TX.
- Preunkert S., Wagenbach D. and Legrand M., 2003. A seasonally resolved alpine ice core record of nitrate: Comparison with anthropogenic inventories and estimation of preindustrial emissions of NO in Europe. *Journal of Geophysical Research* 108, doi:10.1029/2003JD003475.
- Redfield, A.C., 1934. On the proportions of organic derivatives in sea-water and their relation to the composition of plankton. In: R. J. Daniel (Editor), James Johnstone Memorial Volume, University Press of Liverpool, pp. 176-192.
- Rees, A.P., Law, C.S. and Woodward, E.M.S., 2006. High rates of nitrogen fixation during an in-situ phosphate release experiment in the Eastern Mediterranean Sea. *Geophysical Research Letters* 33, doi:10.1029/2006GL025791.
- Ren, H., Sigman, D., Meckler, A.N., Plessen, B., Robinson, R.S., Rosenthal, Y. and Haug, G.H., 2009. Foraminiferal Isotope Evidence of Reduced Nitrogen Fixation in the Ice Age Atlantic Ocean. *Science* 323, 244-248.
- Reschke, S., 1999. Biogeochemie der Schwebstofffracht der Donau und deren Einfluß auf das Sedimentationsgeschehen im nordwestlichen Schwarzen Meer. Ph.D. thesis, Universität Hamburg, Hamburg, 109 pp.
- Ribera d'Alcala, M., Civitarese, G., Conversano, F. and Lavezza, R., 2003. Nutrient ratios and fluxes hint at overlooked processes in the Mediterranean Sea. *Journal of Geophysical Research* 108(C9), doi:10.1029/2002JC001650.
- Rixen, T., Haake, B. and Ittekkot, V., 2000. Sedimentation in the western Arabian Sea: The role of water mass advection, coastal and open ocean upwelling. *Deep Sea Research II* 47, 2155-2178.
- Roether, W., Manca, B.B., Klein, B., Bregant, D., Georgopoulos, D., Beitzel, V., Kovacevic, V. and Luchetta, A., 1996. Recent changes in Eastern Mediterranean deep waters. *Science* 271, 333-335.
- Rohling, E.J., 1994. Review and new aspects concerning the formation of eastern Mediterranean sapropels. *Marine Geology* 122, 1-28.
- Rohling, E.J., Hopmans, E.C. and Damste, J.S.S., 2006. Water column dynamics during the last interglacial anoxic event in the Mediterranean (sapropel S5). *Paleoceanography* 21(2), doi:10.1029/2005PA001237.

References

- Rossignol-Strick, M., Nesteroff, W., Olive, P. and Vergnaudgrazzini, C., 1982. After the Deluge - Mediterranean Stagnation and Sapropel Formation. *Nature* 295, 105-110.
- Rossignol-Strick, M., 1983. African Monsoons, an Immediate Climate Response to Orbital Insolation. *Nature* 304, 46-49.
- Rossignol-Strick, M., 1985. Mediterranean Quaternary sapropels, an immediate response of the African monsoon to variation of insolation. *Palaeogeography, Palaeoclimatology, Palaeoecology* 49, 237-263.
- Ryan, W.B.F., 1972. Stratigraphy of Late Quaternary sediments in the eastern Mediterranean. In: D.J. Stanley (Editor), *The Mediterranean Sea: a Natural Sedimentation Laboratory*. Dowden, Hutchinson and Ross, Stroudsburg, Pa, pp. 149-169.
- Sachs, J.P. and Repeta, D.J., 1999. Oligotrophy and nitrogen fixation during Eastern Mediterranean sapropel events. *Science* 286, 2485-2488.
- Saino, T. and Hattori, A., 1980. N-15 Natural Abundance in Oceanic Suspended Particulate Matter. *Nature* 283, 752-754.
- Schlarbaum, T., Dähnke, K., Bahlmann, E. and Emeis, K.-C., in revision. Dissolved organic nitrogen in the Elbe River and estuary: Results of nitrogen isotope investigations. *Marine Chemistry*.
- Schulz, H., von Rad, U. and Erlenkeuser, H., 1998. Correlation between Arabian Sea and Greenland climate oscillations of the past 110000 years. *Nature* 393, 54-57.
- Sigman, D.M., Altabet, M.A., Michener, R., McCorkle, D.C., Fry, B. and Holmes, R.M., 1997. Natural abundance-level measurement of the nitrogen isotopic composition of oceanic nitrate: an adaptation of the ammonia diffusion method. *Marine Chemistry* 57, 227-242.
- Sigman, D.M., Altabet, M.A., Francois, R., McCorkle, D.C. and Gaillard, J.F., 1999. The isotopic composition of diatom-bound nitrogen in Southern Ocean sediments. *Paleoceanography* 14(2), 118-134.
- Sigman, D.M., Altabet, M.A., McCorkle, D.C., Francois, R. and Fischer, G., 2000. The delta N-15 of nitrate in the Southern Ocean: Nitrogen cycling and circulation in the ocean interior. *Journal of Geophysical Research-Oceans* 105(C8), 19599-19614.
- Sigman, D.M., Casciotti, K.L., Andreani, M., Barford, C., Galanter, M. and Bohlke, J.K., 2001. A bacterial method for the nitrogen isotopic analysis of nitrate in seawater and freshwater. *Analytical Chemistry* 73, 4145-4153.
- Sigman, D.M., Granger, J., DiFiore, P.J., Lehmann, M.M., Ho, R., Cane, G. and van Geen, A., 2005. Coupled nitrogen and oxygen isotope measurements of nitrate along the eastern North Pacific margin. *Global Biogeochemical Cycles* 19(4), doi:10.1029/2005GB002458.
- Sigman, D.M., DiFiore, P.J., Hain, M.P., Deutsch, C., Wang, Y., Karl, D.M., Knapp, A.N., Lehmann, M.F. and Pantoja, S., 2009. The dual isotopes of deep nitrate as a constraint on the cycle and budget of oceanic fixed nitrogen *Deep Sea Research I* 56, 1419-1439.
- Silfer, J.A., Engel, M.H. and Macko, S.A., 1992. Kinetic Fractionation of Stable Carbon and Nitrogen Isotopes During Peptide-Bond Hydrolysis - Experimental-Evidence and Geochemical Implications. *Chemical Geology* 101, 211-221.

- Sirocko, F. and Ittekkot, V., 1992. Organic-Carbon Accumulation Rates in the Holocene and Glacial Arabian Sea - Implications for O₂-Consumption in the Deep-Sea and Atmospheric CO₂ Variations. *Climate Dynamics* 7(4), 167-172.
- Slomp, C.P., Thomson, J. and de Lange, G.J., 2002. Enhanced regeneration of phosphorus during formation of the most recent eastern Mediterranean sapropel (S1). *Geochimica et Cosmochimica Acta* 66, 1171-1184.
- Sprenst, J.I. and Sprenst, P., 1990. *Nitrogen Fixing Organisms: Pure and Applied Aspects*. Chapman and Hall, London, 256 pp.
- Struck, U., Emeis, K.-C., Rau, G.H., Voss, M., Krom, M.D. and Rau, G.H., 2001. Biological productivity during sapropel S5 formation in the eastern Mediterranean Sea - Evidence from stable isotopes of nitrogen and carbon. *Geochimica et Cosmochimica Acta* 65, 3241-3258.
- Suthhof, A., Jennerjahn, T.C., Schafer, P. and Ittekkot, V., 2000. Nature of organic matter in surface sediments from the Pakistan continental margin and the deep Arabian Sea: amino acids. *Deep Sea Research II* 47, 329-351.
- Suthhof, A., Ittekkot, V. and Gaye-Haake, B., 2001. Millennial-scale oscillation of denitrification intensity in the Arabian Sea during the late Quaternary and its potential influence on atmospheric N₂O and global climate. *Global Biogeochemical Cycles* 15(3), 637-649.
- Sweeney, R.E. and Kaplan, I.R., 1980. Natural abundances of ¹⁵N as a source indicator for near-shore marine sedimentary and dissolved nitrogen. *Marine Chemistry* 9, 81-90.
- Tamburini, F., Föllmi, K.B., Adatte, T., Bernasconi, S.M. and Steinmann, P., 2003. Sedimentary phosphorus record from the Oman margin: New evidence of high productivity during glacial periods. *Paleoceanography* 18(1), doi:10.1029/2000PA000616.
- Thingstad, T.F. and Rassoulzadegan, F., 1999. Conceptual models for the biogeochemical role of the photic zone microbial food web, with particular reference to the Mediterranean Sea. *Progress in Oceanography* 44, 271-286.
- Thingstad, T.F., Krom, M.D., Mantoura, R.F.C., Flaten, G.A.F., Groom, S., Herut, B., Kress, N., Law, C.S., Pasternak, A., Pitta, P., Psarra, S., Rassoulzadegan, F., Tanaka, T., Tselepidis, A., Wassmann, P., Woodward, E.M.S., Wexels Riser, C., Zodiatis, G. and Zohary, T., 2005. Nature of phosphorus limitation in the ultraoligotrophic Eastern Mediterranean. *Science* 309, 1068-1071.
- Thomson, J., Higgs, N.C., Wilson, T.R.S., Croudace, I.W., De Lange, G.J. and Van Santvoort, P.J.M., 1995. Redistribution and geochemical behaviour of redox-sensitive elements around S1, the most recent eastern Mediterranean sapropel. *Geochimica et Cosmochimica Acta* 59, 3487-3501.
- Thomson, J., Mercone, D., De Lange, G.J. and Van Santvoort, P.J.M., 1999. Review of recent advances in the interpretation of eastern Mediterranean sapropel S1 from geochemical evidence. *Marine Geology* 153, 77-89.
- Thunell, R.C., Sigman, D.M., Muller-Karger, F., Astor, Y. and Varela, R., 2004. Nitrogen isotope dynamics of the Cariaco Basin, Venezuela. *Global Biogeochemical Cycles* 18(3), doi:10.1029/2003GB002185.

References

- Tissot, B.P. and Welte, D.H., 1978. *Petroleum Formation and Occurrence*. Springer-Verlag, Berlin Heidelberg New York, 538 pp.
- Triantaphyllou, M.V., Antonarakou, A., Kouli, K., Dimiza, M., Kontakiotis, G., Papanikolaou, M.D., Ziveri, P., Mortyn, P.G., Lianou, V., Lykousis, V. and Dermitzakis, M.D., 2009. Late Glacial-Holocene ecostratigraphy of the south-eastern Aegean Sea, based on plankton and pollen assemblages. *Geo-Marine Letters*, doi:10.1007/s00367-009-0139-5.
- Tyrrell, T., 1999. The relative influences of nitrogen and phosphorus on oceanic primary production. *Nature* 400, 525-531.
- Unger, D., Gaye-Haake, B., Neumann, K., Gebhardt, A.C. and Ittekkot, V., 2005. Biogeochemistry of suspended and sedimentary material in the Ob and Yenisei rivers and Kara Sea: amino acids and amino sugars. *Continental Shelf Research* 25, 437-460.
- Voss, M., Nausch, G. and Montoya, J.P., 1997. Nitrogen stable isotope dynamics in the central Baltic Sea: influence of deep-water renewal on the N-cycle changes. *Marine Ecology Progress Series* 158, 11-21.
- Voss, M., Dippner, J.W. and Montoya, J.P., 2001. Nitrogen isotope patterns in the oxygen-deficient waters of the Eastern Tropical North Pacific Ocean. *Deep Sea Research I* 48, 1905-1921.
- Voss, M., Emeis, K.C., Hille, S., Neumann, T. and Dippner, J.W., 2005. Nitrogen cycle of the Baltic Sea from an isotopic perspective. *Global Biogeochemical Cycles* 19(3), doi:10.1029/2004GB002338.
- Voss, M., Deutsch, B., Elmgren, R., Humborg, C., Kuuppo, P., Pastuszak, M., Rolff, C. and Schulte, U., 2006. Source identification of nitrate by means of isotopic tracers in the Baltic Sea catchments. *Biogeosciences* 3, 663-676.
- Wallmann, K., 2003. Feedbacks between oceanic redox states and marine productivity: A model perspective focused on benthic phosphorus cycling. *Global Biogeochemical Cycles* 17(3), doi:10.1029/2002GB001968.
- Wankel, S.D., Kendall, C., Francis, C.A. and Paytan, A., 2006. Nitrogen sources and cycling in the San Francisco Bay Estuary: A nitrate dual isotopic composition approach. *Limnology and Oceanography* 51(4), 1654-1664.
- Wankel, S.D., Chen, Y., Kendall, C., Post, A.F. and Paytan, A., 2009. Sources of aerosol nitrate to the Gulf of Aqaba: Evidence from $\delta^{15}\text{N}$ and $\delta^{18}\text{O}$ of nitrate and trace metal chemistry. *Marine Chemistry*, in press, corrected proof.
- Ward, B.B., Devol, A.H., Rich, J.J., Chang, B.X., Bulow, S.E., Naik, H., Pratihary, A. and Jayakumar, A., 2009. Denitrification as the dominant nitrogen loss process in the Arabian Sea. *Nature* 461, 78-81.
- Warnken, C., 2003. *Biogeochemie von Schwebstoffen, Sinkstoffen und Sedimenten im Ierapetra-Tief (östliches Mittelmeer)*. M.Sc. thesis, Universität Hamburg, Hamburg, 80 pp.

- Westley, M.B., Yamagishi, H., Popp, B.N. and Yoshida, N., 2006. Nitrous oxide cycling in the Black Sea inferred from stable isotope and isotopomer distributions. *Deep Sea Research II* 53, 1802-1816.
- Wüst, G., 1961. On the vertical circulation of the Mediterranean Sea. *Journal of Geophysical Research* 66, 3261-3271.
- Wyrtki, K., 1971. *Oceanographic Atlas of the International Indian Ocean Expedition*. National Science Foundation Publication, Washington DC, 531 pp.
- Yool, A., Martin, A.P., Fernandez, C. and Clark, D.R., 2007. The significance of nitrification for oceanic new production. *Nature* 447, 999-1002.
- York, J.K., Tomasky, G., Valiela, I. and Repeta, D.J., 2007. Stable isotopic detection of ammonium and nitrate assimilation by phytoplankton in the Waquoit Bay estuarine system. *Limnology and Oceanography* 52, 144–155.
- Zahn, R. and Pedersen, T.F., 1991. Late Pleistocene evolution of surface and mid-depth hydrography at the Oman margin: Planktonic and benthic isotope records at Site 724. In: W.D. Prell, N. Niitsuma, K.C. Emeis and P.A. Meyers (Editors), *Proceedings ODP, Scientific Results*. College Station, TX, pp. 291-308.
- Zohary, T. and Robarts, R.D., 1998. Experimental study of microbial P limitation in the eastern Mediterranean. *Limnology and Oceanography* 43(3), 387-395.
- Zohary, T., Herut, B., Krom, M., Mantoura, R.F.C., Pitta, P., Psarra, S., Rassoulzadegan, F., Stambler, N., Tanaka, T., Thingstad, T.F. and Woodward, E.M.S., 2005. P-limited bacteria but N and P co-limited phytoplankton in the Eastern Mediterranean - a microcosm experiment. *Deep Sea Research II* 52, 3011-3023.

Curriculum Vitae

Jürgen Henning Möbius

Born: 14.04. 1978 in Hamburg
Nationality: German
Home address: Lange Reihe 76, 20099 Hamburg

Education

Since

April 2006 Ph.D. student, Institut für Biogeochemie und Meereschemie,
Universität Hamburg
Thesis subject: *Nitrogen cycling in the past and in the present
Mediterranean Sea and Arabian Sea – Implications from stable isotope
studies*

March 2006 Graduation (Diploma)
Diploma-Thesis: *Particle sedimentation during the 1998/1999 El
Niño event in the South China Sea: amino acids and amino
sugars*

2002 Exchange student (spring semester) in geology at
“Universidad de Granada”, Granada, Spain

1999 - 2006 Studies of Geology and Paleontology (Diploma),
Universität Hamburg.
Emphasis on Biogeochemistry and Soil Science

1997 Abitur at Gymnasium Winsen

List of Publications:

Wieland, A., Pape, T., Möbius, J., Klock, J.H. and Michaelis, W., 2008: Carbon pools and isotopic trends in a hypersaline cyanobacterial mat. *Geobiology* 6(2), 171-186.

Koppelman, R., Böttger-Schnack, R., Möbius, J. and Weikert, H., 2009: Trophic relationships of zooplankton in the eastern Mediterranean based on stable isotope measurements. *Journal of Plankton Research* 31(6), 669-686.

Zonneveld, K.A.F., Chen, L., Möbius, J., Mahmoud, M.S., 2009: Environmental significance of dinoflagellate cysts from the proximal part of the Po-river discharge plume (off southern Italy, Eastern Mediterranean). *Journal of Sea Research* 62(4), 189-213.

Möbius, J., Lahajnar, N. and Emeis, K.-C., 2010: Diagenetic control of nitrogen isotope ratios in Holocene sapropels and recent sediments from the Eastern Mediterranean Sea. *Biogeosciences Discussions* 7, 1131-1165.

Emeis, K.-C., Mara, P., Schlarbaum, T., Möbius, J., Dähnke, K., Struck, U., Mihalopoulos, N. and Krom, M.: N-isotope ratios of nitrate, dissolved organic nitrogen and particulate nitrogen in the Eastern Mediterranean Sea. *Journal of Geophysical Research – Biogeochemistry* (under review)

Möbius, J., Gaye, B., Lahajnar, N., Bahlmann, E. and Emeis, K.-C.: Influence of diagenesis on sedimentary $\delta^{15}\text{N}$ in the Arabian Sea over the last 130 kyr. Submitted to *Marine Geology*